

## ABSTRACT

BARTHOLOMEW, NATHANAEL. Polyacrylamide For Turbidity Control in Runoff: Effects of Polyacrylamide, Soil, and Solution Properties. (Under the direction of Richard McLaughlin).

Eroded soil discharged from construction sites is a major water quality issue. North Carolina regulations require that the turbidity of discharged waters from construction sites to non-trout streams or reservoirs not exceed 50 nephelometer turbidity units (NTU) and 10 NTU in trout waters. Polyacrylamide (PAM) has been demonstrated to reduce erosion and turbidity in runoff, but there is little information on the interactions between PAM properties and that of the water or suspended solids. Our study tested eight PAM products (Cytec Superfloc A100, A110, A150, N300, 1606; Ciba Soilfix Polybead; Applied Polymer Systems 705; Chemtall 923VHM) at concentrations from 0 to 10 mg L<sup>-1</sup> for turbidity reduction in suspensions of 13 soils from active construction sites around North Carolina. For five soil suspensions, with turbidities of up to 3000 NTU, PAM reduced turbidity to below 50 NTU in 30 s. In addition turbidity reductions to the 10 NTU level were observed for two soils. Overall, turbidity reductions of greater than 86% were achieved for all soils. Optimal PAM concentrations of soils tested were 1-2 mg L<sup>-1</sup>, with higher concentrations causing turbidity increases in some soils. Sediment properties drastically affected the response to PAM, which indicates the need to have site-specific recommendations for PAM use. Sediments with turbidity reductions below the 50 NTU standard had kaolinite as the dominant clay mineral (70-90%), a pH between 5-6, and very low organic matter. Soils from the Coastal Plain had poor turbidity reduction with most PAMs. APS705, which contains a mixture of polymers

with different molecular weights and charge density, was the only polymer that effectively reduced turbidity in all Coastal Plain soils. An evaluation using combinations of low and high molecular weight PAM products to try and mimic APS705 effects gave limited turbidity reduction of Coastal Plain soil suspensions. Combined treatment of gypsum and PAM appears to have either positive or negative effects depending on PAM concentration and soil properties. When gypsum was added to a Piedmont soil sample, it decreased the efficacy of PAM at polymer concentrations below  $1 \text{ mg L}^{-1}$ . For PAM concentrations at or above  $1 \text{ mg L}^{-1}$ , gypsum had a positive combined effect, although no significant effect occurred above  $50 \text{ mg L}^{-1}$  gypsum. In soils from the Coastal Plain, there was a positive combined gypsum and PAM effect at all PAM concentrations. However, APS 705 alone was more effective at reducing turbidity than other PAMs combined with gypsum. PAM effectively decreased turbidity of most soil suspensions and could be very useful in reducing construction site runoff turbidity to meet water quality standards.

**Polyacrylamide For Turbidity Control in Runoff:  
Effects of Polyacrylamide, Soil, and Solution Properties.**

by

NATHANAEL BARTHOLOMEW

A thesis submitted to the Graduate Faculty of North Carolina State University in partial  
fulfillment of the requirements for the Degree of Master of Science

DEPARTMENT OF SOIL SCIENCE

Raleigh

2003

Approved by:

---

Dr. R. A. McLaughlin  
Chair of Advisory Committee

---

Dr. D. L. Hesterberg

---

Dr. D.R.U.Knappe

## **Biography**

Nathanael Bartholomew was born April 12, 1977 in Payson, Utah. He spent most of his childhood in Springville, Utah. During his high school years, Nathanael became interested in science. He began his studies at Brigham Young University in Chemical Engineering. After one year of college, Nathanael spent the next two years as a missionary for the Church of Jesus Christ of Latter-day Saints in Sweden. After coming home Nathanael decided to change majors and after taking an introduction to soil science class by Bruce Webb ended up in Agronomy with an emphasis in Environmental Science. Nathanael was involved with many undergraduate research projects in the Agronomy Department. The studies included: 1) sodic soil reclamation using gypsum, polyacrylamide and sulfuric acid, 2) mapping of invasive species using gps, and 3) phosphorus movement in soil profiles on agricultural fields. After completion of his Bachelors degree, Nathanael pursued a M.S. in Soil Science at North Carolina State University under the direction of Dr. Rich McLaughlin. After graduation, Nathanael will continue his education toward a Ph.D. at the University of Minnesota.

## **Acknowledgements**

There are many people that I would like to recognize for their support leading to the completion of my M.S. degree. First I would like to thank my wife for her patience during the last two years. I'd like to thank her for always sticking with me even when I haven't used my head. I'd like to thank her for the support that leads to good grades and a completed degree. Next I would like to thank my parents for the way that they brought me up. Dad always taught me that I needed to be proud of what I do. I'd like to acknowledge my advisor, Rich for being patient with me even when he probably thought that things would never get done. Also, I'd like to thank him for his quiet support and good example of how to do research and how to effectively present research at professional meetings. I'd like to thank Dr. Dean Hesterberg for his support and willingness to always listen to my questions. I'd also like to thank him for his kindness, even with Ashley attending soil chemistry. I'd like to thank David Crouse for his friendship and support, knowing that I was a lucky student to walk into his path. I'd also like to thank Mark, Dawn, Jamie, Sara, Tabitha, Wes, Eric, Rob, Tim, Mindy, Amy, David, John, Kim, Carrie, Ross, Erik, Justin, Gary, Jared, Amber, Nathan, Ryan, Leigh Ann and Jaren for their friendship. They defined my experience at NC State. Last but not least I'd like to thank my friend Bruce Webb for his advice to stay in soil science. Without his guidance I would have never come to North Carolina State to study soil science.

# Table of Contents

<b>List of Figures</b> .....	v
<b>List of Tables</b> .....	xii
<b>Introduction</b> .....	1
PAM Background .....	4
Flocculation .....	6
Environmental Issues .....	10
References .....	14
<b>Polyacrylamide and Soil Interactions</b> .....	
Introduction .....	22
Materials and Methods .....	26
Soil Analysis .....	26
PAM Interactions .....	28
Mixed Polymers .....	31
Results and Discussion .....	32
Soil Analysis .....	32
PAM Interactions .....	33
Statistical Analysis .....	38
Mixed Polymer .....	41
Conclusions .....	42
References .....	43
<b>Combined Gypsum and PAM Treatment</b> .....	
Introduction .....	77
Materials and Methods .....	80
Results and Discussion .....	82
Conclusions .....	87
References .....	88
<b>Appendix</b> .....	110

## List of Figures

	Page
Figure 1.1 Industrial applications of anionic polyacrylamide (Barvenik, 1994).	17
Figure 1.2 Copolymerization of acrylamide and acryloyloxyethyl-trimethyl ammonium chloride to form cationic PAM (Barvenik, 1994).	18
Figure 1.3 Nonionic PAM polymerization (Barvenik, 1994).	19
Figure 1.4 Copolymerization of acrylamide and sodium acrylate to form anionic PAM (Barvenik, 1994).	20
Figure 1.5 Molecular structure of anionic PAM.	21
Figure 2.1 Mineral content of coarse (2 – 0.2 mm) and fine (< 0.2 mm) clay fractions of typical North Carolina soils (Coleman et al., 1949).	45
Figure 2.2 Soil sample numbers coincide with the highway division they originated from.	46
Figure 2.3 Example of Initial PAM testing using soil 11 from the Mountain Region. Figure shown in linear-log scale.	47
Figure 2.4 Turbidity reduction as a function of input concentration for four PAM products differing in charge density (c.d.) (percent hydrolysis) and molecular weight (in $\text{Mg mol}^{-1}$ ) over nine concentrations on soil sample 9. For each PAM concentration, data points with different letters are significantly different ( $p = 0.05$ ). Figure shown in linear-log scale.	48
Figure 2.5 Turbidity reduction as a function of input concentration for four PAM products differing in charge density (c.d.) (percent hydrolysis) and molecular weight (in $\text{Mg mol}^{-1}$ ) over nine concentrations on soil sample 5. For each PAM concentration, data points with different letters are significantly different ( $p = 0.05$ ). Figure shown in linear-log scale.	49
Figure 2.6 Turbidity reduction as a function of input concentration for four PAM products differing in charge density (c.d.) (percent hydrolysis) and molecular weight (in $\text{Mg mol}^{-1}$ ) over nine concentrations on soil sample 12. For each PAM concentration, data points with different letters are significantly different ( $p = 0.05$ ). Figure shown in linear-log scale.	50
Figure 2.7 Turbidity reduction as a function of input concentration for five PAM products differing in charge density (c.d.) (percent hydrolysis) and molecular	

weight (in  $\text{Mg mol}^{-1}$ ) over nine concentrations on soil sample 13. For each PAM concentration, data points with different letters are significantly different ( $p = 0.05$ ). Figure shown in linear-log scale. 51

Figure 2.8 Turbidity reduction as a function of input concentration for five PAM products differing in charge density (c.d.) (percent hydrolysis) and molecular weight (in  $\text{Mg mol}^{-1}$ ) over nine concentrations on soil sample 11. For each PAM concentration, data points with different letters are significantly different ( $p = 0.05$ ). Figure shown in linear-log scale. 52

Figure 2.9 Turbidity reduction as a function of input concentration for four PAM products differing in charge density (c.d.) (percent hydrolysis) and molecular weight (in  $\text{Mg mol}^{-1}$ ) over nine concentrations on soil sample 7. For each PAM concentration, data points with different letters are significantly different ( $p = 0.05$ ). Figure shown in linear-log scale. 53

Figure 2.10 Turbidity reduction as a function of input concentration for four PAM products differing in charge density (c.d.) (percent hydrolysis) and molecular weight (in  $\text{Mg mol}^{-1}$ ) over nine concentrations on soil sample 14. For each PAM concentration, data points with different letters are significantly different ( $p = 0.05$ ). Figure shown in linear-log scale. 54

Figure 2.11 Turbidity reduction as a function of input concentration for five PAM products differing in charge density (c.d.) (percent hydrolysis) and molecular weight (in  $\text{Mg mol}^{-1}$ ) over nine concentrations on soil sample 2. For each PAM concentration, data points with different letters are significantly different ( $p = 0.05$ ). Figure shown in linear-log scale. 55

Figure 2.12 Turbidity reduction as a function of input concentration for five PAM products differing in charge density (c.d.) (percent hydrolysis) and molecular weight (in  $\text{Mg mol}^{-1}$ ) over nine concentrations on soil sample 3. For each PAM concentration, data points with different letters are significantly different ( $p = 0.05$ ). Figure shown in linear-log scale. 56

Figure 2.13 Turbidity reduction as a function of input concentration for four PAM products differing in charge density (c.d.) (percent hydrolysis) and molecular weight (in  $\text{Mg mol}^{-1}$ ) over nine concentrations on soil sample 6. For each PAM concentration, data points with different letters are significantly different ( $p = 0.05$ ). Figure shown in linear-log scale. 57

Figure 2.14 Turbidity reduction as a function of input concentration for four PAM products differing in charge density (c.d.) (percent hydrolysis) and molecular weight (in  $\text{Mg mol}^{-1}$ ) over nine concentrations on soil sample 8. For each PAM concentration, data points with different letters are significantly different ( $p = 0.05$ ). Figure shown in linear-log scale. 58



Figure 2.15 Turbidity reduction as a function of input concentration for five PAM products differing in charge density (c.d.) (percent hydrolysis) and molecular weight (in $\text{Mg mol}^{-1}$ ) over nine concentrations on soil sample 1. For each PAM concentration, data points with different letters are significantly different ( $p = 0.05$ ). Figure shown in linear-log scale.	59
Figure 2.16 Turbidity reduction as a function of input concentration for four PAM products differing in charge density (c.d.) (percent hydrolysis) and molecular weight (in $\text{Mg mol}^{-1}$ ) over nine concentrations on soil sample 4. For each PAM concentration, data points with different letters are significantly different ( $p = 0.05$ ). Figure shown in linear-log scale.	60
Figure 2.17 Comparison of treatments involving low and high molecular weight PAMs. For each PAM concentration, data points with different letters are significantly different ( $p = 0.05$ ). Figure shown in linear-log scale.	61
Figure 2.18 Comparison of treatments involving low and high molecular weight PAMs. For each PAM concentration, data points with different letters are significantly different ( $p = 0.05$ ). Figure shown in linear-log scale.	62
Figure 3.1 Soil sample numbers coincide with the highway division they originated from. Soil samples used in gypsum evaluation came from 1, 2, 3, 4, 8, 11 and 13 (NCDOT Divisions).	90
Figure 3.2 Turbidity reduction as a function of input PAM concentration. Flocculation by Superfloc A110 (18% charge density, $15 \text{ Mg mol}^{-1}$ molecular weight) alone and with gypsum at four different concentrations on soil 8. For each PAM concentration, data points with different letters are significantly different ( $p = 0.05$ ). The “0” data point for PAM is graphed at 0.01 due to limitations in using a linear-log scale.	91
Figure 3.3 Turbidity reduction as a function of input PAM concentration. Flocculation by Chemtall 923VHM (30% charge density, $14\text{-}17.5 \text{ Mg mol}^{-1}$ molecular weight) alone and with gypsum at four different concentrations on soil 8. For each PAM concentration, data points with different letters are significantly different ( $p = 0.05$ ). The “0” data point for PAM is graphed at 0.01 due to limitations in using a linear-log scale.	92
Figure 3.4 Turbidity reduction as a function of input PAM concentration. Flocculation by Ciba Soilfix (30% charge density, $15 \text{ Mg mol}^{-1}$ molecular weight) alone and with gypsum at four different concentrations on soil 8. For each PAM concentration, data points with different letters are significantly different ( $p = 0.05$ ). The “0” data point for PAM is graphed at 0.01 due to limitations in using a linear-log scale.	93

Figure 3.5 Turbidity reduction as a function of input PAM concentration. Flocculation by APS 705 (mixed charge density, mixed molecular weight) alone and with gypsum at four different concentrations on soil 8. For each PAM concentration, data points with different letters are significantly different ( $p = 0.05$ ). The “0” data point for PAM is graphed at 0.01 due to limitations in using a linear-log scale. 94

Figure 3.6 Turbidity reduction as a function of input PAM concentration. Flocculation by APS 706b (block) (mixed charge density, mixed molecular weight) alone and with gypsum at four different concentrations on soil 8. For each PAM concentration, data points with different letters are significantly different ( $p = 0.05$ ). The “0” data point for PAM is graphed at 0.01 due to limitations in using a linear-log scale. 95

Figure 3.7 Turbidity reduction as a function of input PAM concentration with no gypsum and 5 different PAM products on soil 8. For each PAM concentration, data points with different letters are significantly different ( $p = 0.05$ ). The “0” data point for PAM is graphed at 0.01 due to limitations in using a linear-log scale. 96

Figure 3.8 Turbidity reduction as a function of input PAM concentration with 10 mg L<sup>-1</sup> gypsum and 5 different PAM products on soil 8. For each PAM concentration, data points with different letters are significantly different ( $p = 0.05$ ). The “0” data point for PAM is graphed at 0.01 due to limitations in using a linear-log scale. 97

Figure 3.9 Turbidity reduction as a function of input PAM concentration with 20 mg L<sup>-1</sup> gypsum and 5 different PAM products on soil 8. For each PAM concentration, data points with different letters are significantly different ( $p = 0.05$ ). The “0” data point for PAM is graphed at 0.01 due to limitations in using a linear-log scale. 98

Figure 3.10 Turbidity reduction as a function of input PAM concentration with 50 mg L<sup>-1</sup> gypsum and 5 different PAM products on soil 8. For each PAM concentration, data points with different letters are significantly different ( $p = 0.05$ ). The “0” data point for PAM is graphed at 0.01 due to limitations in using a linear-log scale. 99

Figure 3.11 Turbidity reduction as a function of input PAM concentration with 100mg L<sup>-1</sup> gypsum and 5 different PAM products on soil 8. For each PAM concentration, data points with different letters are significantly different ( $p = 0.05$ ). The “0” data point for PAM is graphed at 0.01 due to limitations in using a linear-log scale. 100

Figure 3.12 Turbidity reduction by Superfloc A100 (7% charge density, 16 Mg mol<sup>-1</sup> molecular weight) alone and with gypsum at three different concentrations

for soil sample 11. The “0” data point for PAM is graphed at 0.01 due to limitations in using a linear-log scale.	101
Figure 3.13 Turbidity reduction by Superfloc A100 (7% charge density, 16 Mg mol <sup>-1</sup> molecular weight) alone and with gypsum at three different concentrations for soil sample 13. The “0” data point for PAM is graphed at 0.01 due to limitations in using a linear-log scale.	102
Figure 3.14 Turbidity reduction by Superfloc A100 (7% charge density, 16 Mg mol <sup>-1</sup> molecular weight) alone and with gypsum at four different concentrations for soil sample 1. The “0” data point for PAM is graphed at 0.01 due to limitations in using a linear-log scale.	103
Figure 3.15 Turbidity reduction by Superfloc A100 (7% charge density, 16 Mg mol <sup>-1</sup> molecular weight) alone and with gypsum at three different concentrations for soil sample 2. The “0” data point for PAM is graphed at 0.01 due to limitations in using a linear-log scale.	104
Figure 3.16 Turbidity reduction by Superfloc A100 (7% charge density, 16 Mg mol <sup>-1</sup> molecular weight) alone and with gypsum at three different concentrations for soil sample 4. The “0” data point for PAM is graphed at 0.01 due to limitations in using a linear-log scale.	105
Figure 3.17 Turbidity reduction by Superfloc A100 (7% charge density, 16 Mg mol <sup>-1</sup> molecular weight) alone and with gypsum at three different concentrations for soil sample 3. The “0” data point for PAM is graphed at 0.01 due to limitations in using a linear-log scale.	106
Figure A.1 X-ray diffraction patterns for phyllosilicate mineralogy of the fine clay fraction of soil sample 1. Numbers above peaks are d-spacings in nanometers.	111
Figure A.2 X-ray diffraction patterns for phyllosilicate mineralogy of the coarse clay fraction of soil sample 1. Numbers above peaks are d-spacings in nanometers.	112
Figure A.3 X-ray diffraction patterns for phyllosilicate mineralogy of the fine clay fraction of soil sample 2. Numbers above peaks are d-spacings in nanometers.	113
Figure A.4 X-ray diffraction patterns for phyllosilicate mineralogy of the coarse clay fraction of soil sample 2. Numbers above peaks are d-spacings in nanometers.	114

Figure A.5 X-ray diffraction patterns for phyllosilicate mineralogy of the fine clay fraction of soil sample 3. Numbers above peaks are d-spacings in nanometers.	115
Figure A.6 X-ray diffraction patterns for phyllosilicate mineralogy of the coarse clay fraction of soil sample 3. Numbers above peaks are d-spacings in nanometers.	116
Figure A.7 X-ray diffraction patterns for phyllosilicate mineralogy of the fine clay fraction of soil sample 4. Numbers above peaks are d-spacings in nanometers.	117
Figure A.8 X-ray diffraction patterns for phyllosilicate mineralogy of the coarse clay fraction of soil sample 4. Numbers above peaks are d-spacings in nanometers.	118
Figure A.9 X-ray diffraction patterns for phyllosilicate mineralogy of the fine clay fraction of soil sample 5. Numbers above peaks are d-spacings in nanometers.	119
Figure A.10 X-ray diffraction patterns for phyllosilicate mineralogy of the coarse clay fraction of soil sample 5. Numbers above peaks are d-spacings in nanometers.	120
Figure A.11 X-ray diffraction patterns for phyllosilicate mineralogy of the fine clay fraction of soil sample 6. Numbers above peaks are d-spacings in nanometers.	121
Figure A.12 X-ray diffraction patterns for phyllosilicate mineralogy of the coarse clay fraction of soil sample 6. Numbers above peaks are d-spacings in nanometers.	122
Figure A.13 X-ray diffraction patterns for phyllosilicate mineralogy of the fine clay fraction of soil sample 7. Numbers above peaks are d-spacings in nanometers.	123
Figure A.14 X-ray diffraction patterns for phyllosilicate mineralogy of the coarse clay fraction of soil sample 7. Numbers above peaks are d-spacings in nanometers.	124
Figure A.15 X-ray diffraction patterns for phyllosilicate mineralogy of the fine clay fraction of soil sample 9. Numbers above peaks are d-spacings in nanometers.	125
Figure A.16 X-ray diffraction patterns for phyllosilicate mineralogy of the coarse clay fraction of soil sample 9. Numbers above peaks are d-spacings in	

nanometers.	126
Figure A.17 X-ray diffraction patterns for phyllosilicate mineralogy of the fine clay fraction of soil sample 11. Numbers above peaks are d-spacings in nanometers.	127
Figure A.18 X-ray diffraction patterns for phyllosilicate mineralogy of the coarse clay fraction of soil sample 11. Numbers above peaks are d-spacings in nanometers.	128
Figure A.19 X-ray diffraction patterns for phyllosilicate mineralogy of the fine clay fraction of soil sample 13. Numbers above peaks are d-spacings in nanometers.	129
Figure A.20 X-ray diffraction patterns for phyllosilicate mineralogy of the coarse clay fraction of soil sample 13. Numbers above peaks are d-spacings in nanometers.	130

## List of Tables

	Page
Table 2.1 PAM products used in initial evaluation of PAM interactions.	63
Table 2.2 PAM products used in replicate testing for PAM interactions evaluation.	64
Table 2.3 PAM products used in mixed polymer evaluation.	65
Table 2.4 Properties for soils that had 98 to 99.7% reductions in suspension turbidity with PAM (2 mg L <sup>-1</sup> ).	66
Table 2.5 Properties for soils that had diminished turbidity reduction at PAM concentrations greater than 1 mg L <sup>-1</sup> .	67
Table 2.6 Properties for soils that had a little flocculation with PAM at lower concentrations (< 1 mg L <sup>-1</sup> ), but flocculated at higher PAM concentrations.	68
Table 2.7 Properties for soils that had a little or no flocculation with any single component PAM. APS705 (commercially mixed) PAM was the only effective polymer.	69
Table 2.8 Stepwise regression results on the effect of soil properties on PAM (Superfloc A100) effectiveness for soil samples with kaolinite as the dominant clay mineralogy. All other soil properties were not significant at p = 0.05.	70
Table 2.9 Summary of individual regression analysis on the effect of soil properties on PAM effectiveness (Superfloc A100) for soil samples with kaolinite as the dominant clay mineralogy.	71
Table 2.10 Stepwise regression results on the effect of soil properties on PAM effectiveness (Superfloc A100) for soil samples with > 20% smectite or vermiculite clay mineralogy. All other soil properties were not significant at p = 0.05.	72
Table 2.11 Summary of individual regression analysis on the effect of soil properties on PAM effectiveness (Superfloc A100) for soil samples with > 20% smectite or vermiculite clay mineralogy.	73
Table 2.12 Stepwise regression results on the effect of soil properties on PAM effectiveness (Superfloc A100) for all 13 NC DOT soil samples. All other soil properties were not significant at p = 0.05.	74

Table 2.13 Pearson correlation coefficients for sand correlation to all other soil properties.	75
Table 2.14 Summary of individual regression analysis on the effect of soil properties on PAM effectiveness (Superfloc A100) for all 13 NC DOT soil samples.	76
Table 3.1 Comparison of the amount of smectite and vermiculite in the clay fraction of recalcitrant soils (1, 2, 4, 6, 7) with soils that had turbidity reductions (with PAM) that met the 50 NTU standard (5, 9, 11, 13).	107
Table 3.2 Properties of PAM products used in gypsum evaluation. All polymers except SF A100 were used in replicate testing (soil 8).	108
Table 3.3 Table comparing the soil properties of the four Coastal Plain soils.	109
Table A.1 Average NTU readings for soils with the most effective flocculation with PAM. For each PAM concentration, data points with different letters are significantly different ( $p = 0.05$ ).	131
Table A.2 Average NTU readings for soils with diminished turbidity reduction at high PAM concentrations. For each PAM concentration, data points with different letters are significantly different ( $p = 0.05$ ).	132
Table A.3 Average NTU readings for soils with little flocculation at low PAM concentrations. For each PAM concentration, data points with different letters are significantly different ( $p = 0.05$ ).	133
Table A.4 Average NTU readings for soils with minimal PAM effect (except APS705). For each PAM concentration, data points with different letters are significantly different ( $p = 0.05$ ).	134
Table A.5 Statistical significance of flocculant treatment by gypsum concentration for soil 8 (lsd $\alpha = 0.05$ ).	135
Table A.6 Statistical significance of gypsum concentration by PAM concentration for soil 8 (lsd $\alpha = 0.05$ ).	136

## Introduction

Eroded soil discharged from construction sites is a major water quality issue. Erosion from construction sites accounts for approximately  $5.4 \times 10^8$  Mg yr<sup>-1</sup> solids discharged into surface waters (Przepiora et al., 1998). Sediment carried from construction sites causes increases in the turbidity of natural waters. This turbidity keeps sunlight from penetrating into water by both reflecting and absorbing light. In slow moving water, light absorption causes increases in water temperature and decreases of oxygen mixing into deeper waters. Reduction in light decreases the growth of benthic macrophytes. High turbidity waters also have reduced aquatic plant (phytoplankton) growth. Decreased phytoplankton growth reduces the food source for zooplankton and fish larvae. Turbidity can also have negative effects on normal fish hatching. Direct, lethal effects on adult fish are rarely seen, but high levels of suspended solids are associated with gill damage and abrasion (Clark et al., 1985). Rainbow trout (*Salmo gairdneri*) develop a higher incidence of fin rot when exposed to high turbidity waters for several months. In general, fish populations are indirectly reduced because of high turbidity by: 1) decreased food supply, 2) destruction of habitat, and 3) decreased reproductive success (Clark et al., 1985).

In 1973 North Carolina enacted one of the nation's strictest sediment and erosion control plans (Burby et al., 1990). According to the sediment and erosion control act of 1973, any construction site that disturbs greater than one acre must have an erosion control plan and have the erosion control measures in place 15 working days after land is disturbed (NC DENR, 2002). The primary goal of the act is to keep sediment within the boundaries of construction sites. Out of 128 constructions sites evaluated in North Carolina in 1990, Burby et al. (1990) deemed 39% as keeping sediment on site. Thirty-three percent allowed serious



(>0.85 m<sup>3</sup>) levels of sediment to leave sites. A large portion of sediment losses could have been controlled by proper placement and maintenance of sediment control measures, but it was believed that “Part of the sedimentation problem obviously cannot or, for economic reasons, should not be prevented from occurring. For example, some particles are too fine to be captured in entrapment devices” (Burby et al., 1990). Fennessey and Jarrett (1994) also stated that runoff containing more than 20% of soil particles finer than 20 µm (fine silt) would require chemical flocculation to meet desired discharge water quality. Line and White (2001) evaluated three temporary sediment traps with rock outlets in the North Carolina Coastal Plain and Piedmont regions. They found that sediment traps retained only 21 to 40% of clay and 43 to 72% of silt.

N.C. Administrative Code 15ANCAC 02B .0211 requires that the turbidity of discharged waters from construction sites to non-trout streams or reservoirs not exceed 50 nephelometric turbidity units (NTU) and not exceed 10 NTUs in trout waters. However, the code also states that “compliance with this turbidity standard can be met when land management activities employ Best Management Practices (BMPs) . . . recommended by the Designated Nonpoint Source Agency (North Carolina Sediment Control Commission)” (NC DENR, 2002).

In October 2000, there was a case in Jackson County, NC where the development of a golf course led to down-stream damage of a lake due to high turbidity discharge. The golf course developer being sued had followed an erosion control plan that was certified by the Department of Water Quality (DWQ). It was decided before an Administrative Law Judge that the Department of Environment and Natural Resources (DENR) had erroneously interpreted the turbidity standard in a manner that allows water quality standards to be

violated so long as sedimentation control BMPs are being followed. The ruling cast doubt on the validity of the turbidity standard. However, in conclusion to the issue, the staff of DWQ recommended that the current turbidity standard be retained, but improvements in BMP design and ground cover requirements were needed (Ross and Gardner, 2002).

Przepiora et al. (1997) evaluated the turbidity of two sedimentation basins in urban construction sites in the North Carolina Piedmont. Over a twelve-month period turbidity readings of discharged water always exceeded 50 NTU ranging from 120 to 3200 NTU. Przepiora et al. (1998) concluded that more effective technologies for removing suspended solids would have to be found to reach the turbidity requirements set forth in NC Administrative Code 15 ANCAC 02B .0211.

Since the 1970s polyacrylamide (PAM) has emerged as an effective soil erosion amendment (Orts et al., 1999). The majority of PAM produced is used in industry (Fig. 1.1) in multiple applications of water treatment as a flocculant. Sojka and Lentz (1997) found PAM to be an excellent flocculant for silt and clay particles that were dispersed in furrow irrigation. Water treated with PAM (5-20 mg L<sup>-1</sup>) caused soil to settle to the furrow bottom. PAM technology could potentially help keep construction site discharge to the high water quality requirements set by North Carolina and other states.

## **PAM Background**

PAM is a water-soluble synthetic polymer. There are three types of PAM, each having different charge characteristics. A unique chemical reaction is used to produce each type of PAM. The three types of PAM are: cationic, nonionic and anionic. All of the PAM types are used in water treatment, but due to unique properties they each have slightly different applications. The degree of negative (or positive) charge that PAM has is called the charge density. In anionic PAM, charge density is defined by the degree of hydrolysis; i.e., the percentage of OH<sup>-</sup> groups substituted for NH<sub>2</sub> groups on the polymer during polymerization (Green et al., 2000). In cationic PAM, the charge density is the percent of positively charged units in the polymer (Fig. 1.2).

Cationic PAM is used mainly as a flocculant for sewage sludge and various industrial wastes (Barvenik, 1994). Cationic PAM may have adverse effects on aquatic life and presently is not used in erosion control (Goodrich et al., 1991; Sojka and Lentz, 1997).

Nonionic PAM is used as a flocculant in solid-liquid separations, usually as an aid to primary coagulants such as aluminum and iron salts. Nonionic PAM is also used in erosion control, although in limited applications (Barvenik, 1994). Nonionic PAM is actually slightly anionic (1-2 % charge density) due to the hydrolysis of acrylamide units during the manufacturing process (Barvenik, 1994). Figure 1.3 shows the polymerization reaction for nonionic PAM.

The majority of anionic PAM is used in water treatment and industrial wastewater treatment (Barvenik, 1994). Since the 1970s there has been increased use of anionic PAM as a soil amendment for erosion control (Orts et al., 1999). However, erosion control (agriculture) applications only account for 2 % of all PAM produced. High molecular weight

(mw) anionic PAM (12—18 Mg mol<sup>-1</sup>), with a charge density ranging from 7 to 50 is typically used in erosion control (Orts et al., 1999). Anionic PAM is commonly produced (Fig. 1.4) by copolymerization of acrylamide and acrylic acid (or a salt of acrylic acid) (Barvenik, 1994). Figure 1.5 illustrates the molecular structure of anionic PAM.

PAM is typically purchased as a dry powder. Dry PAM has active polymer concentrations of 75 to 90 %, the remainder being water, processing aids, and buffers (Barvenik, 1994). PAM is most efficient and effective if dissolved in water before application to soil (Lentz and Sojka, 1994; Nadler et al., 1994). When mixing PAM solutions, PAM should always be added to water that is stirred or agitated (water should never be added to PAM) (Sojka and Lentz, 1997). The polymer solution must be rapidly agitated for at least 30-60 minutes for dry granular PAM to be thoroughly dissolved (Barvenik, 1994). Higher molecular weight PAMs require more time to dissolve and the solutions are more viscous (Levy and Agassi, 1995). Anionic PAM with a molecular weight between 15-20 Mg mole<sup>-1</sup> forms extremely viscous solutions above 1-2% PAM concentrations (Barvenik, 1994). PAM is soluble in cold water, and heating does not increase the rate of dissolution (Montgomery, 1968). Pumping liquid PAM solutions may shear PAM molecules, reducing its viscosity and reducing its effectiveness to bridge soil particles in suspension (Bjorneberg, 1998).

## **Flocculation**

Flocculation occurs when PAM binds (bridges) between multiple soil particles in suspension. Polymers need to be of a high molecular weight to successfully bridge multiple soil particles (Gregory, 1989; Laird, 1997; Green et al., 2000). High molecular weight PAM is long enough to bind to multiple soil particles, with 15 Mg mole<sup>-1</sup> PAM being approximately 10µm in length (Orts et al., 1999). Bridging occurs best when polymer adsorption leaves a significant portion of the polymer in the aqueous phase. This allows multiple particles to bind to the same polymer chain (Gregory, 1989). In the case of excess polymer adsorption, bridging is prevented because insufficient free particle surface for bridging is available. Flocculation by bridging leads to larger, more stable aggregates than flocs formed through the reduction of the electrical double layer by addition of salts. Colloid scientists usually refer to aggregation caused by reduction of double-layer repulsion and charge neutralization as coagulation and flocculation as aggregation caused by polymer bridging (Gregory, 1989; Helalia and Letey, 1988; Laird, 1997). PAM desorption from soil particles is thought to be very limited because of the small probability that all polymer segments could detach simultaneously (Nadler and Letey, 1989; Theng, 1982).

Cationic, nonionic and anionic PAMs are hypothesized to have unique binding mechanisms to soil particles. The major binding mechanism of cationic PAM is electrostatic (coulombic) interactions between positively charged trimethyl ammonium groups on the polymer and negative clay surfaces (Aly and Letey, 1988; Helalia and Letey, 1988; Theng, 1982; Ben-Hur, 1992). Aly and Letey (1988) observed a decrease in cationic PAM adsorption to soil as electrolyte concentration of soil suspensions increased. They concluded that the decrease in cationic adsorption was due to cation competition with PAM for the

electrostatic bonds. In addition Laird (1997) showed a large release of exchangeable  $\text{Ca}^{2+}$  with reaction of cationic PAM to  $\text{Ca}^{2+}$  saturated soil. Cationic PAM both coagulates and flocculates suspended solids by: 1) decreasing particle repulsion and 2) increasing bridging between clay particles (Aly and Letey, 1988).

Nonionic PAM tends to coil in aqueous systems rather than form a chain, which may decrease its ability to bind to multiple soil particles (Laird, 1997; Helalia and Letey, 1988; Theng, 1982). Theng (1982) and Ben-Hur (1992) hypothesized that entropy is the driving force for nonionic PAM binding to soil particles. PAM adsorption on clay surfaces generally leads to desorption of solvent molecules. Desorption of these molecules increases the entropy (disorder) of the solution (universe). Natural systems (including PAM/soil suspensions) move from conditions of low to high entropy (Theng, 1982). Amide nitrogens are also thought to be involved in the binding of nonionic PAM to clay surfaces. Although nonionic PAM exists as a random coil in solution, it is believed to extend into the aqueous phase during adsorption. Theng (1982) reported that an average of 60% of nonionic polymer chains extend into the aqueous phase, which are available to bridge between multiple soil particles. Nonionic PAM along with cationic forms of PAM is believed to be able to enter into the interlayer space of 2:1 clays, whereas anionic polymers cannot (Theng, 1982; Ben-Hur et al., 1992).

Intramolecular electrostatic repulsion extends anionic polymers. Anionic PAM is generally more effective for flocculation and stabilization of soil particles than nonionic polymers because of enhanced particle bridging due to greater polymer extension (Laird, 1997). Although anionic PAM is expected to extend in solution, polymers with charge densities of 40% or greater tend to coil around cations in solution (Malik, 1991).

There are many possible mechanisms for anionic PAM adsorption to soil particles. The mechanisms involved in the flocculation of 1:1 clays and those involving 2:1 clays are hypothesized to be different. Some of the binding mechanisms proposed for 1:1 clays (kaolinite) are: 1) hydrogen bonding (Laird 1997), 2) ligand exchange (Aly and Letey 1988; Theng 1982), 3) anion exchange (Peng and Di 1994; Theng 1982), 4) hydrophobic bonding (Laird 1997), and 5) cation bridging (Laird, 1997; Aly and Letey, 1988). Mechanisms proposed for 2:1 clays (vermiculite, smectite) are: 1) cation bridging (Laird, 1997; Aly and Letey, 1988) and 2) van der Waals forces (Laird, 1997; Shainberg et al., 1990).

Adsorption of negatively charged PAM to any mineral surface is most often attributed to cation bridging (Laird, 1997; Ben-Hur et al., 1992; Aly and Letey, 1988; Nadler and Letey, 1989, Theng, 1982; Green et al., 2000; Orts et al., 1999; Sojka and Lentz, 1997). Multivalent cations act as bridges between the anionic groups (carboxyl) of the polymer and the negative clay surfaces. In the presence of electrolytes the thickness of the diffuse double layer at the clay and polymer surfaces is suppressed, resulting in decreased repulsive forces and greater polymer adsorption (Shainberg and Levy, 1994).

Shainberg et al., (1990) hypothesized that there are two different types of cation bridging between polymers and soil. The first type is an interaction between anionic groups of the polymer with an exchangeable cation through a water molecule to yield an “outer-sphere” complex. This mode of interaction happens in aqueous solutions. The second type is cation bridging between anionic groups of the polymer in direct association with exchangeable cations in the soil to form an “inner-sphere” complex. The drying of a soil induces inner-sphere complex formation (Shainberg et al, 1990). The adsorption of PAM onto soil constituents is irreversible when the system is allowed to dry because the short-

range van der Waals force holds them together (Zang and Miller, 1996; Laird, 1997; Letey, 1994).

Cation bridging may be the major mechanism in the adsorption of PAM to 2:1 clays, but other mechanisms may be more instrumental in the adsorption of PAM to kaolinitic clays (Laird, 1997). Peng and Di (1994) found that the addition of  $\text{Ca}^{2+}$  and  $\text{Al}^{3+}$  to kaolinite suspensions containing PAM decreased clay flocculation. They hypothesized that if cation bridging is the main adsorption mechanism, then the addition of multivalent cations should have increased the flocculation of soil particles. They also observed that the density of PAM adsorption on edges was much higher than on faces. Peng and Di (1994) attributed adsorption of PAM to edge faces to hydrogen bonding between polymer amide groups and exposed oxygen of kaolinite surfaces. Theng (1982) stated that under acidic conditions, anionic polymers could adsorb to clays by either anion exchange or ligand exchange. Because kaolinite ion exchange capacity is pH dependent, under acidic conditions it can exhibit anionic exchange, or positive surface charge, attracting anionic PAM. Ligand exchange would occur when the anionic carboxylic group on the polymer enters the inner coordination layer of edge aluminum to form a coordination complex. The final hypothesized binding mechanism between PAM and kaolinite is hydrophobic bonding (Laird, 1997). This occurs when the carbon backbone (nonpolar) of PAM forms a van der Waals bond with the basal (uncharged siloxane) surface of kaolinite (Laird, 1997).



## **Environmental Issues**

The issues associated with the release of PAM into the environment are quite different for the cationic forms compared to the nonionic or anionic forms. For this reason, they will be discussed separately.

Cationic PAM is not currently used in environmental applications because of its toxicity to fish. Cationic PAM binds to negatively charged fish gills, resulting in suffocation (Sojka and Lentz, 1997; Goodrich et al., 1991). Low concentrations of cationic PAM (0.3-10 mg L<sup>-1</sup>) are known to cause damage to fish and invertebrates (Barvenik, 1994). However, under environmental conditions, it is possible the toxicity would be largely mitigated. Because PAM irreversibly binds to soil particles (Letey, 1994; Seybold, 1994; Zang and Miller, 1996), it is conceivable that limited or no toxicity to fish occurs under typical conditions found on construction sites due to the high concentrations of suspended sediment.

Most testing of PAM toxicity has been performed in distilled water, which does not accurately describe cationic PAM toxicity in natural environments (McCollister et al., 1965; Biesinger et al., 1976). Goodrich et al. (1991) found that the addition of 5 mg L<sup>-1</sup> humic acid to distilled water decreased fish toxicity of cationic PAM seven to sixteen fold. Limited laboratory studies have been done on the effectiveness of cationic PAM as an amendment for erosion control (Aly and Letey, 1988; Helalia and Letey, 1988; Laird, 1997; Letey, 1994). Cationic polymers have shown greater adsorption to clays than the anionic and nonionic types and may be more effective as a flocculant to reduce turbidity of soil suspensions (Letey, 1994; Malik and Letey, 1991; Barvenik, 1994). However, further testing reflecting the normal range of environmental conditions will need to be done before cationic PAM is accepted for use in environmental applications.

Anionic and nonionic forms of PAM are nontoxic to fish (Seybold, 1994). However, the potential for the introduction of residual monomer acrylamide in PAM applications is one area of concern. Acrylamide is a known neurotoxin and carcinogen to humans and has a LD<sub>50</sub> (mammals) between 110 and 280 mg kg<sup>-1</sup> body weight (Seybold, 1994). By US law (From Sojka and Lentz, 1997: "Products (PAM) labeled for sale in the USA as erosion polymers are formulated to the same EPA and FDA standards as those used in potable water treatment and for food processing and packaging uses. By US law, they may contain no more than 0.05% monomer.") the concentration of residual acrylamide in PAM cannot exceed 0.05% (Sojka and Lentz, 1997; Barvenik, 1994). Wallace and Wallace (1986) found typical acrylamide concentrations in PAM to be below 0.0002%. Even with such low concentrations of acrylamide in PAM, it is still a major source of acrylamide released into the environment (Abdelmagid and Tabatabai, 1982). However, acrylamide is biodegradable and does not accumulate in soils. At ambient temperatures the half-life of acrylamide in soil ranged from 18 to 45 hours when added at 25 mg kg<sup>-1</sup> (Lande et al., 1979). Abdelmagid and Tabatabai (1982) demonstrated that acrylamide is hydrolyzed, releasing NH<sub>4</sub><sup>+</sup> under various soil conditions. Dry beans (*Phaseolus vulgaris*), sugarbeet (*Beta vulgaris* L.), and corn (*Zea mays* L.) treated with 1120 kg ha<sup>-1</sup> PAM (50-100 times normal application) showed no detectable acrylamide monomer in the tissues (Sojka and Lentz, 1997).

PAM exhibits low toxicity in mammals (Barvenik, 1994). McCollister et al. (1965) examined workmen from PAM production plants over five years and found no health effects associated with PAM inhalation. An additional study of unintentional occupational exposure to PAM indicated that there was no association with tumors, suggesting that residual monomer acrylamide (carcinogen) is not a major concern (Stephens, 1991). PAM

degradation in soil systems is approximately 10% per year primarily through shear-induced chain scission and photodegradation. However, degradation does not produce the monomer acrylamide due to the removal of the amine group from the polymer backbone (hydrolysis) (Orts et al., 1999; Barvenik, 1994; Abdelmagid and Tabatabai, 1982). Aqueous solutions of PAM may provide a substrate for mold growth if nutrients are present, although PAM degradation does not occur due to microbial attack (Montgomery, 1964). PAM has not been shown to have any negative effects on plant growth or nutrition and is safe to use as a soil amendment (Barvenik, 1994; Sojka and Lentz, 1997).

Increase in PAM solution viscosity is another potential environmental issue. PAM solution viscosity increased 5% for every 10 mg L<sup>-1</sup> increase in PAM concentration for a PAM product with a molecular weight of 15 Mg mol<sup>-1</sup> and an 18% charge density (Bjorneberg, 1998). A 2,500 mg L<sup>-1</sup> solution of PAM (30 % c.d., high m.w.) caused death in 100% of fish population, probably due to solution viscosity (McCollister, 1965). This concentration is 125-500 times that used in agriculture applications to irrigation water (Orts et al., 1999).

The environmental benefits of PAM are much greater than the possible risks involved with its use. Lentz and Sojka, (1994) showed that PAM treatment generally improved furrow discharge water quality. Compared with the controls, PAM treatment reduced losses of ortho-phosphate, nitrates, and biological oxygen demand (BOD) by 30%; total-phosphorus by 47%; and total sediment by 58% (Lentz and Sojka, 1994). Lentz et al., (1998) found ortho-P and total-P concentrations in control discharge to be five to seven times that of PAM treated furrow irrigation (10 mg L<sup>-1</sup> PAM concentration).

Additional environmental benefits from PAM use come from the reduction of the degradation of natural waters due to sediment pollution. Some of the environmental problems associated with sediment in water are: 1) benthic communities damaged by sediment blanketing community, 2) high turbidity reduces both plankton and aquatic plant production, 3) nutrients attached to sediment lead to the eutrophication of surface waters, 4) increase in turbidity affects light penetration and can decrease oxygen concentration and increase water temperature (Clark et al., 1985). Environmental benefits also include economic benefits resulting from decreased damage caused by sediment pollution.

## References

- Alley, S.M. and J. Letey. 1988. Polymer and water quality effects on flocculation of montmorillonite. *Soil Sci. Soc. Am. J.* 52:1453-1458.
- Abdelmagid, H.M. and M.A. Tabatabai. 1982. Decomposition of acrylamide in soils. *J. Environ. Qual.* 11:701-704.
- Arora, H.S. and N.T. Coleman. 1979. The influence of electrolyte concentration on flocculation of clay suspensions. *Soil Sci.* 127:134-139.
- Barvenik, F.W. 1994. Polyacrylamide characteristics related to soil applications. *Soil Sci.* 158:235-243.
- Ben-Hur, M., M. Malik, J. Letey, and U. Mingelgrin. 1992. Adsorption of polymers on clays as affected by clay charge and structure, polymer properties, and water quality. *Soil Sci.* 153:349-356.
- Biesinger, K.E., A.E. Lemke, W.E. Smith, and R.M. Tyo. 1976. Comparative toxicity of polyelectrolytes to selected aquatic animals. *Polyelectrolyte Tox.* 48:183-187.
- Bjorneberg, D.L. 1998. Temperature, concentration, and pumping effects on PAM viscosity. *Trans. ASAE.* 41:1651-1655.
- Burby, R.J., E.J. Kaiser, M.I. Luger, R.G. Paterson, H.R. Malcom and A.C. Beard. 1990. A report card on urban erosion and sedimentation control in North Carolina. *Carolina Plan.* 16:28-36.
- Clark, E.H., J.A. Haverkamp, and W. Chapman. 1985. *Eroding soils: The off-farm impact.* The Conservation Foundation, Washington, DC.
- Fennessey, L.A.J., and A.R. Jarrett. 1994. The dirt in a hole: A review of sedimentation basins for urban areas and construction sites. *J. Soil Water Cons.* 49:317-323.
- Goldberg, S. and R.A. Glaubig. 1987. Effect of saturating cation, pH, and aluminum and iron oxide on the flocculation of kaolinite and montmorillonite. *Clays Clay Min.* 35:220-227.
- Goodrich, M.S., L.H. Dulak, M.A. Friedman, and J.J. Lech. 1991. Acute and long-term toxicity of water-soluble cationic polymers to rainbow trout (*Oncorhynchus mykiss*) and the modification of toxicity by humic acid. *Environ. Tox. Chem.* 10:509-515.
- Green, S.V., D.E. Stott, L.D. Norton, and J.G. Graveel. 2000. Polyacrylamide molecular weight and charge effects on infiltration under simulated rainfall. *Soil Sci. Soc. Am. J.* 64:1786-1791.

- Gregory, John. 1989. Fundamentals of flocculation. *Critical Rev. Environ. Control.* 19:185-230.
- Helalia, A.M. and J. Letey. 1988. Polymer type and water quality effects on soil dispersion. *Soil Sci. Soc. Am. J.* 52:243-246.
- Laird, D.A. 1997. Bonding between polyacrylamide and clay mineral surfaces. *Soil Sci.* 162:826-832.
- Lande, S.S., S.J. Bosch, and P.H. Howard. 1979. Degradation and leaching of acrylamide in soil. *J. Environ. Qual.* 8:133-137.
- Lentz, R.D. and R.E. Sojka. 1994. Field results using polyacrylamide to manage furrow erosion and infiltration. *Soil Sci.* 158:274-282.
- Lentz, R.D., R.E. Sojka, and C.W. Robbins. 1998. Reducing phosphorus losses from surface-irrigated fields: emerging polyacrylamide technology. *J. Environ. Qual.* 27:305-312.
- Letey, J. 1994. Adsorption and desorption of polymers on soil. *Soil Sci.* 158:244-248.
- Levy, G.J., and M. Agassi. 1995. Polymer molecular weight and degree of drying effects on infiltration and erosion of three different soils. *Aust. J. Soil. Res.* 33:1007-1018.
- Line, D.E., and N.M. White. 2001. Efficiencies of temporary sediment traps on two North Carolina Construction sites. *Trans ASAE.* 44:1207-1215.
- Malik, M., and J. Letey. 1991. Adsorption of polyacrylamide and polysaccharide polymers on soil materials. *Soil Sci. Soc. Am. J.* 55:380-383.
- McCollister, D.D., C.L. Hake, S.E. Sadek, and V.K. Rowe. 1965. Toxicologic investigations of polyacrylamides. *Tox. Applied Pharm.* 7:639-651.
- Montgomery, W.H. 1968. Polyacrylamide. *Water Soluble Resins.* Wayne, NJ.
- Nadler, A and J. Letey. 1989. Adsorption isotherms of polyanions on soils using tritium labeled compounds. *Soil Sci. Soc. Am. J.* 53:1375-1378.
- Nadler, A., M. Magaritz, and L. Leib. 1994. PAM application techniques and mobility in Soil. *Soil Sci.* 158:249-254.
- North Carolina Department of Environment and Natural Resources. 2002. Administrative code section 15ANCAC 02B .0211. Fresh surface water quality standards for class c waters. NC DENR, Div. Of Environmental Management, Raleigh, NC.
- Orts, W.J., R.E. Sojka, G.M. Glenn, and R.A. Gross. 1999. Preventing soil erosion with polymer additives. *Polymer News.* 24:406-413.

- Pang, F.F., and P. Di. 1994. Effect of multivalent salts-calcium and aluminum on the flocculation of kaolin suspension with anionic polyacrylamide. *J. Colloid Interface Sci.* 164:229-237.
- Przepiora, A., D. Hesterberg, J.E. Parsons, J.W. Gilliam, D.K. Cassel, and W. Faircloth. 1997. Calcium sulfate as a flocculant to reduce sedimentation basin water turbidity. *J. Environ. Qual.* 26:1605-1611.
- Przepiora, A., D. Hesterberg, J.E. Parsons, J.W. Gilliam, D.K. Cassel, and W. Faircloth. 1998. Field evaluation of calcium sulfate as a chemical flocculant for sedimentation basins. *J. Environ. Qual.* 27:669-678.
- Ross, W.G. Jr., C.H. Gardner. 2002. N.C. Division of Water Quality makes recommendations on turbidity standard. *Sediments.* 9:1,3.
- Seybold, C.A. 1994. Polyacrylamide review: soil conditioning and environmental fate. *Comm. Soil Sci. Plant Anal.* 11:767-834.
- Shainberg, I. and G.J. Levy. 1994. Organic polymers and soil sealing in cultivated soils. *Soil Sci.* 158:267-273.
- Shainberg, I., D.N. Warrington, and P. Rengasamy. 1990. Water quality and PAM interactions in reducing surface sealing. *Soil Sci.* 149:301-307.
- Sojka, R.E., and R.D. Lentz. 1997. Reducing Furrow Irrigation Erosion with Polyacrylamide (PAM). *J. Prod. Agric.* 10:47-51.
- Stephens, S.H. 1991. Final report on the safety assessment of polyacrylamide. *J. Am. Coll. Toxicol.* 10:193-202.
- Theng, B.K.G. 1982. Clay-Polymer interactions: summary and perspectives. *Clays Clay Min.* 30:1-10.
- Wallace, A. and G.A. Wallace. 1986. Effects of soil Conditioners on emergence and growth of tomato, cotton, and lettuce seedlings. *Soil Sci.* 141:313-316.
- Zhang, X.C. and W.P. Miller. 1996. Polyacrylamide effect on infiltration and erosion in furrows. *Soil Sci. Soc. Am. J.* 60:866-872.

Industry	Applications
Mineral and coal processing	Thickening and dewatering of concentrates and tailings Separation of coal fines and clay Purifying aluminum ores (Bayer process) Clarification of process steams Dispersants and antiscalants (low MW)
Petroleum production	Tertiary oil recovery Reservoir profile modification Well cementing Drilling muds
Paper making	Retention aids Dry strength aids (with alum) Dispersants (low MW) Drainage and dewatering aids
Water treating	Clarification, thickening and dewatering of wastewaters and sludges (commonly as flocculant aids to primary coagulants) Raw/potable water clarification (flocculant aid) Alum sludge dewatering Dispersants and antiscalants (low MW) Boiler and cooling applications Desalination Heavy metals removal (with pH adjustment)
Food processing	Washing fruits and vegetables Clarification of sugar juice and liquor Scale control in sugar production (low MW)
Miscellaneous applications	Superabsorbers (cross-linked PAMs) Chemical grouting Textile additives Friction reduction Adhesives Viscosity enhancement/gelling applications Laboratory applications Cosmetics

Figure 1.1 Industrial applications of anionic polyacrylamide (Barvenik, 1994).



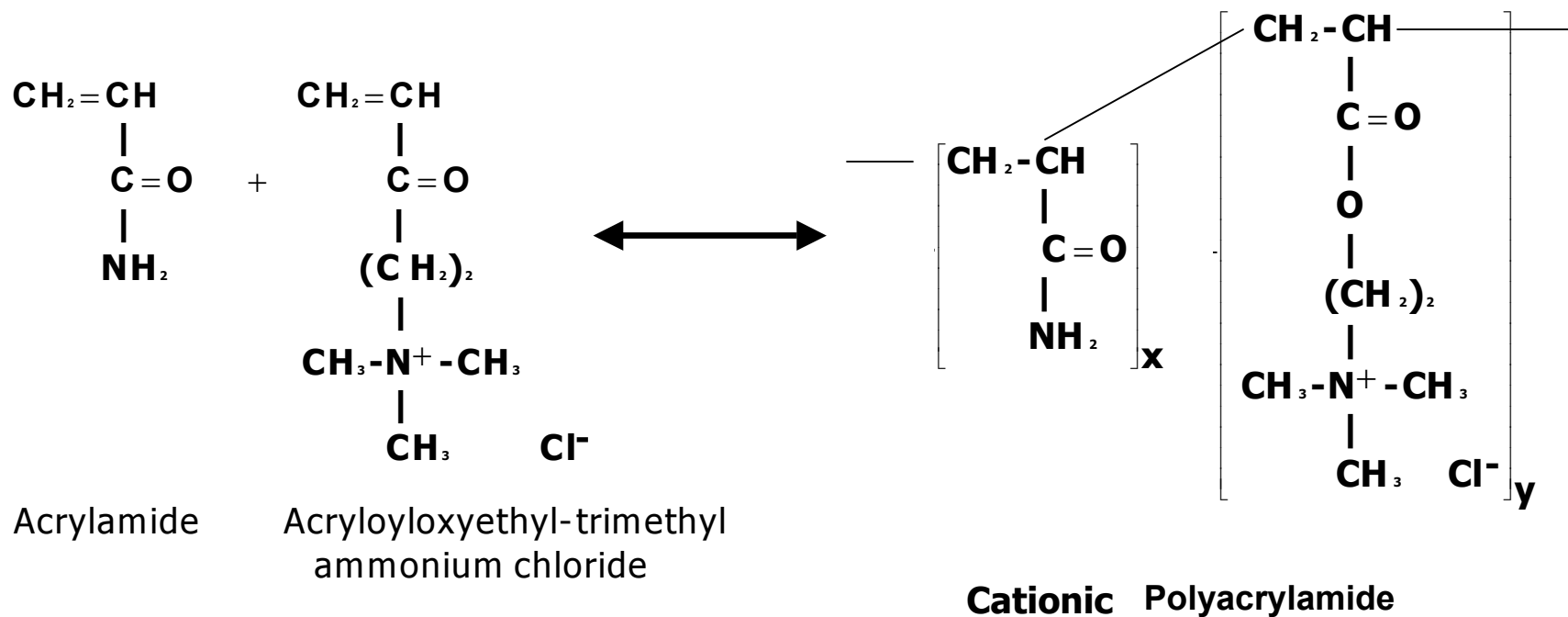
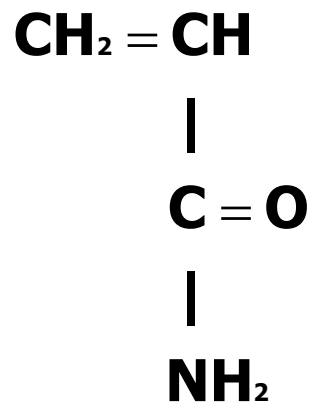
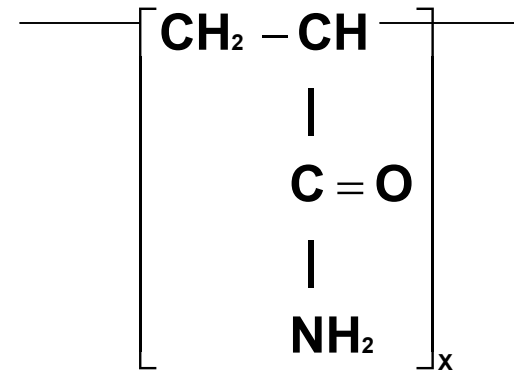


Figure 1.2 Copolymerization of acrylamide and acryloyloxyethyl-trimethyl ammonium chloride to form cationic PAM (Barvenik, 1994).



**Acrylamide**

Polymerization  
↔



**Nonionic  
Polyacrylamide**

Figure 1.3 Nonionic PAM polymerization (Barvenik, 1994).

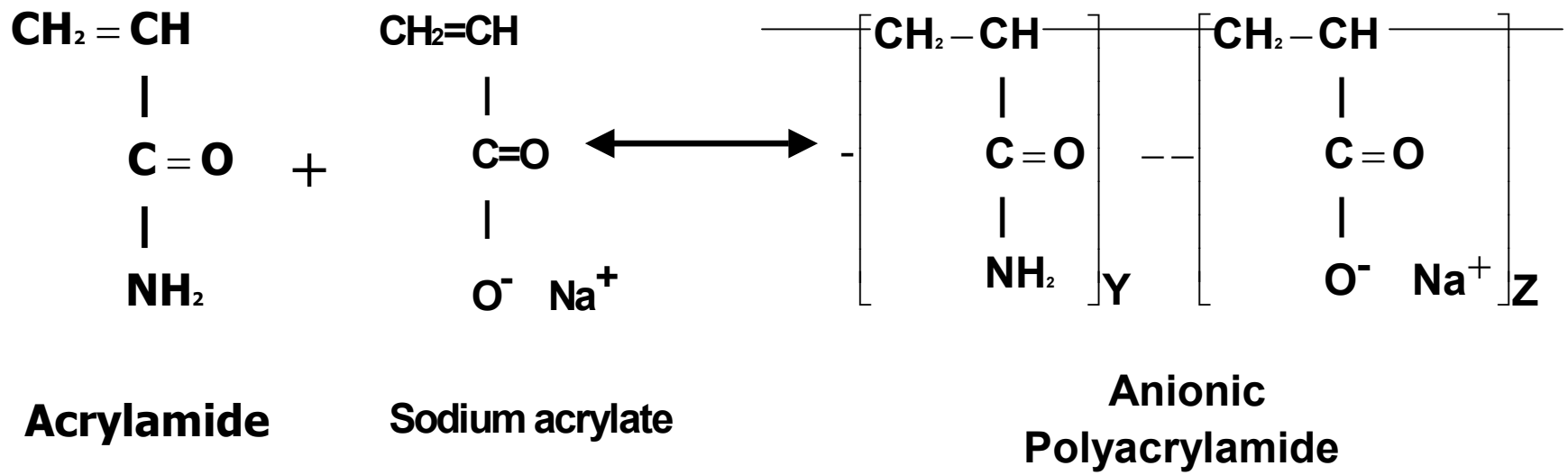


Figure 1.4 Copolymerization of acrylamide and sodium acrylate to form anionic PAM (Barvenik, 1994).

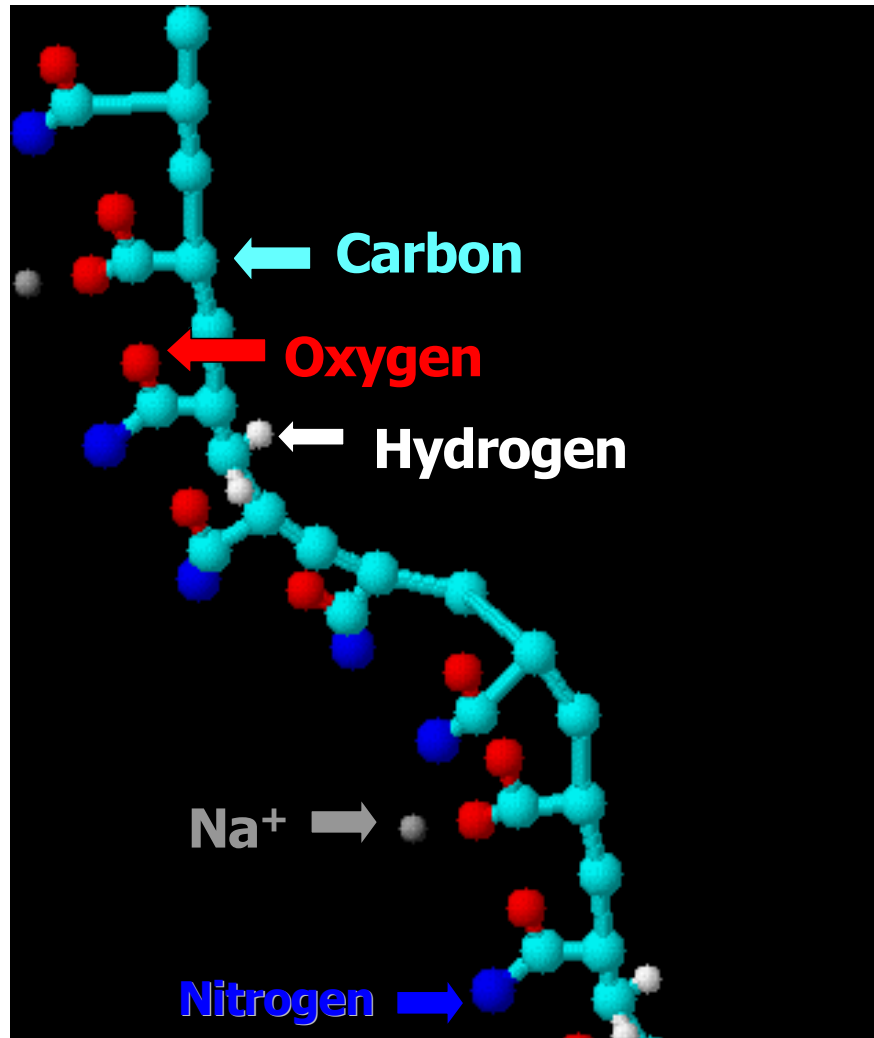


Figure 1.5 Molecular structure of anionic PAM.

# PAM Interactions

## Introduction

The effectiveness of PAM as a flocculant is affected by the characteristics of the soil being treated. Some of the characteristics that may be significant in adsorption and flocculation of soil particles by PAM are: 1) mineralogy, 2) exchangeable cations, 3) pH, 4) soil texture, 5) organic matter content, and 6) iron oxide content. In addition, how PAM interacts with individual soils may depend on the configuration of the PAM molecule itself (charge density and molecular weight).

Laird (1997) demonstrated that the efficacy of anionic PAM for clay flocculation varies with mineralogy (kaolinite > illite >> quartz). In addition, Ben-Hur et al. (1992) found adsorption of anionic PAM on illite 200 to 400 times greater than that of anionic PAM adsorption to smectite clays. Anionic PAM is highly effective in the acid kaolinite and acid illite systems (Laird, 1997). Arora and Coleman (1979) showed that the addition of small amounts of smectite, which they theorized might have deposited on positively charged clay edges of kaolinite, caused a significant increase in critical salt concentration values for kaolinite. Goldberg and Glaubig (1987) also showed that mixtures of kaolinite and montmorillonite behaved more like montmorillonite in coagulation experiments. Flocculation (with PAM) of soils containing mixtures of smectite and kaolinite would likely decrease compared to kaolinite soils alone. PAM adsorption to quartz is poor due to lack of aluminol groups ( $>Al-OH$ ), which are present on lateral edges of kaolinite and illite (Laird, 1997). Aluminol groups have a point of zero charge between a pH of 5 and 7. Under acidic conditions, edges of kaolinite and illite are positively charged, increasing adsorption of anionic PAM. Active sites on

quartz are silanol groups ( $>\text{Si—OH}$ ), which are neutral in acidic environments. The lack of positive charge sites, or divalent cations on quartz surfaces leads to poor adsorption of anionic PAM. Coleman et al. (1949) compared the clay mineralogy of seven soils typical of the Coastal Plain, Piedmont, and Mountain regions of North Carolina (Fig. 2.1). The greatest differences in mineralogy between regions were the increase of smectite (montmorillonite) and the absence of iron and aluminum oxides in the Coastal Plain. In addition Coleman et al. (1949) demonstrated that there were large differences in mineralogy within each region.

Cation bridging is believed to be a major mechanism of PAM adsorption, although it may not be as important in kaolinite. Divalent cations provide a bridge between negatively charged polymer and clay surfaces (Letey, 1994). Laird (1997) showed that soils saturated with  $\text{Ca}^{2+}$  resulted in greater flocculation with PAM than soils saturated by  $\text{Na}^+$ . Soils with divalent exchangeable cations will result in increased cation bridging and better flocculation with the addition of PAM (Nadler and Letey, 1989). The significance of divalent cations in solution or on exchange sites may differ according to soil mineralogy (Laird, 1997; Peng and Di, 1994).

Goldberg and Glaubig (1987) determined that the critical coagulation concentration of all tested clays, clay mixtures and oxides were pH dependent. The pH dependence of kaolinite was greater than montmorillonite, although a 50/50 mixture behaved more like montmorillonite. Peng and Di (1994) hypothesized that adsorption of anionic PAM to kaolinite is strongly dependent on pH. In contrast, adsorption of nonionic PAM on kaolinite was demonstrated to be independent of pH. Peng and Di (1994) found an optimal pH range of 5-7 with lower and higher pH levels leading to

decreased flocculation. Possible explanations for this phenomenon are that at low pH values PAM becomes protonated and neutralized. The neutralization of carboxyl groups on the polymer causes the polymer to coil on itself, decreasing its ability to bridge between soil particles. At higher pH values, kaolinite edge and surface charges become more negative, which increases repulsion of anionic PAM.

Soil texture is an important factor in the efficacy of PAM surface applications for erosion control (Green et al., 2000; Nadler et al., 1994; Miller et al., 1998). However, all articles that cited the importance of soil texture on PAM efficacy dealt with stabilization of soil aggregates and not flocculation. I hypothesize that the ratio of silt to clay may effect the flocculation of soil suspension with the addition of PAM, although not overall soil texture.

Kretzschmar et al. (1997) found that the removal of natural organic matter from clay reduced the stability of clay colloids in critical coagulation experiments with kaolinite soils. It was suggested that the effect of organic matter on colloidal stability was due to electrostatic and steric stabilization. The stabilizing effect of natural organic matter in coagulation experiments may not be the same as those with polymer interactions, although negatively charged organic matter would likely repel anionic polyacrylamide except at low pH (hydrophobic reactions) (Helalia and Letey, 1988; Nadler and Letey, 1989).

Little information is available on the interactions of iron oxides and PAM. Flocculation testing of soil suspensions using Georgia kaolinite, and Tumut illite found kaolinite to be significantly ( $p=0.05$ ) more effective in flocculation than illite (Laird, 1997). However, iron oxides were not removed before flocculation testing was

performed and they did not mention the iron oxide content of each soil. Theng (1982) stated that ligand exchange might be an important mechanism for anionic PAM binding. Iron oxides may be involved in flocculation with PAM if polymer carboxyl groups ( $\text{COO}^-$ ) exchange with hydroxyl groups ( $>\text{Fe-OH}$ ).

The objectives of this study were: 1) to evaluate the PAM-induced flocculation of soils from across NC having diverse soil characteristics that may have potential significance on PAM efficacy and 2) to evaluate which PAM types are most effective at flocculating soils of given mineralogical or chemical characteristics. Based on past studies the soil properties of interest were: exchangeable cations, mineralogy, pH, texture, organic matter (content), and iron oxide content.



## **Materials and Methods**

### **Soil Analysis**

Soil particle size analysis was completed by the hydrometer method (Gee and Bauder, 1986), after soil organic matter was removed by the addition of hydrogen peroxide (Day, 1965). Chemical dispersion was accomplished by the addition of Na-hexametaphosphate. An electric mixer was used for physical dispersion for a 5-minute duration on each soil sample. This analysis was performed on two samples from each soil and the values reported here are an average.

Clay mineralogy ( $< 2 \mu\text{m}$ ) was determined by x-ray diffraction analysis (Whittig and Allardice, 1986). Soils that had already received chemical and physical dispersement from the particle size analysis were used for mineralogical analysis determination (Kunze and Dixon, 1986). X-ray diffraction patterns were interpreted by measuring (integrating) the area under the curve of each clay mineral (smectite, vermiculite, mica, and kaolinite) in the Mg-glycerol saturated samples. The area of each clay mineral was divided by the total area of all clay minerals to give the percent of each clay mineral present in the soil.

Soil pH was determined using a pH electrode with distilled water and a 1:1 soil to water ratio. Two samples were used and an average pH value was reported.

Exchangeable cations and organic carbon content were determined in the North Carolina State University Soil Science Department Analytical Services lab. Minerals were extracted by the Mehlich-3 procedure and measured using an ICP-emission spectrometer (Mehlich, 1984). Two samples from each soil were given to the lab and average values are reported for each parameter.

Extractable soil iron was determined by ammonium oxalate and citrate-bicarbonate-dithionite (CBD) extraction. Ammonium oxalate extraction was done to determine the amount of amorphous and organically bound Fe. CBD extracts all forms of iron oxide (crystalline and noncrystalline)(Jackson et al., 1986).

Oxalate extractable iron was determined by measuring 0.15 g (0.3 g in gray soils) of soil in a 50 ml centrifuge tube. Thirty mL of oxalate extract was added to the soil and the tube was then covered in aluminum foil. All tubes were shaken for 2 hours on a reciprocating shaker. Samples were centrifuged at 15000 rpm for 15 minutes and the supernatant solutions were saved and Fe was measured by atomic absorption (AA) spectrometry (Jackson et al., 1986).

CBD extractable iron was determined by first weighing 1 g soil (3 g in gray soils) into 100 mL polypropylene centrifuge tubes. 50 mL of Na-citrate/bicarbonate solution was added to each tube, and the tubes were heated (75-80 °C) in a water bath while adding a total of 2 g Na-dithionite over a 15 minute time period. Saturated NaCl solution was then added to promote flocculation. Samples were centrifuged for 5 minutes at 2000 rpm and Fe was measured by AA spectrometry (Jackson et al., 1986).

## **PAM Interactions**

Thirteen soil samples were provided by the North Carolina Department of Transportation (NCDOT) from active construction sites within 13 of their 14 geographic divisions (Fig. 2.2). This provided a fairly comprehensive range of materials representing North Carolina sediment sources. The samples were taken from subsoils, which were exposed during the grading process, although the original depths are not known. Soil samples were allowed to air-dry, after which they were ground with a mortar and pestle until they passed through a 2-mm sieve.

We evaluated 11 PAM products which had a wide range in molecular weight and charge density. The molecular weight of the polymers ranged from 14 to 28 Mg mol<sup>-1</sup> and the charge density ranged from neutral to 50% molar charge (Table 2.1). Applied Polymer Systems (APS) PAM products contained a mixture of polymers containing different molecular weight and charge density. The PAM products used were: Superfloc 1606, A150, A150 HMW, A100, and N300 (Cytec Industries, West Patterson, NJ, USA), Chemtall 923 VHM (Chemtall Inc., Riceboro, GA, USA), Soilfix Polybead (Ciba Specialty Chemicals, Suffolk, VA, USA), and APS 702aa, 702b, 702c, and 730b (Applied Polymer Systems Inc., Woodstock, GA, USA). Initially, an evaluation of all polymers (11) with all soils (13) was performed (Table 2.1; Fig 2.3).

The flocculation tests involved suspending soil in water, adding PAM, and then measuring the turbidity of the soil solution after a short amount of time. Five grams of soil were placed into a 100 mL specimen cup and 100 mL of distilled water was added. PAM was then added by pipette to bring the PAM concentration in the cup to a range of concentration from 0 to 10 mg PAM L<sup>-1</sup>.

All PAM used in the evaluation was received in granular form. Stock solutions containing PAM (0.1% w/w) were made by slowly adding the PAM to a flask of stirring, distilled water and mixing for at least 24 hours at room temperature. Each soil suspension with PAM was shaken for 10 seconds (no previous physical or chemical dispersion) and placed on the lab bench to settle under gravity. Twenty seconds after shaking, a nephelometer (Analite 152, McVan Instruments, Mulgrave, Australia) probe was inserted into the solution and a nephelometric turbidity (NTU) reading was taken 10 seconds later at a depth between 10 and 38 mm.

After an initial flocculation screening with each soil and all 11 PAMs, the four or five best flocculants for each soil were chosen for replicated testing (Table 2.2). The criteria for the selection of the best PAM were a combination of the greatest turbidity reduction and the lowest concentration of polymer needed to decrease turbidity. Cytec Industries A110 (SF A836) is commonly used in erosion control and was included in replicate testing (Orts et al., 1999). Applied Polymer Systems 705 was used in replicate testing instead of other (702aa, 702b, 702c, 705, and 730b) commercially mixed polymers. These experiments used the same procedure as is described for the screening tests, but with three treatment replicates.

Soil characteristics were evaluated as potential indicators of the relative effectiveness of PAMs in reducing turbidity. Stepwise multiple regression (SAS Institute, Cary, NC) analysis was performed on soil turbidity reduction for one PAM product (Cytec Superfloc A100).

The binding mechanisms for smectite and vermiculite are different than those for soils with kaolinite and smectite (Laird, 1997; Peng and Di, 1994). Soils were grouped

according to soil mineralogy for initial statistical analysis. Soils that had less than 20% smectite or vermiculite in either the fine or coarse clay fraction with dominant kaolinite clay mineralogy were grouped together (sample 5, 9, 11, 12, 13, 14). Soil samples 1, 2, 3, 4, 6, and 7 all had greater than 20% smectite or vermiculite in either the fine or coarse clay fraction. Arora and Coleman demonstrated that raising the smectite fraction in a smectite/kaolinite from 15 to 20% caused the greatest increase in critical salt concentration (85-270 meq L<sup>-1</sup>). These soils would likely to react more like smectite (or vermiculite) than kaolinite (Arora and Coleman, 1979). Multivariate analysis (stepwise regression analysis) for soil properties (texture, exchangeable cations, pH, organic carbon, Fe oxide) was performed for each group of soils. The dependant variable, named  $\ln p_{ct}$ , in the experiments was equal to the  $\log (100 * ((\text{initial turbidity} - \text{final turbidity}) / \text{initial turbidity}))$ .

## Mixed Polymers

The mixed PAM product APS 705 was often the most effective in reducing turbidity, but we do not know what PAMs are in the formulation. We designed a series of experiments to determine if the results could be replicated using a mixture of PAMs having a variety of molecular weights and charge densities. We selected soil sample 4 from the Coastal Plain Region because it was the most recalcitrant in responding (flocculating) to single component PAMs but did respond to APS 705. The products used in the mixture were all from Cytec Industries (West Paterson, NJ, USA). The individual products mixed were Superfloc N300, A100, A150, N300LMW, A100LMW, and A150LMW. Polymers with a “LMW” suffix have a molecular weight of approximately  $4 \text{ Mg mole}^{-1}$ , and those products without the suffix have molecular weights approximately  $14\text{-}16 \text{ Mg mole}^{-1}$  (Table 2.3).

Combinations and single PAMs were used in this experiment to differentiate what parameters were significant in the evaluation. Treatments included: A100LMW, A150LMW, N300, A100 + A100LMW, A150LMW + N300, N300LMW + A150, and N300 + A150. Polymer mixtures contained 50% (w/w) of each polymer added. The treatments were intended to evaluate if the effectiveness of APS 705 was due to low molecular weight PAM alone, high molecular weight PAM alone, combined high and low molecular weight with the same charge density, or a combination of different molecular weights and charge densities. All PAM used in the evaluation was in granular form and was mixed with distilled water as described above. In the case of PAM mixtures, the PAM products were mixed in dry form before being added to water. The PAM mixture solutions were evaluated in flocculation experiments as described above.

## Results and Discussion

### Soil Analysis Properties

Soil textures ranged from sand to clay with soils ranging from 38 to 500 g kg<sup>-1</sup> clay, 30 to 390 g kg<sup>-1</sup> silt and 285 to 932 g kg<sup>-1</sup> sand (Tables 2.4-2.7). Dominant clay mineralogies were found to include smectite, vermiculite, kaolinite and mica. The pH ranged from 3.7 to 8.0 and organic carbon ranged from 0.9 to 7.2 g kg<sup>-1</sup>. Exchangeable Ca<sup>2+</sup> ranged from 0.1 to 9.0 cmol<sub>c</sub> kg<sup>-1</sup>, exchangeable Mg<sup>2+</sup> ranged from 0.1 to 1.3 cmol<sub>c</sub> kg<sup>-1</sup>, and sodium adsorption ratio (SAR) ranged from 0.2 to 1.9. Oxalate extractable iron ranged from 1.1 to 14.9 mmol kg<sup>-1</sup> and Citrate-Bicarbonate-Dithionite extractable iron ranged from 8.2 to 861.2 mmol kg<sup>-1</sup>. Most soil properties in NC DOT soil samples are representative of soil properties found throughout North Carolina (Daniels et al, 1999). These diverse properties were the focus of why flocculation of soil suspensions differed so greatly between NC DOT soil samples.

## **PAM Interactions**

Minimal turbidities were reached with PAM concentrations generally between 0.5 and 2 mg L<sup>-1</sup> with all PAM and soil combinations (Fig 2.4-2.16). In most cases, PAM reduced turbidity in soil suspensions. Soils varied greatly in terms of PAM flocculation efficiency with turbidity reductions ranging from 86 to 99.7% compared to untreated controls. Five soils had turbidity reductions of at least 98 % within 30 seconds, with three reaching the 50 NTU level and two dropping below 10 NTU (Fig. 2.4-2.8). In four soils (Fig. 2.8-2.11) turbidity declined to a minimum with increasing PAM concentration, then increased at concentrations greater than 1 mg L<sup>-1</sup>. Increasing the PAM concentration in these soils to 5 mg L<sup>-1</sup> caused diminished turbidity reduction. In three other soils (Fig. 2.12-2.14), PAM had no observable effect until the concentration exceeded 0.5 mg/L. At higher PAM concentrations these soils had turbidity reductions of 86, 91, and 97%, but only one of the soils met the 50 NTU standard. The final two soils (Fig. 2.15-2.16) exhibited little or no flocculation with single component PAMs. However, a commercially mixed PAM application (APS 705) reduced turbidity by 87% (Fig. 2.15-2.16).

Soils (samples 9, 5, 12, 13; Fig 2.4-2.7) that demonstrated the greatest turbidity reduction with PAM have several common soil properties (Table 2.4). They all were greater than 140 g kg<sup>-1</sup> clay and 220 g kg<sup>-1</sup> silt. Silt may be involved in the flocculation of clays. Clays bridged to silt particles by polymer chains will flocculate quicker than clay-to-clay flocculation. Montgomery (1965) stated that PAM will “integrate the finer particles with coarser particles” forming flocs which fall out of solution quicker than fine-to-fine particles. However, texture may not be the actual issue because all the soils



were from the Piedmont or Mountain Regions. The common feature with the Piedmont and Mountain soils is that they have much higher amounts of iron oxides than soils from the coastal plain (Coleman et al., 1949). These soils (5, 9, 12, 13) had the highest CBD extractable iron (304-761 mmol kg<sup>-1</sup>) of all soils tested, oxalate extractable values (7.7-20.4 mmol kg<sup>-1</sup>) were also relatively high (Table 2.4-2.7). The dominant clay mineralogy of these soils was kaolinite with between 68 and 90% kaolinite on both the fine and coarse clay fractions. Only three other soils (sample 6, 7, 11) tested had above 50% kaolinite in both coarse and fine clay fractions (Table 2.4-2.7). Laird (1997) stated that kaolinite soils have greater adsorption and flocculation than other soils, which the results of this study agree. Each of the soils had very low amounts of smectite or vermiculite clays (<12%) in either the fine or coarse clay fractions (Table 2.4). Low levels of exchangeable Ca<sup>2+</sup> and Mg<sup>2+</sup> (0.2-1.6 meq L<sup>-1</sup>) indicate that cation bridging may have limited affect on PAM binding to kaolinite clays. Each of the soils also has relatively low organic carbon (0.9-3.5 g kg<sup>-1</sup>), which may also be a factor to greater flocculation (Helalia and Letey, 1988; Nadler and Letey, 1989). Soil pH in these soils ranged from 5 to 5.6, which is within the optimal pH level for kaolinite clays (Peng and Di, 1994).

There are no apparent similarities between soils (11, 2, 7, 14) that have a diminished flocculation at high PAM concentrations. In each of these soils turbidity was reduced to a minimum level with PAM application at or near 1 mg L<sup>-1</sup>. At PAM concentrations higher than 1 mg L<sup>-1</sup> there was a negative effect from excess polymer adsorbed to the soil and remaining in solution. This can possibly be explained by two different mechanisms: 1) An increase in viscosity of the soil and polymer suspension, or 2) steric stabilization of the suspended soil particles (Gregory, 1989).

Viscosity is defined as the internal friction of a fluid due to molecular cohesion (Hillel, 1998). In other words, it is the ease that adjacent layers of a fluid slide over one another. Increasing the amount of polymer in solution increases the viscosity. Bjorneberg, (1998) demonstrated that PAM (SuperflocA110) solution viscosity increased 5% with every 10 mg L<sup>-1</sup> increase in PAM concentration. The 5% increase in viscosity would cause any flocculated sediment to fall slower out of suspension causing an increase in turbidity. Stokes law states that the time (t) a particle takes to fall in suspension is equal to:  $t = 18hn/(d^2g(p_s-p_f))$ . In my experiment height (h), particle diameter (d), acceleration of gravity (g), and particle density (p<sub>s</sub>) are constant, which means that viscosity (n) and fluid density (p<sub>f</sub>) are the only possible parameters that change. A 5% increase in viscosity leads to a 5% increase in the time required for particles to settle. A small increase in required settling time could cause a large increase in suspended particles due to the short settling time (30 s) in our flocculation experiment.

The second possible explanation for an increase in turbidity of high concentration PAM solutions is steric stabilization or repulsion (Lentz et al., 1996, Gregory, 1989). This occurs when excess polymer is adsorbed to particles and segments of polymer chains extend into the aqueous phase. Excessive polymer creates a thick layer around particles in suspension. This polymer layer makes the distance between individual soil particles large enough that van der Waals attraction may be too weak to cause adhesion and flocculation (Gregory, 1989). Sterically stabilized soil dispersions can be destabilized by changing the solvency of the medium for the stabilized chains. In some cases adding salts (especially sulfates) and increasing the temperature of the solution will cause flocculation (Gregory, 1989).

There were no unique soil properties associated with soils that exhibited a negative trend in turbidity reduction at high PAM concentrations. Therefore, I hypothesize that all soils will have diminished flocculation effectiveness at high PAM levels. However, the concentration that causes diminished flocculation effect varies considerably among soils. Peng and Di (1994) found maximum flocculation at 5 to 8 mg L<sup>-1</sup> PAM application with kaolinite soils. This optimal PAM application falls within the negative trend region for soil samples 2, 7, 11, and 14.

Soils 3, 6 and 8 all had limited soil flocculation at low PAM concentrations (<0.1). One explanation for the effect is the pH of the solutions. The pH values (7.4, 3.7, and 4.8) were all outside the optimal pH range (pH 5-7) proposed by Peng and Di (1994). PAM molecules may have coiled when H<sup>+</sup> ions in solution caused the protonation of carboxyl groups on the polymer making it less effective. At higher pH kaolinite edges become more negative leading to poor PAM adsorption. A second explanation is that these three soils have less silt (30, 70, and 130 g kg<sup>-1</sup>) than soils that had turbidity reductions at low PAM concentrations (Table 2.4-2.6). The clay to silt ratio was greater in these soils than in other soils which agrees with the statement that PAM will “integrate the finer particles with coarser particles” forming flocs which fall out of solution quicker than fine-to-fine particles (Montgomery, 1965).

Soils 1 and 4 had little or no flocculation with any of the single polymers. Both soils had high amounts of 2:1 clays (smectite and vermiculite), which may have caused poor flocculation (Laird, 1997). Highly dispersible clays (2:1 clays) with little silt (54 and 110 g kg<sup>-1</sup>) for PAM to bridge between may have caused an increase in the amount of fine-to-fine suspended aggregates which were not large enough to fall out of suspension

in our experiment. Both soils also had very low amounts of CBD extractable iron (8 and 18 mmol kg<sup>-1</sup>) compared with other soils. There was not a common reason for poor flocculation related to exchangeable cations or pH, because the soils have contrasting values for both. APS 705 worked significantly (tukey, p=0.05) better on both of these soils than all other PAM products (Fig. 2.15-2.16). There remains the possibility that mixtures of polymers may lead to better flocculation of recalcitrant soils than single polymers. Montgomery (1968) in reference to water treatment with anionic PAM stated that there are “many cases in which the nature of the suspended solids requires that a combination of flocculants be used”. It was not explained which suspended solid properties require combined treatment, although the use of polymer mixtures was used to obtain lower suspended solids.

## Statistical Analysis

Soils that have dominant kaolinite mineralogy (sample 5, 9, 11, 12, 13, 14) had three explanatory variables that were significant at the  $p = 0.05$  level. Approximately 48% of the variation in turbidity reduction was explained by the pH of the soils, with  $\text{Ca}^{2+}$  and CBD extractable iron attributing for 19 and 11% of the variation in turbidity reduction respectively (Table 2.8). These results agree with other research. In kaolinite soils high in iron oxides, flocculation is pH dependant (Goldberg and Glaubig, 1987; Peng and Di, 1994). The parameter estimate for pH (-9.46) indicates that as pH values increase (towards neutral values) turbidity decreases. The parameter estimate for  $\text{Ca}^{2+}$  (4.46) indicates that larger amounts of  $\text{Ca}^{2+}$  caused diminished turbidity reduction, which is in agreement with other research on kaolinite soils (Peng and Di, 1994). Simple regression analysis was also performed on individual soil properties related to turbidity reduction by PAM (Table 2.9). This analysis demonstrated that oxalate extractable iron might also be a significant variable ( $p = 0.04$ ).

Soils (samples 1, 2, 3, 4, 6, 7) that contained greater than 20% vermiculite or smectite were found to have four variables that explained variation in turbidity reduction. CBD extractable iron accounted for 83% of the variation in turbidity reduction with  $\text{Ca}^{2+}$ , pH and oxalate extractable iron accounting for 7, 5, and 3% of variation in turbidity reduction respectively (Table 2.10). Two possible explanations can be given for the large (83%) positive (negative parameter estimate) correlation between iron oxide content and PAM effectiveness. First, iron oxides may have reduced the dispersion of soils leaving larger particles for PAM to floc out of suspension (Goldberg and Glaubig, 1987). Second, iron oxides were present on the exterior of 2:1 clays, which provided binding

(ligand exchange) sites for PAM. Calcium was significantly ( $p = 0.008$ ) related to turbidity reduction by PAM. The negative parameter estimate ( $-0.297$ ) indicates that increases in  $\text{Ca}^{2+}$  leads to greater turbidity reduction. This agrees with the hypothesis that cation bridging is important in PAM adsorption to 2:1 clays (Letey, 1994; Laird, 1997). Turbidity reduction related to pH was significant ( $p = 0.005$ ), although it did not account for as much variation in turbidity reduction as soils dominated by kaolinite clays (0.48 compared to 0.046). Goldberg and Glaubig (1987) also found pH dependence of kaolinite soils to be greater than smectitic soils. Individual regression analysis (Table 2.11) shows  $\text{Ca}^{2+}$  and oxalate Fe as insignificant variables. These variables may account for variation in turbidity when included in the multivariate regression, although they may not be involved in adsorption mechanisms.

Turbidity reduction with PAM was compared with soil properties to see if general trends were present among all 13 soils. A stepwise regression analysis was used to obtain a multivariate regression model for soil properties compared to turbidity reduction ( $\ln p_{ct}$ ). The five soil properties that were significant ( $p \leq 0.05$ ) were sand, mica ( $< 1 \mu\text{m}$ ), mica (1-2  $\mu\text{m}$ ), smectite ( $< 1 \mu\text{m}$ ), and sodium adsorption ratio (SAR). These variables accounted for 62, 19, 13, 4 and 0.5% of the variation in turbidity reduction respectively (Table 2.12). The regression model was:  $\ln p_{ct} = 0.004(\text{sand}) - 17.9 (\text{mica (1-2 } \mu\text{m)}) + 27.0 (\text{mica } (< 1 \mu\text{m})) + 1.06 (\text{smectite } (< 1 \mu\text{m})) - 0.217 (\text{SAR})$  (Table 2.12). Because  $\ln p_{ct}$  is equal to the log of 100 minus turbidity reduction, the lower value for  $\ln p_{ct}$  the higher the turbidity reduction. Therefore the equation indicates that the greater the sand content of the soil, the less turbidity reduction. An analysis for the sand content in a soil would be a simple and inexpensive method to determine how PAM would work for a

particular soil. Because sand is highly correlated to other soil properties, it may not be directly involved in flocculation of soils (Table 2.13). However, despite obvious covariation, sand remains a good indicator of a soil's potential turbidity reduction with PAM.

Additional regression analysis of individual soil properties demonstrates that many of the soil properties were significant ( $p = 0.05$ ) (Table 2.14). However, because of correlation between soil properties, the majority of the variables were dropped from the overall stepwise equation. Because of the complexity (covariates) of the multivariate regression analysis, individual flocculation tests with fixed levels of each soil property may give a greater understanding of how much individual soil properties affect flocculation of soil suspensions with PAM.

## Mixed Polymer

Combined polymer treatment using Cytec Industries polymers was similar to flocculation with APS 705 alone (Fig. 2.17-2.18) with soil 4 (Fig. 2.16). Initially, it appeared that the combined treatment of Superfloc N300 and A150LMW resulted in a positive combined effect, but the second test (Fig. 2.18) demonstrated that the effect was due to N300. APS 705 may contain a polymer similar to N300 because of similar effect on soil 4. Earlier testing also showed similar flocculation trends for APS 705 and N300 (Fig. 2.8-2.9) where addition of the flocculant caused significantly (Tukey,  $p=0.05$ ) less flocculation at low PAM concentrations ( $<0.5 \text{ mg L}^{-1}$ ), and significantly (Tukey,  $p = 0.05$ ) more flocculation at high PAM concentrations ( $> 1 \text{ mg L}^{-1}$ ). Coastal Plain soils (samples 1- 4) tested generally contained more 2:1 clays with higher surface charges than soils from the Piedmont and Mountain Regions. Neutral polymers would likely be less repulsed by negative clay surface charges than charged polymers and may be more effective in 2:1 clay flocculation. Coastal Plain soils also had lower amounts of CBD-extractable iron than all other soil samples (8-16 compared to 68-761  $\text{mmol kg}^{-1}$ ). Ligand exchange is not believed to be a binding mechanism for neutral polymers (limited R-COO<sup>-</sup> groups) to soils. This may explain why neutral PAM (N300) worked well on Coastal Plain soils since there would be no reliance on iron oxides for binding. Additional testing with combined coagulant and polymer systems will have to be performed to understand how to have better flocculation in soils from the Coastal Plain. Combined PAM and gypsum treatment will be covered in chapter 3 as a possible solution to recalcitrant soils.



## Conclusions

PAM effectively decreased the turbidity of most soil suspensions and could be very useful in reducing construction site runoff turbidity. Sediment properties drastically affected the response to PAM, which indicates the need to have site-specific recommendations for PAM use. Soils with dominant kaolinite clay fractions flocculated well with all PAMs. Variation in turbidity reduction in soils dominated by kaolinite clays was mostly due to pH (48%). In soils with > 20% smectite or vermiculite, CBD extractable iron accounted for 83% of the variance in turbidity reduction. In a statistical evaluation of all 13 soils, sand content accounted for 62% of variation in turbidity.

Soil suspensions with low pH had poorer PAM responses possibly due to the negatively charged polymers coiling in suspension, causing them to be less effective unless higher concentrations of polymer were applied. Several soils demonstrated diminished turbidity reduction at high PAM concentrations, suggesting the need for accurate PAM dosing. Increased 2:1 clays, decreased silt or lack of iron oxides could be the reasons for poor flocculation of soils from the Coastal Plain. For soils from the Coastal Plain Region, it is recommended that APS 705 be used over other PAM products. N300 may also be useful for recalcitrant soil flocculation, as negative surface charge from clays and organic carbon and extreme pH values (<5 or >7) will not cause neutral polymers be repulsed or coil in solution.

## References

- Arora, H.S. and N.T. Coleman. 1979. The influence of electrolyte concentration on flocculation of clay suspensions. *Soil Sci.* 127:134-139.
- Coleman, N.T., M.L. Jackson, and A. Mehlich. 1949. Mineral composition of the clay fraction of several Coastal Plain, Piedmont, and Mountain soils of North Carolina. *Soil Sci. Soc. Am. Proc.* 13:81-85.
- Daniels, R.B., S.W. Buol, H.J. Kliess, and C.A. Ditzler. 1999. Soil systems in North Carolina. *NCSU Tech. Bull.* 314.
- Day, P.R. 1965. Particle fractionation and particle-size analysis. p. 547-567. *In* C.A. Black et al. (ed.) *Methods of soil analysis, Part I. Agronomy* 9:545-567.
- Gee, G.W. and J.W. Bauder. 1986. Particle-size analysis. P. 383-409 *In* *Methods of soil analysis, part 1. 2<sup>nd</sup> ed.* ASA and SSSA. Madison, WI.
- Goldberg, S. and R.A. Glaubig. 1987. Effect of saturating cation, pH, and aluminum and iron oxide on the flocculation of kaolinite and montmorillonite. *Clays Clay Min.* 35:220-227.
- Green, S.V., D.E. Stott, L.D. Norton, and J.G. Graveel. 2000. Polyacrylamide molecular weight and charge effects on infiltration under simulated rainfall. *Soil Sci. Soc. Am. J.* 64:1786-1791.
- Gregory, J. 1989. Fundamentals of flocculation. *Crit. Rev. Environ. Control.* 19:185-230.
- Hillel, D. 1998. *Environmental Soil Physics.* Academic Press. London.
- Kretschmar, R., D. Hesterberg, and H. Sticher. 1997. Effects of adsorbed humic acid on surface charge and flocculation of kaolinite. *Soil Sci. Soc. Am. J.* 61: 101-108.
- Jackson, M.L., C.H. Lim, and L.W. Zelazny. 1986. Oxides, hydroxides, and aluminosilicates. pp. 101-150 *In* A. Klute (ed.) *Methods of soil analysis, part 1. physical and mineralogical methods,* ASA-SSA, Madison, WI.
- Kretschmar, R., W.P. Robarge, and S.B. Weed. 1993. Flocculation of kaolinitic soil clays: effects of humic substances and iron oxides. *Soil Sci. Soc. Am. J.* 57: 1277-1283.
- Kunze, G. W. and J. B. Dixon. 1986. Pretreatment for mineralogical analysis. p. 91-100 *In* A. Klute (ed.) *Methods of soil analysis. Part 1. 2nd ed.* ASA and SSSA, Madison, WI.

- Laird, D.A. 1997. Bonding between polyacrylamide and clay mineral surfaces. *Soil Sci.* 162:826-832.
- Letey, J. 1994. Adsorption and desorption of polymers on soil. *Soil Sci.* 158:244-248.
- Mehlich A. 1984. Mehlich-3 soil test extractant: a modification of Mehlich-2 extractant. *Commun Soil Sci Plant Anal.* 15:1409–16.
- Miller, W.P., R.L. Willis and G.J. Levy. 1998. Aggregate stabilization in kaolinitic soils by low rates of anionic polyacrylamide. *Soil Manag.* 14:101-105.
- Montgomery, W.H. 1968. Polyacrylamide. *Water Soluble Resins.* Wayne, NJ.
- Nadler, A and J. Letey. 1989. Adsorption isotherms of polyanions on soils using tritium labeled compounds. *Soil Sci. Soc. Am. J.* 53:1375-1378.
- Nadler, A., M. Magaritz, and L. Leib. 1994. PAM application techniques and mobility in Soil. *Soil Sci.* 158:249-254.
- Pang, F.F., and P. Di. 1994. Effect of multivalent salts-calcium and aluminum on the flocculation of kaolin suspension with anionic polyacrylamide. *J. Colloid Interface Sci.* 164:229-237.
- Whittig, L. D. and W. R. Allardice. 1986. X-ray diffraction techniques. p. 331-362 *In* A. Klute (ed.) *Methods of soil analysis. Part 1.* 2nd ed. ASA and SSSA, Madison, WI.

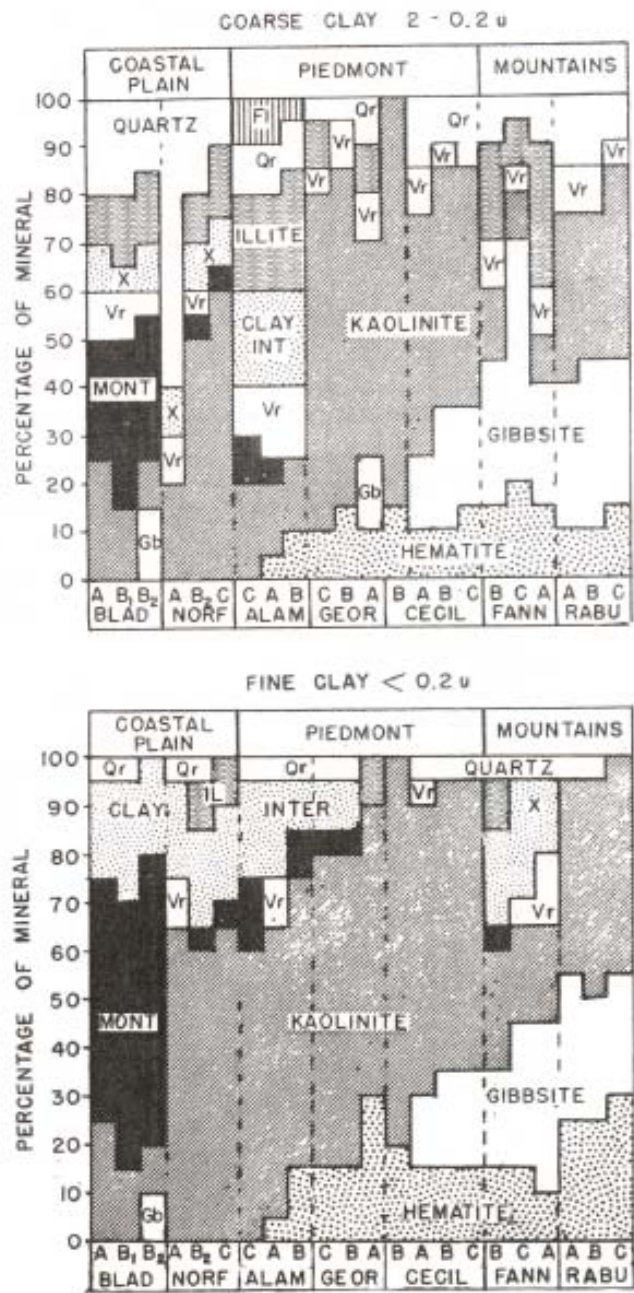


Figure 2.1 Mineral content of coarse (2 – 0.2 mm) and fine (< 0.2 mm) clay fractions of typical North Carolina soils (Coleman et al., 1949).

## NCDOT Divisions

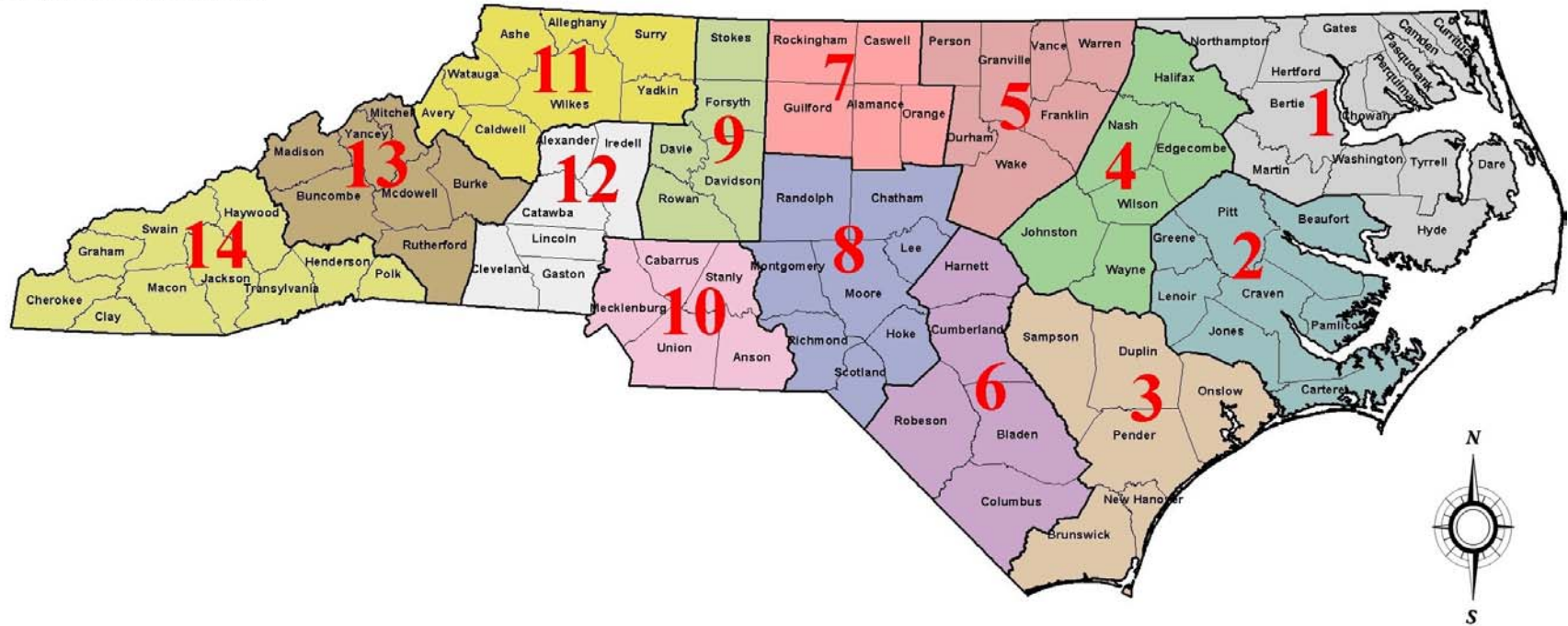


Figure 2.2 Soil sample numbers coincide with the highway division they originated from. No sample was obtained from division 10.

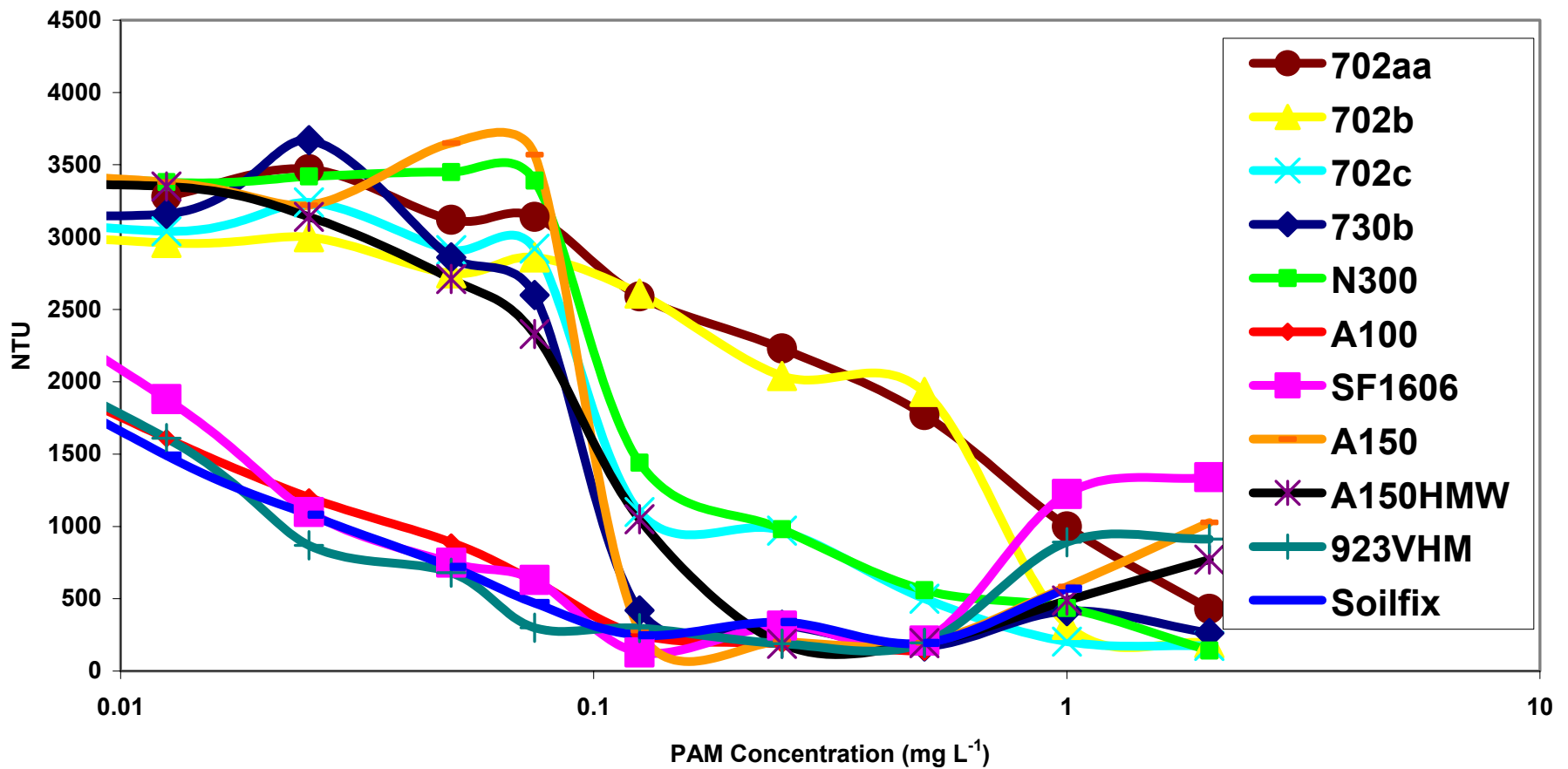


Figure 2.3 Example of Initial PAM testing using soil 11 from the Mountain Region. Figure shown in linear-log scale.

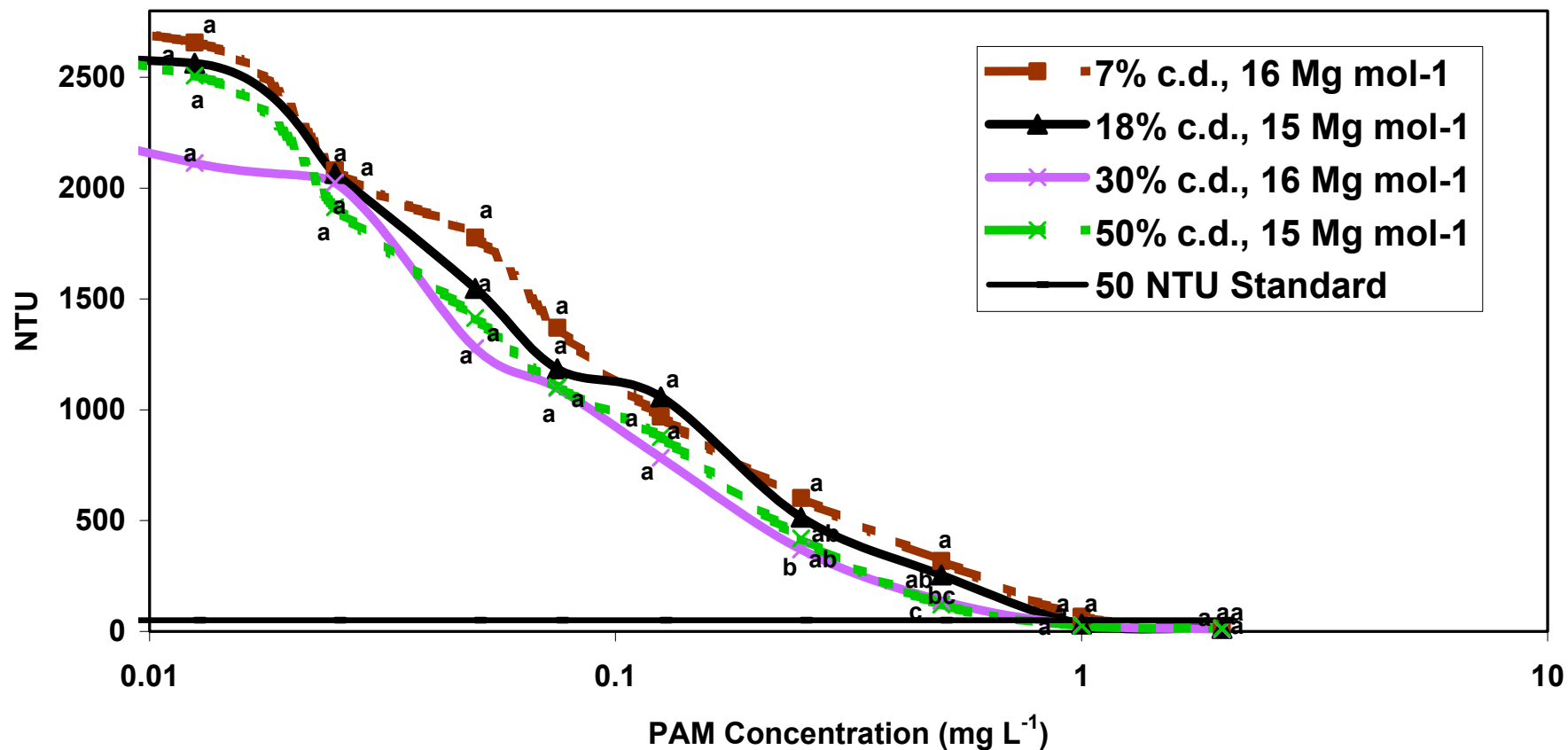


Figure 2.4 Turbidity reduction as a function of input concentration for four PAM products differing in charge density (c.d.) (percent hydrolysis) and molecular weight (in Mg mol<sup>-1</sup>) over nine concentrations on soil sample 9. For each PAM concentration, data points with different letters are significantly different ( $p = 0.05$ ). Figure shown in linear-log scale.

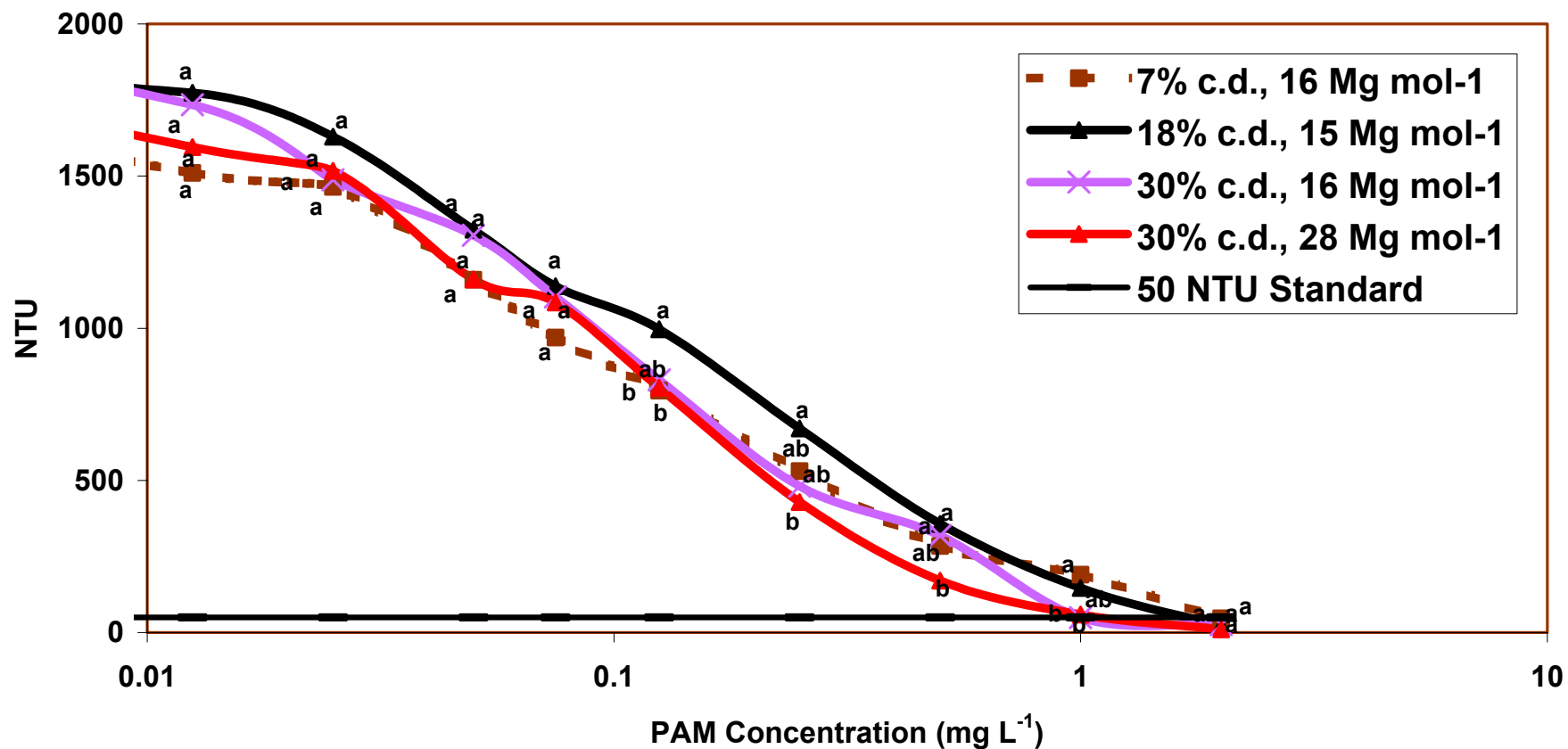


Figure 2.5 Turbidity reduction as a function of input concentration for four PAM products differing in charge density (c.d.) (percent hydrolysis) and molecular weight (in Mg mol<sup>-1</sup>) over nine concentrations on soil sample 5. For each PAM concentration, data points with different letters are significantly different ( $p = 0.05$ ). Figure shown in linear-log scale.



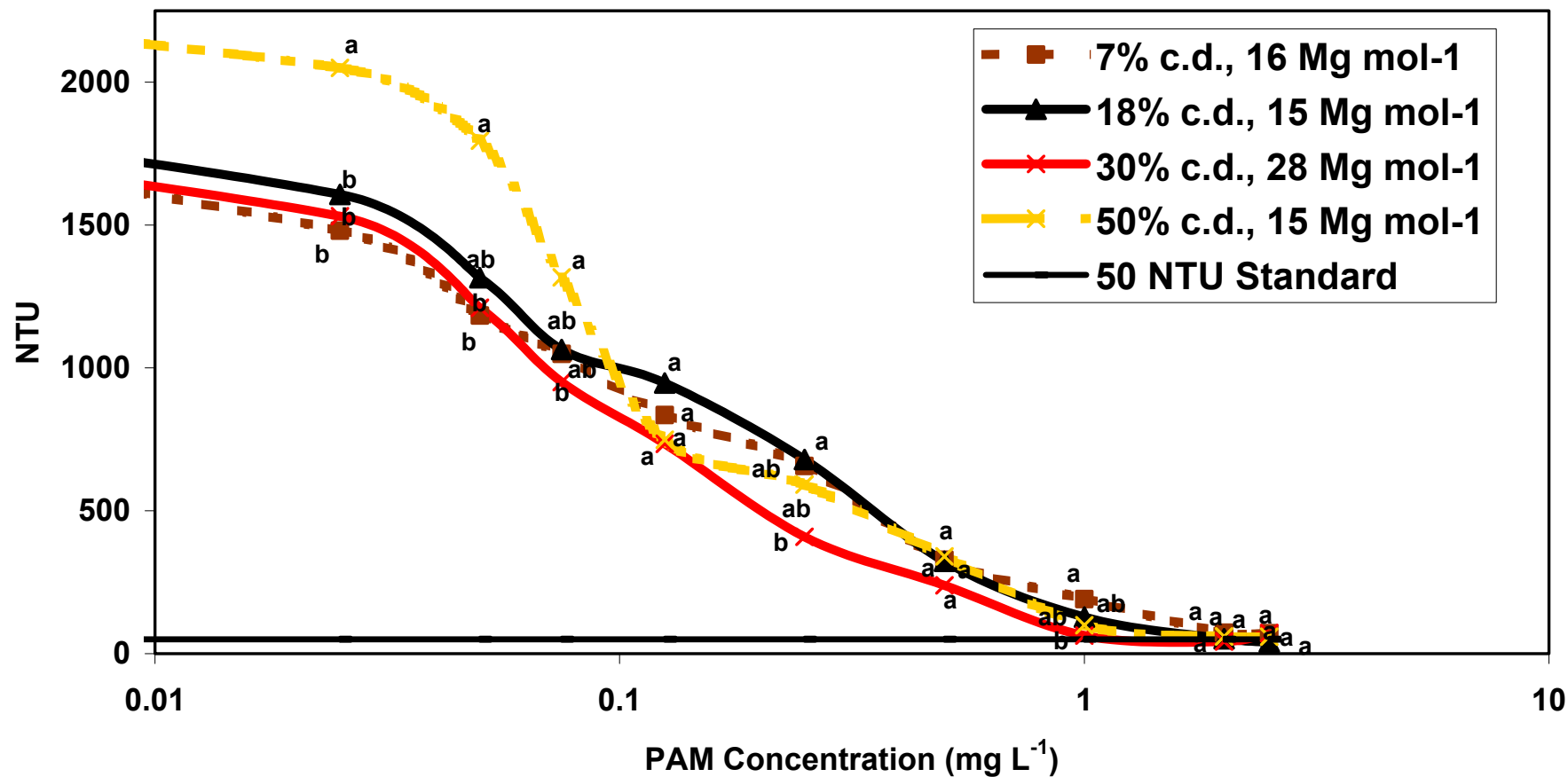


Figure 2.6 Turbidity reduction as a function of input concentration for four PAM products differing in charge density (c.d.) (percent hydrolysis) and molecular weight (in  $\text{Mg mol}^{-1}$ ) over nine concentrations on soil sample 12. For each PAM concentration, data points with different letters are significantly different ( $p = 0.05$ ). Figure shown in linear-log scale.

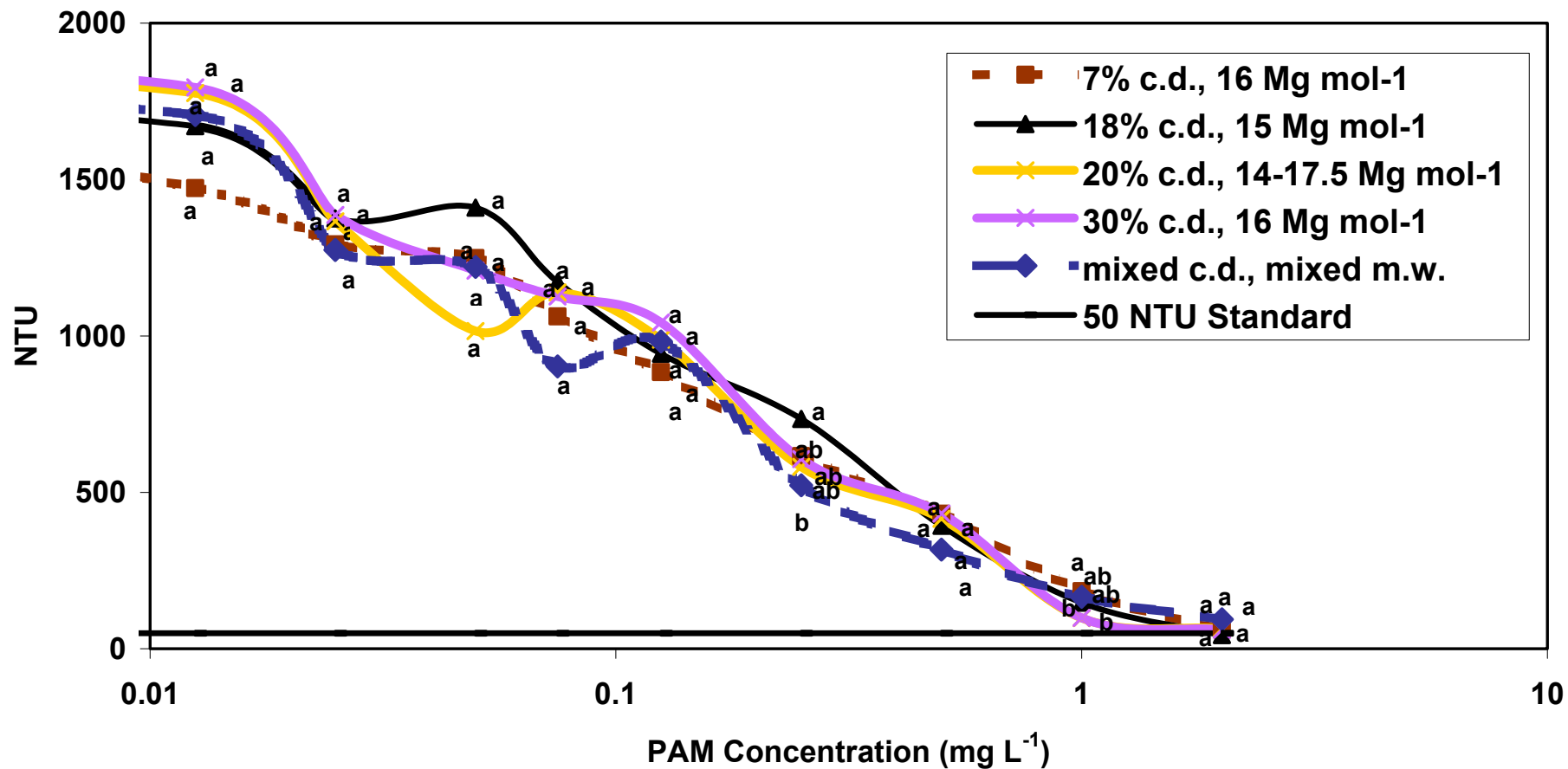


Figure 2.7 Turbidity reduction as a function of input concentration for five PAM products differing in charge density (c.d.) (percent hydrolysis) and molecular weight (in  $\text{Mg mol}^{-1}$ ) over nine concentrations on soil sample 13. For each PAM concentration, data points with different letters are significantly different ( $p = 0.05$ ). Figure shown in linear-log scale.

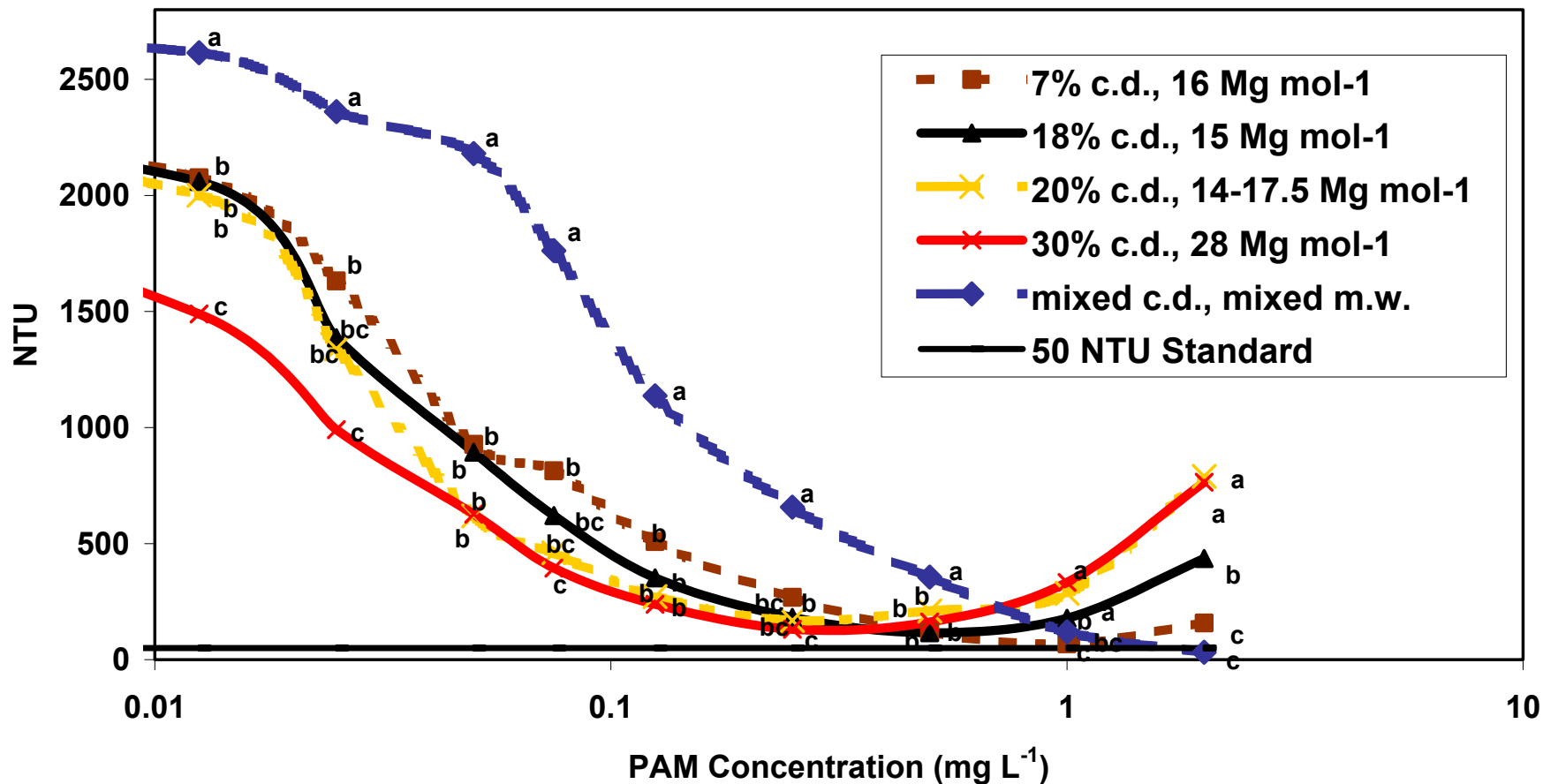


Figure 2.8 Turbidity reduction as a function of input concentration for five PAM products differing in charge density (c.d.) (percent hydrolysis) and molecular weight (in  $\text{Mg mol}^{-1}$ ) over nine concentrations on soil sample 11. For each PAM concentration, data points with different letters are significantly different ( $p = 0.05$ ). Figure shown in linear-log scale.

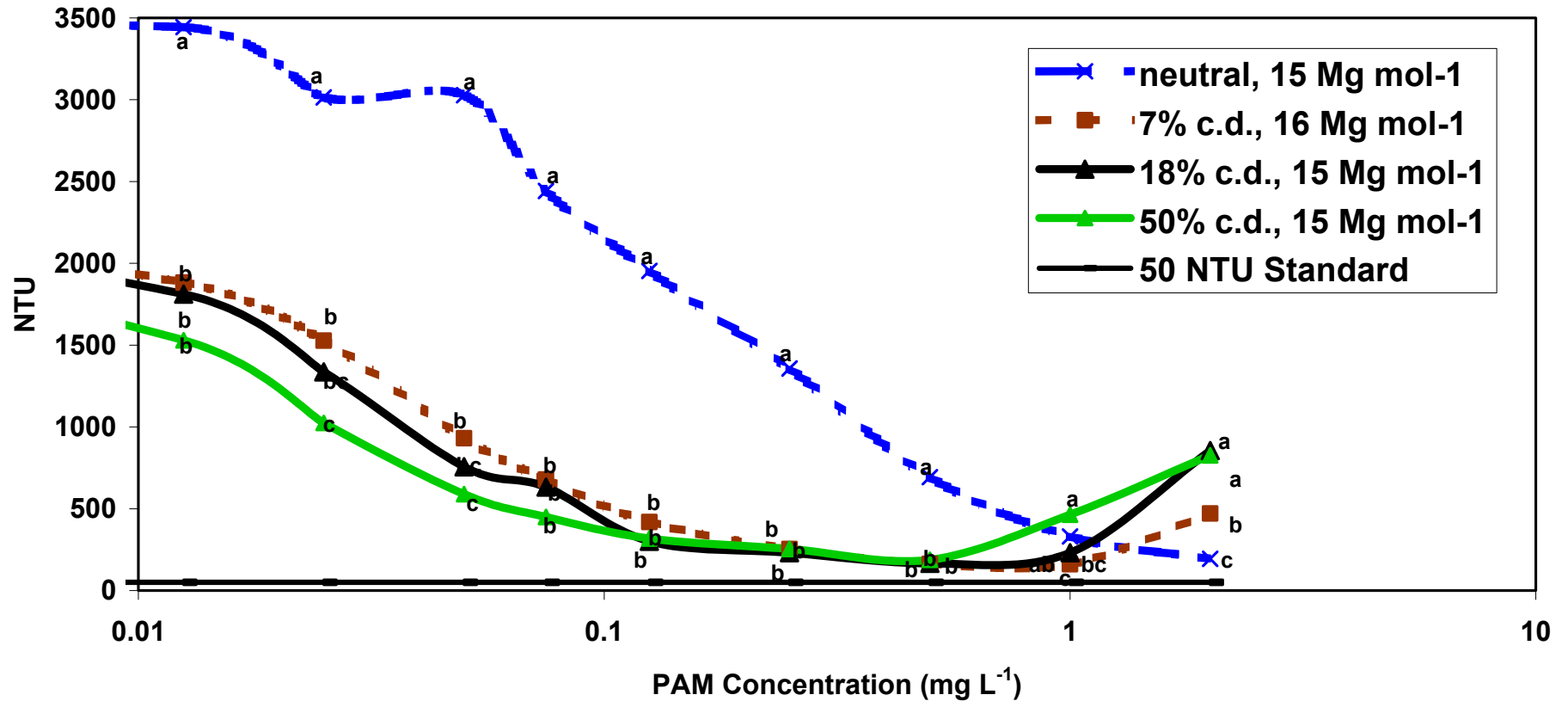


Figure 2.9 Turbidity reduction as a function of input concentration for four PAM products differing in charge density (c.d.) (percent hydrolysis) and molecular weight (in Mg mol<sup>-1</sup>) over nine concentrations on soil sample 7. For each PAM concentration, data points with different letters are significantly different ( $p = 0.05$ ). Figure shown in linear-log scale.

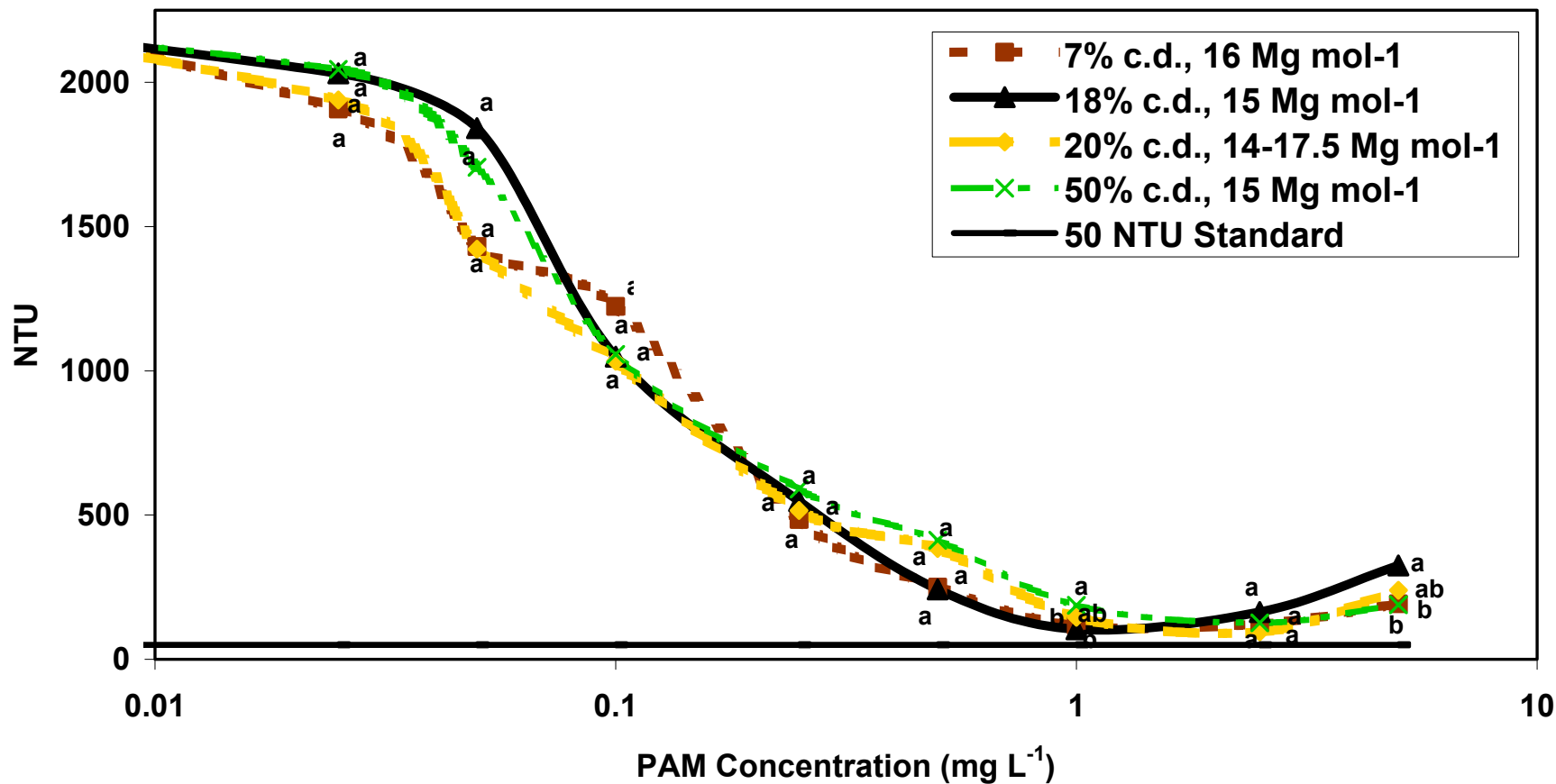


Figure 2.10 Turbidity reduction as a function of input concentration for four PAM products differing in charge density (c.d.) (percent hydrolysis) and molecular weight (in  $\text{Mg mol}^{-1}$ ) over nine concentrations on soil sample 14. For each PAM concentration, data points with different letters are significantly different ( $p = 0.05$ ). Figure shown in linear-log scale.

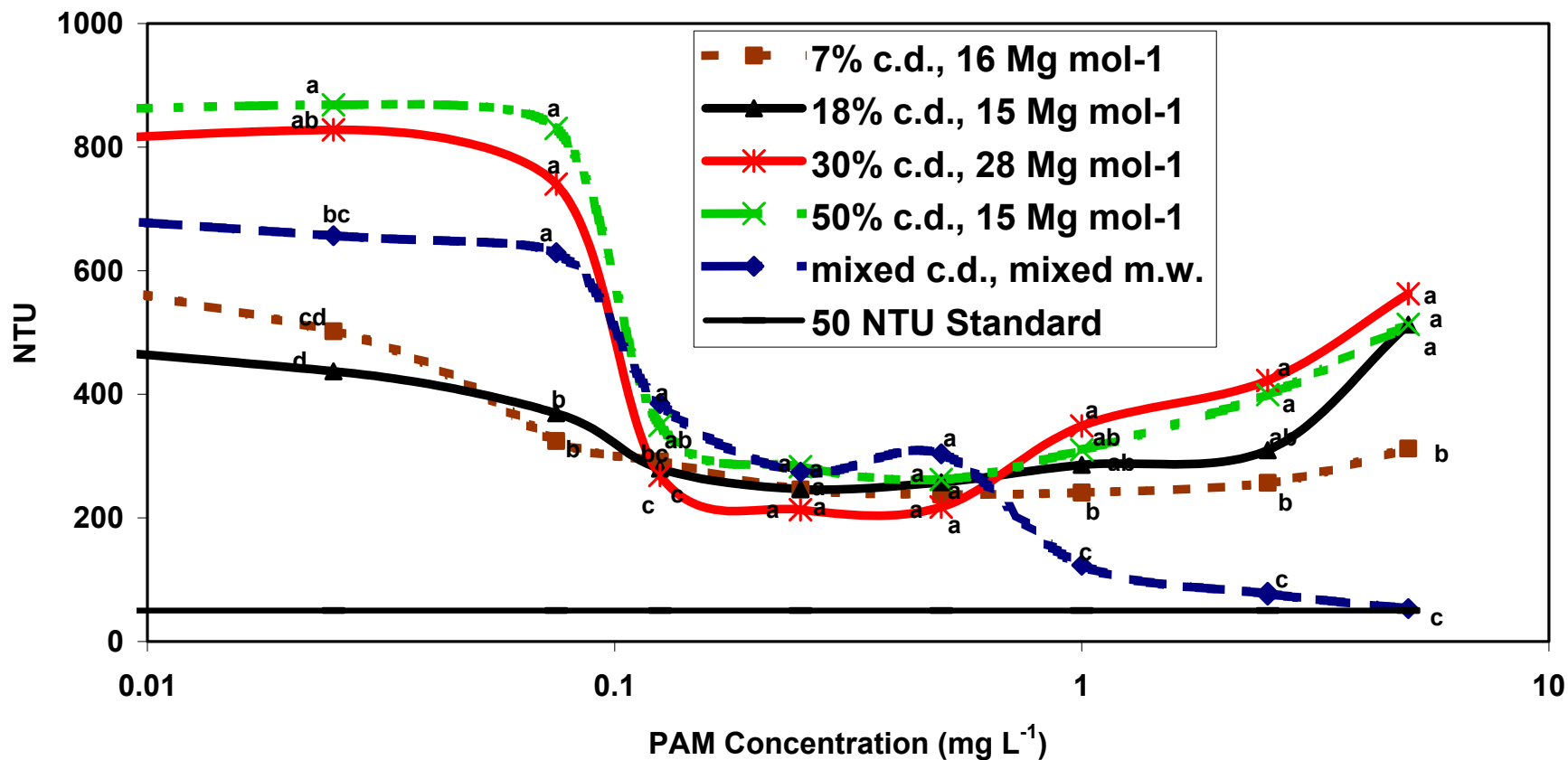


Figure 2.11 Turbidity reduction as a function of input concentration for five PAM products differing in charge density (c.d.) (percent hydrolysis) and molecular weight (in  $\text{Mg mol}^{-1}$ ) over nine concentrations on soil sample 2. For each PAM concentration, data points with different letters are significantly different ( $p = 0.05$ ). Figure shown in linear-log scale.

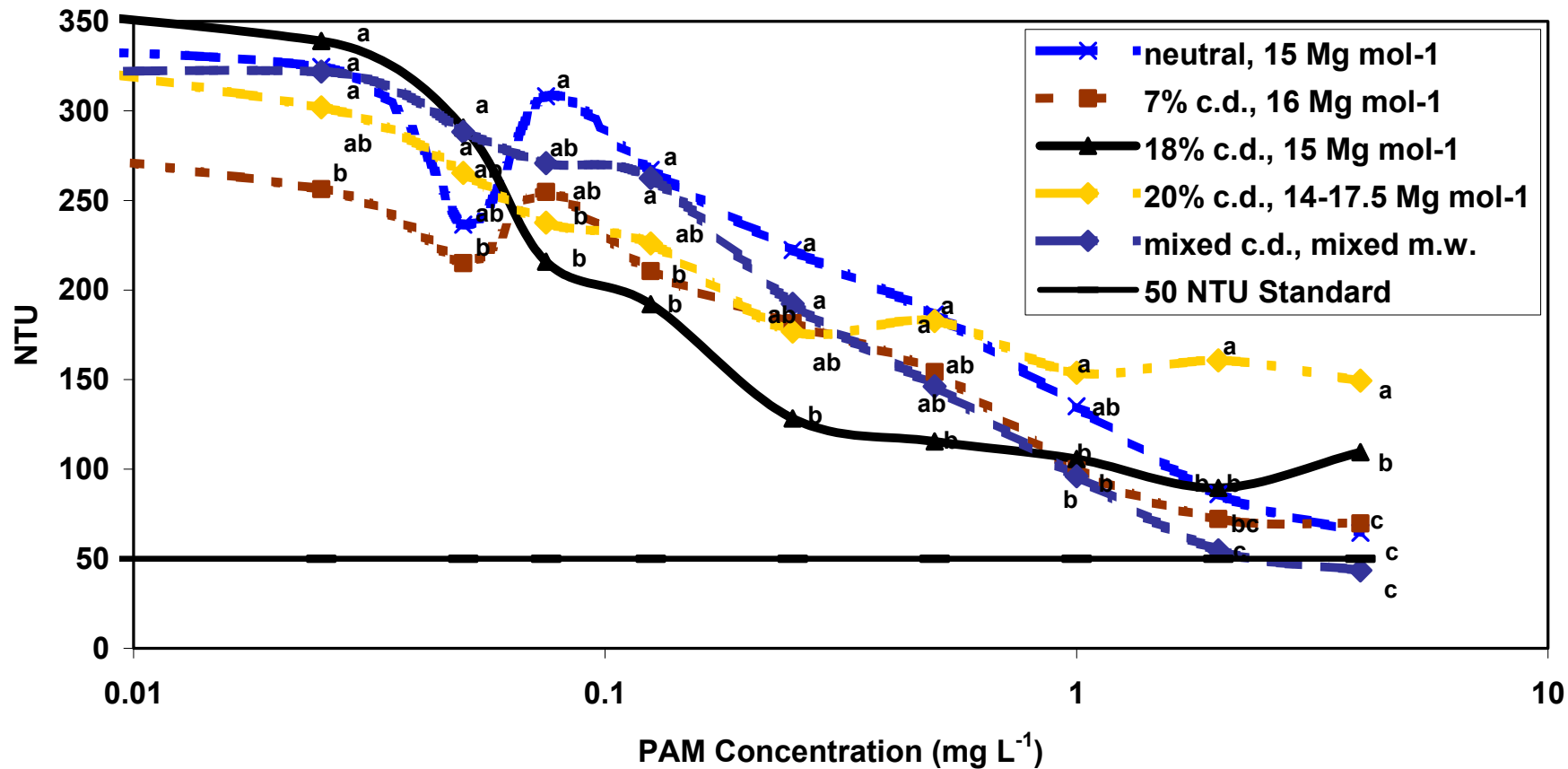


Figure 2.12 Turbidity reduction as a function of input concentration for five PAM products differing in charge density (c.d.) (percent hydrolysis) and molecular weight (in Mg mol<sup>-1</sup>) over nine concentrations on soil sample 3. For each PAM concentration, data points with different letters are significantly different ( $p = 0.05$ ). Figure shown in linear-log scale.

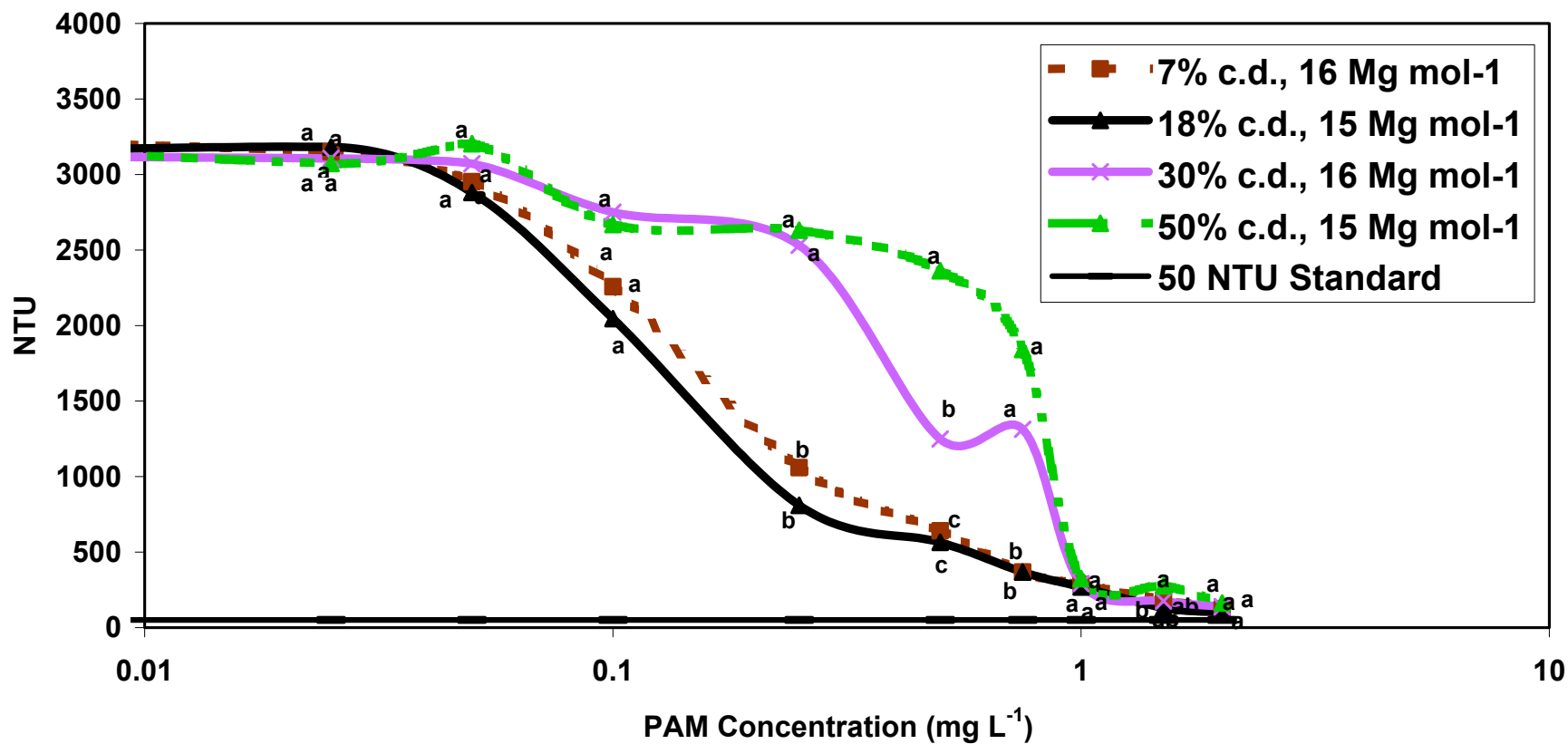


Figure 2.13 Turbidity reduction as a function of input concentration for four PAM products differing in charge density (c.d.) (percent hydrolysis) and molecular weight (in  $\text{Mg mol}^{-1}$ ) over nine concentrations on soil sample 6. For each PAM concentration, data points with different letters are significantly different ( $p = 0.05$ ). Figure shown in linear-log scale.



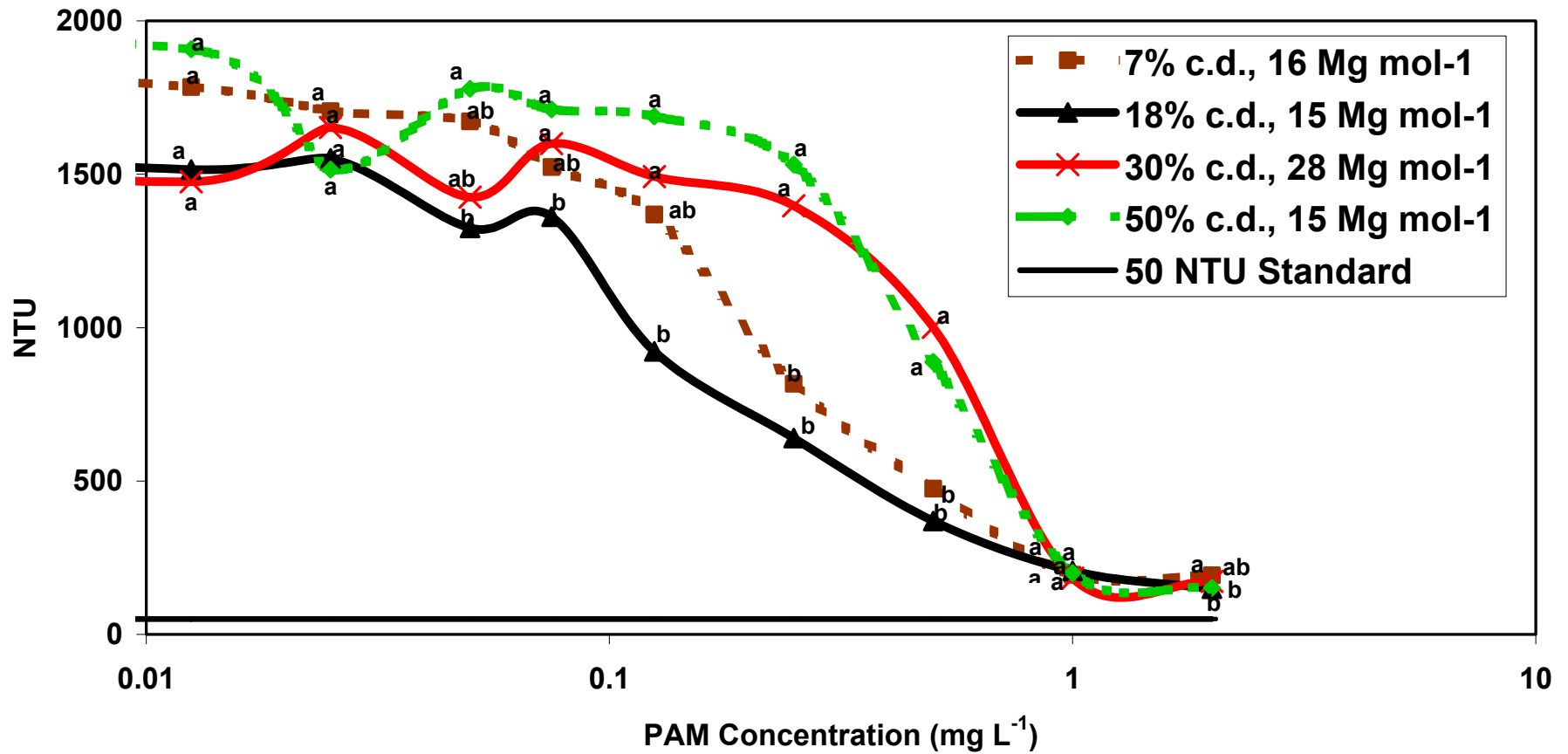


Figure 2.14 Turbidity reduction as a function of input concentration for four PAM products differing in charge density (c.d.) (percent hydrolysis) and molecular weight (in  $\text{Mg mol}^{-1}$ ) over nine concentrations on soil sample 8. For each PAM concentration, data points with different letters are significantly different ( $p = 0.05$ ). Figure shown in linear-log scale.

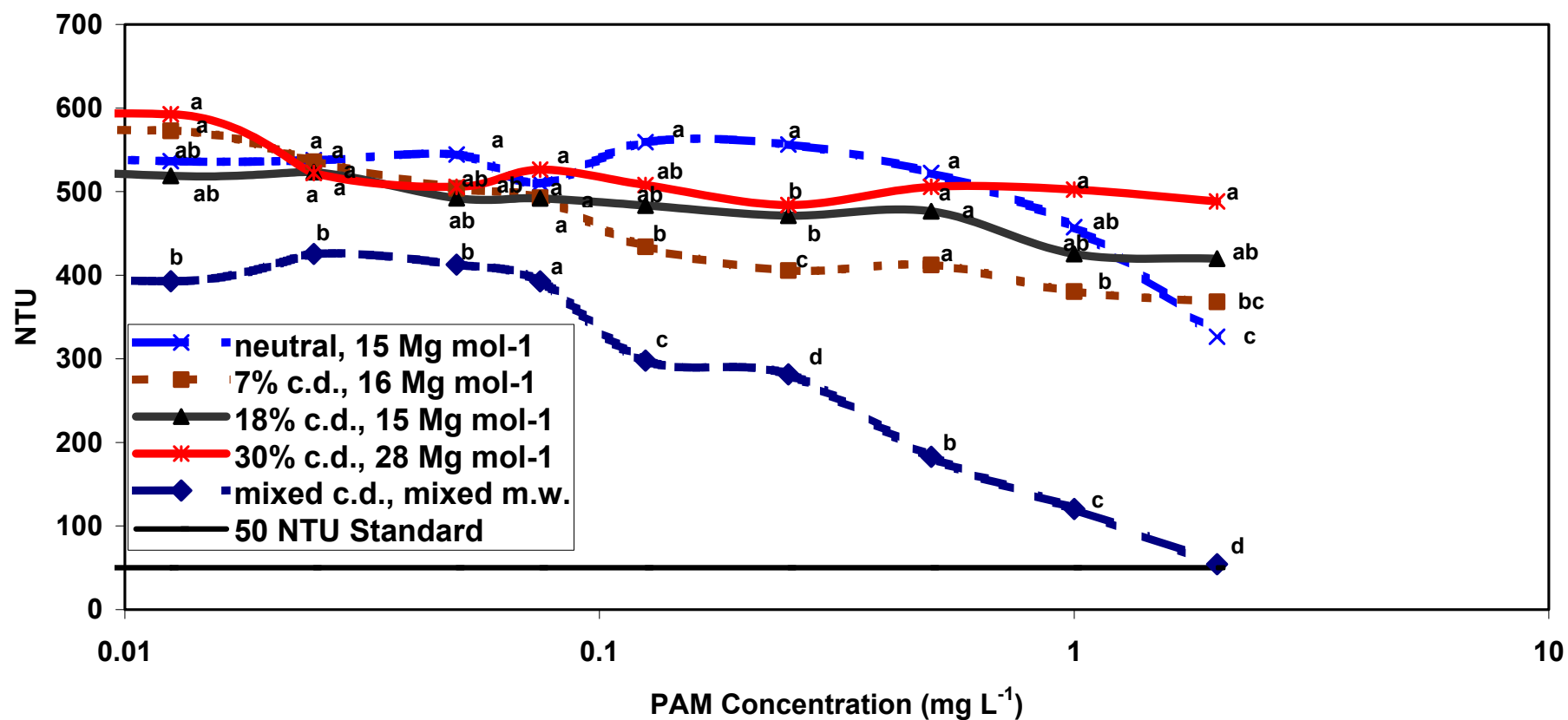


Figure 2.15 Turbidity reduction as a function of input concentration for five PAM products differing in charge density (c.d.) (percent hydrolysis) and molecular weight (in Mg mol<sup>-1</sup>) over nine concentrations on soil sample 1. For each PAM concentration, data points with different letters are significantly different ( $p = 0.05$ ). Figure shown in linear-log scale.

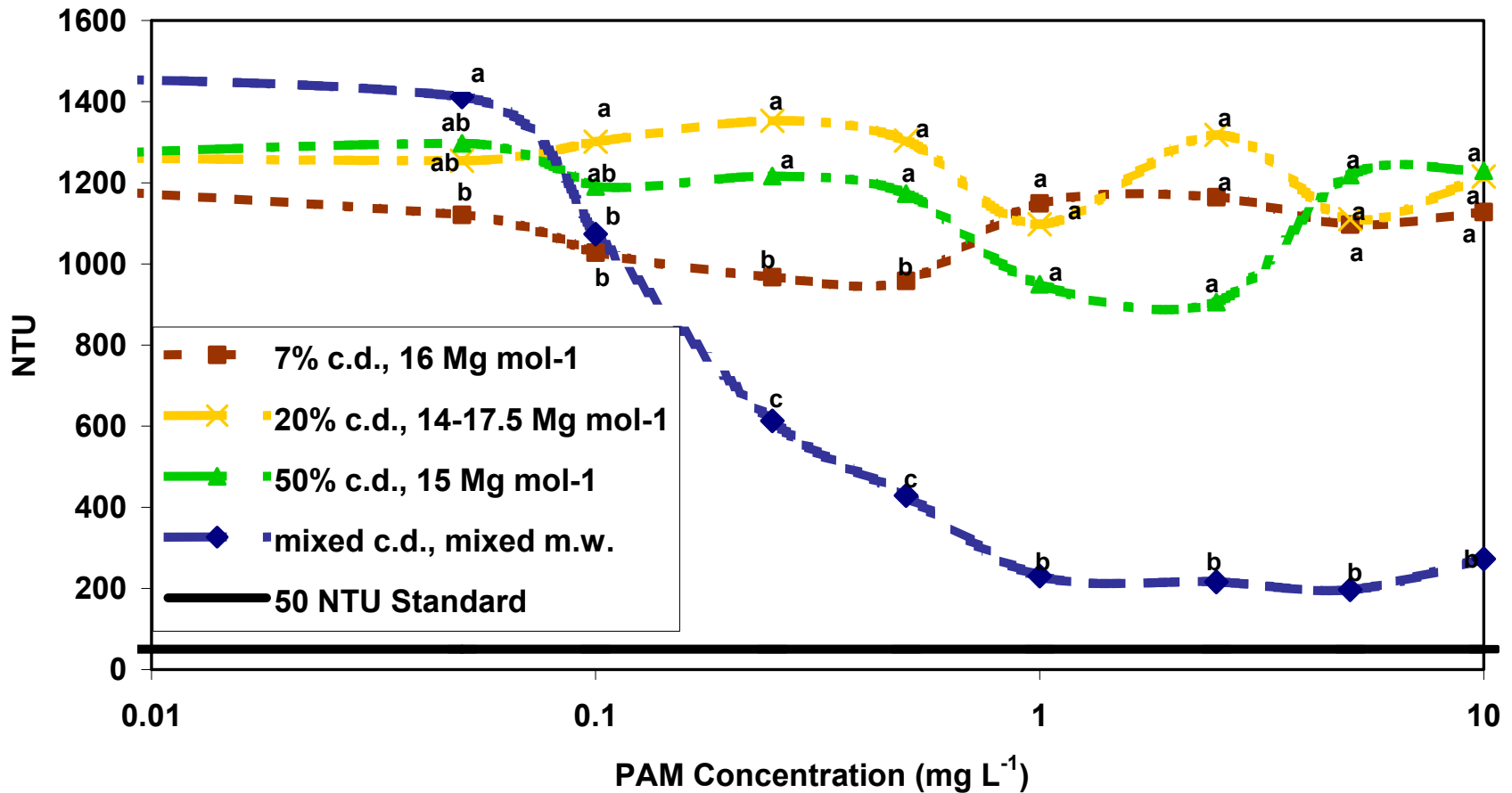


Figure 2.16 Turbidity reduction as a function of input concentration for four PAM products differing in charge density (c.d.) (percent hydrolysis) and molecular weight (in Mg mol<sup>-1</sup>) over nine concentrations on soil sample 4. For each PAM concentration, data points with different letters are significantly different ( $p = 0.05$ ). Figure shown in linear-log scale.

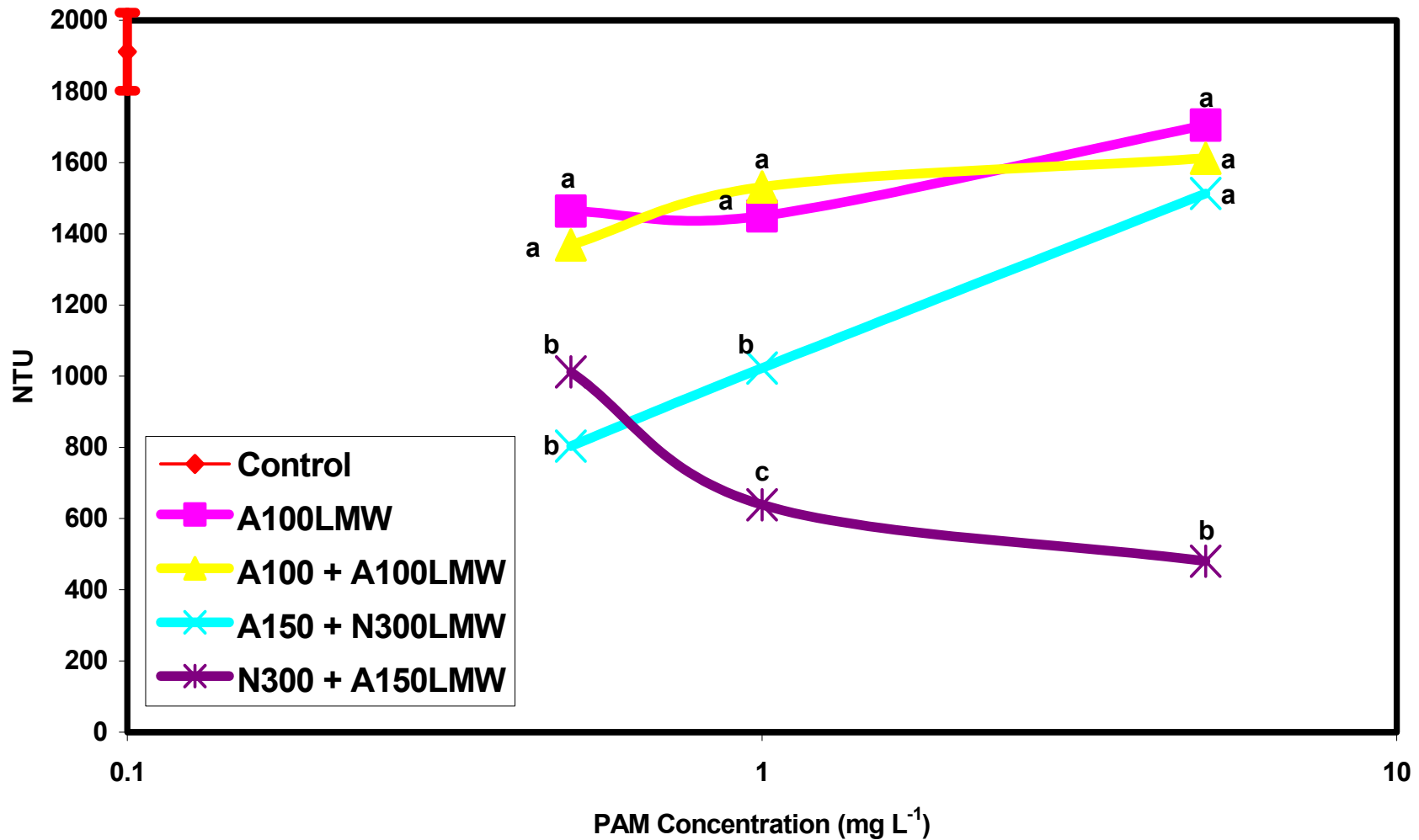


Figure 2.17 Comparison of treatments involving low and high molecular weight PAMs. For each PAM concentration, data points with different letters are significantly different ( $p = 0.05$ ). Figure shown in linear-log scale

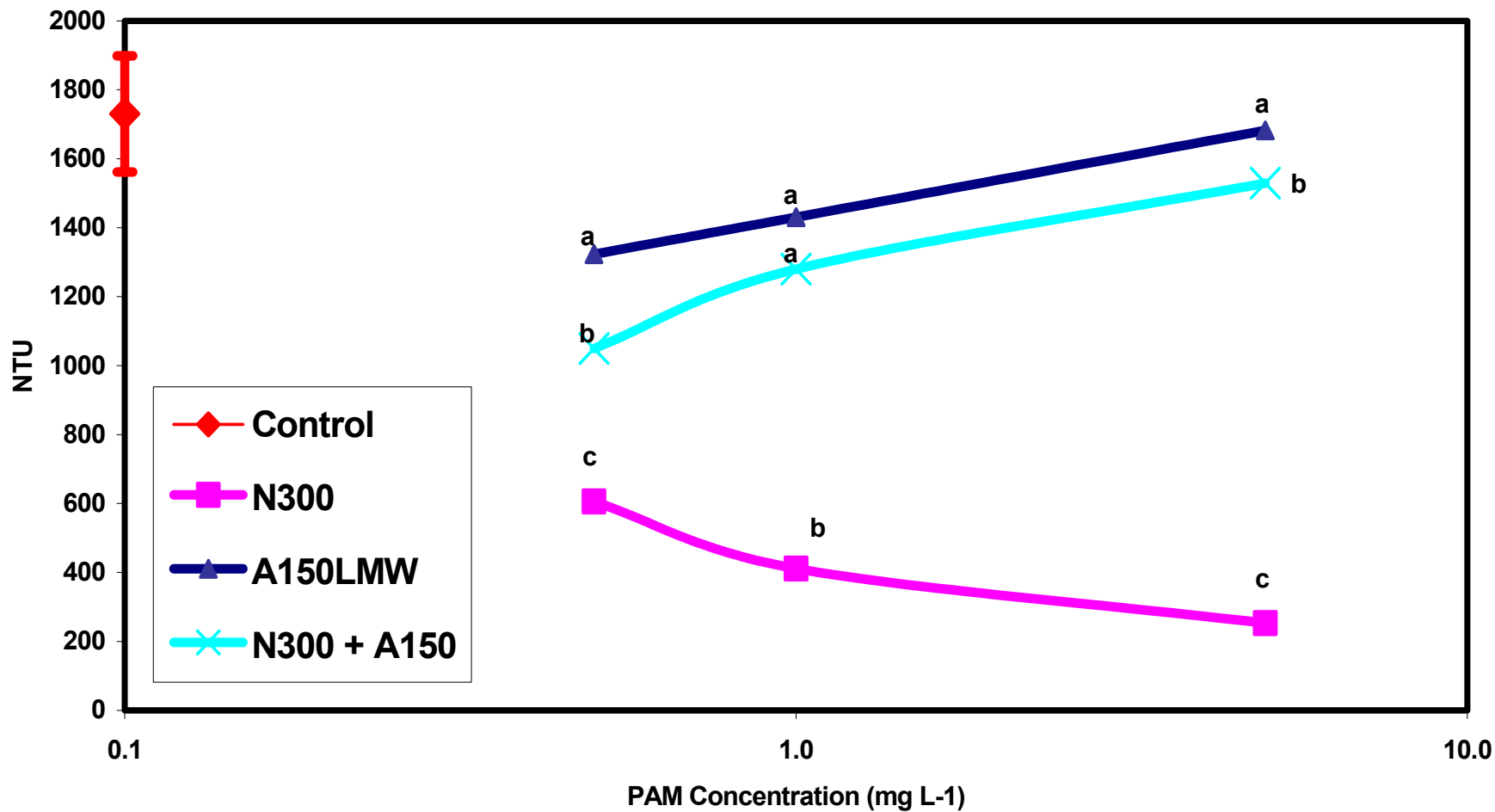


Figure 2.18 Comparison of treatments involving low and high molecular weight PAMs. For each PAM concentration, data points with different letters are significantly different ( $p = 0.05$ ). Figure shown in linear-log scale

<b>Flocculant</b>	<b>Molecular Weight</b>	<b>Charge Density</b>
SF N300	15 Mg mol <sup>-1</sup>	neutral
SF A100	16 Mg mol <sup>-1</sup>	7%
SF A150	15 Mg mol <sup>-1</sup>	50%
SF A150HMW	17 Mg mol <sup>-1</sup>	50%
SF 1606	28 Mg mol <sup>-1</sup>	30%
Soilfix Polybead	16 Mg mol <sup>-1</sup>	30%
APS702aa	mixed	mixed
APS702b	mixed	mixed
APS702c	mixed	mixed
APS730b	mixed	mixed
Chemtall 923VHM	14-17.5 Mg mol <sup>-1</sup>	20%

Table 2.1 PAM products used in initial evaluation of PAM interactions.

<b>Flocculant</b>	<b>Molecular Weight</b>	<b>Charge Density</b>
SF N300	15 Mg mol <sup>-1</sup>	neutral
SF A100	16 Mg mol <sup>-1</sup>	7%
SF A110	15 Mg mol <sup>-1</sup>	18%
SF A150	15 Mg mol <sup>-1</sup>	50%
SF 1606	28 Mg mol <sup>-1</sup>	30%
Soilfix Polybead	16 Mg mol <sup>-1</sup>	30%
APS705	mixed	mixed
Chemtall 923VHM	14-17.5 Mg mol <sup>-1</sup>	20%

Table 2.2 PAM products used in replicate testing for PAM interactions evaluation.

<b>Flocculant</b>	<b>Molecular Weight</b>	<b>Charge Density</b>
SF N300	15 Mg mol <sup>-1</sup>	neutral
SF A100	16 Mg mol <sup>-1</sup>	7%
SF A150	15 Mg mol <sup>-1</sup>	50%
SF N300LMW	4 Mg mol <sup>-1</sup>	neutral
SF A100LMW	4 Mg mol <sup>-1</sup>	7%
SF A150LMW	4 Mg mol <sup>-1</sup>	50%

Table 2.3 PAM products used in mixed polymer evaluation.



Soil	Turbidity Reduction (PAM) (100X(NTU <sub>0</sub> -NTU)/NTU <sub>0</sub> )	Low Turbidity (NTU) with PAM	PAM Conc. at low NTU (mg L <sup>-1</sup> )	Texture	Sand (g kg <sup>-1</sup> )	Silt (g kg <sup>-1</sup> )	Clay (g kg <sup>-1</sup> )	Ca <sup>2+</sup> (cmol <sub>c</sub> Kg <sup>-1</sup> )	Mg <sup>2+</sup> (cmol <sub>c</sub> Kg <sup>-1</sup> )	SAR
5	99.5%	11	2	clay	285	215	500	0.9	0.4	0.5
9	99.7%	9	2	sandy loam	524	336	140	1.1	0.7	0.4
12	98.2%	40	2.5	clay loam	440	280	280	0.7	0.6	0.4
13	97.6%	44	2	clay loam	375	305	320	0.1	0.1	0.8

Soil	pH (1:1, H <sub>2</sub> O)	Organic Carbon (g kg <sup>-1</sup> )	Smectite (<1 μm)	Smectite (1-2 μm)	Vermiculite (<1 μm)	Vermiculite (1-2 μm)	Mica (<1 μm)	Mica (1-2 μm)	Kaolinite (<1 μm)	Kaolinite (1-2 μm)	Oxalate Fe (mmol kg <sup>-1</sup> )	CBD Fe (mmol kg <sup>-1</sup> )
5	5.1	3.5	8%	0%	12%	10%	0%	1%	80%	88%	7.7	568.9
9	5.6	0.9	6%	0%	9%	3%	10%	30%	75%	68%	9.0	304.4
12	5.1	1.0	-----	-----	-----	-----	-----	-----	-----	-----	20.4	505.6
13	5.0	1.6	0%	0%	9%	2%	1%	2%	90%	96%	13.9	761.2

Table 2.4 Properties for soils that had 98 to 99.7% reductions in suspension turbidity with PAM (2 mg L<sup>-1</sup>).

Soil	Turbidity Reduction (PAM) (100X(NTU <sub>0</sub> -NTU)/NTU <sub>0</sub> )	Low Turbidity (NTU) with PAM	PAM Conc. at low NTU (mg L <sup>-1</sup> )	Texture	Sand (g kg <sup>-1</sup> )	Silt (g kg <sup>-1</sup> )	Clay (g kg <sup>-1</sup> )	Ca <sup>2+</sup> (cmol <sub>c</sub> Kg <sup>-1</sup> )	Mg <sup>2+</sup> (cmol <sub>c</sub> Kg <sup>-1</sup> )	SAR
2	93.2%	63	5	sandy loam	720	178	102	0.5	0.3	1.6
7	94.2%	161	1	sandy loam	540	352	108	4.1	1.3	0.3
11	98.9%	32	1	sandy loam	550	390	60	1.3	0.8	0.3
14	96.4%	95	2.5	clay loam	370	290	340	0.4	0.3	0.5

Soil	pH (1:1, H <sub>2</sub> O)	Organic Carbon (g kg <sup>-1</sup> )	Smectite (<1 μm)	Smectite (1-2 μm)	Vermiculite (<1 μm)	Vermiculite (1-2 μm)	Mica (<1 μm)	Mica (1-2 μm)	Kaolinite (<1 μm)	Kaolinite (1-2 μm)	Oxalate Fe (mmol kg <sup>-1</sup> )	CBD Fe (mmol kg <sup>-1</sup> )
2	4.8	3.3	0%	0%	42%	59%	7%	4%	52%	37%	2.6	16.4
7	5.8	0.9	0%	1%	19%	49%	0%	0%	81%	50%	4.3	88.3
11	5.6	0.9	0%	0%	10%	2%	19%	34%	71%	64%	7.6	91.6
14	4.9	7.2	-----	-----	-----	-----	-----	-----	-----	-----	14.9	293.9

Table 2.5 Properties for soils that had diminished turbidity reduction at PAM concentrations greater than 1 mg L<sup>-1</sup>.

Soil	Turbidity Reduction (PAM) (100X(NTU <sub>0</sub> -NTU)/NTU <sub>0</sub> )	Low Turbidity (NTU) with PAM	PAM Conc. at low NTU (mg L <sup>-1</sup> )	Texture	Sand (g kg <sup>-1</sup> )	Silt (g kg <sup>-1</sup> )	Clay (g kg <sup>-1</sup> )	Ca <sup>2+</sup> (cmol <sub>c</sub> Kg <sup>-1</sup> )	Mg <sup>2+</sup> (cmol <sub>c</sub> Kg <sup>-1</sup> )	SAR
3	85.9%	44	4	sand	932	30	38	9.0	0.20	0.2
6	96.7%	99	2	sandy clay loam	625	130	245	0.2	0.1	1.9
8	91.1%	149	2	sandy loam	775	70	155	0.2	0.2	0.9

Soil	pH (1:1, H <sub>2</sub> O)	Organic Carbon (g kg <sup>-1</sup> )	Smectite (<1 μm)	Smectite (1-2 μm)	Vermiculite (<1 μm)	Vermiculite (1-2 μm)	Mica (<1 μm)	Mica (1-2 μm)	Kaolinite (<1 μm)	Kaolinite (1-2 μm)	Oxalate Fe (mmol kg <sup>-1</sup> )	CBD Fe (mmol kg <sup>-1</sup> )
3	7.4	2.0	90%	60%	0%	2%	10%	27%	0%	11%	9.6	10.2
6	3.7	5.9	21%	13%	0%	4%	0%	5%	79%	78%	9.3	135.1
8	4.8	1.4	-----	-----	-----	-----	-----	-----	-----	-----	1.1	67.8

Table 2.6 Properties for soils that had a little flocculation with PAM at lower concentrations (< 1 mg L<sup>-1</sup>), but flocculated at higher PAM concentrations.

Soil	Turbidity Reduction (PAM) (100X(NTU <sub>0</sub> -NTU)/NTU <sub>0</sub> )	Low Turbidity (NTU) with PAM	PAM Conc. at low NTU (mg L <sup>-1</sup> )	Texture	Sand (g kg <sup>-1</sup> )	Silt (g kg <sup>-1</sup> )	Clay (g kg <sup>-1</sup> )	Ca <sup>2+</sup> (cmol <sub>c</sub> Kg <sup>-1</sup> )	Mg <sup>2+</sup> (cmol <sub>c</sub> Kg <sup>-1</sup> )	SAR
1	87.3%	54	2	sand	900	54	46	4.3	0.2	0.5
4	86.7%	197	5	loamy sand	840	110	50	0.2	0.1	0.7

Soil	pH (1:1, H <sub>2</sub> O)	Organic Carbon (g kg <sup>-1</sup> )	Smectite (<1 μm)	Smectite (1-2 μm)	Vermiculite (<1 μm)	Vermiculite (1-2 μm)	Mica (<1 μm)	Mica (1-2 μm)	Kaolinite (<1 μm)	Kaolinite (1-2 μm)	Oxalate Fe (mmol kg <sup>-1</sup> )	CBD Fe (mmol kg <sup>-1</sup> )
1	8.0	1.5	64%	13%	7%	11%	18%	26%	11%	42%	5.2	8.2
4	5.0	4.6	0%	0%	52%	50%	10%	7%	38%	43%	6.8	18.2

Table 2.7 Properties for soils that had a little or no flocculation with any single component PAM. APS705 (commercially mixed) PAM was the only effective polymer.

<b>Summary of stepwise regression</b>				
<b>Variable included</b>	<b>Parameter Estimate</b>	<b>Partial R<sup>2</sup></b>	<b>F-value</b>	<b>P-value</b>
intercept	37.5	N/A	70.26	<0.0001
pH	-9.464	0.48	14.79	0.0014
Ca <sup>2+</sup> (cmol <sub>c</sub> kg <sup>-1</sup> )	4.459	0.187	11.59	0.0043
CBD Fe (mmol kg <sup>-1</sup> )	0.003	0.108	12.01	0.0042

Table 2.8 Stepwise regression results on the effect of soil properties on PAM (Superfloc A100) effectiveness for soil samples with kaolinite as the dominant clay mineralogy. All other soil properties were not significant at  $p = 0.05$ .

<b>Summary of individual regression analysis</b>			
<b>Variable</b>	<b>Adjusted R<sup>2</sup></b>	<b>t-value</b>	<b>P-value</b>
sand (g kg <sup>-1</sup> )	0.148	-1.99	0.0644
silt (g kg <sup>-1</sup> )	0.004	-1.04	0.3158
clay (g kg <sup>-1</sup> )	0.092	1.65	0.1179
Ca <sup>2+</sup> (cmol <sub>c</sub> kg <sup>-1</sup> )	0.213	-2.37	0.0309
Mg <sup>2+</sup> (cmol <sub>c</sub> kg <sup>-1</sup> )	0.154	-2.02	0.0603
sodium adsorption ratio	0.008	1.07	0.3012
pH	0.448	-3.85	0.0014
organic carbon (g kg <sup>-1</sup> )	0.140	1.94	0.0704
CBD Fe (mmol kg <sup>-1</sup> )	0.000	0.85	0.4066
oxalate Fe (mmol kg <sup>-1</sup> )	0.193	2.25	0.0388

Table 2.9 Summary of individual regression analysis on the effect of soil properties on PAM effectiveness (Superfloc A100) for soil samples with kaolinite as the dominant clay mineralogy.

Summary of stepwise regression				
Variable included	Parameter Estimate	Partial R <sup>2</sup>	F-value	P-value
intercept	2.220	N/A	19.51	0.001
CBD Fe (mmol kg <sup>-1</sup> )	-0.020	0.831	73.7	<0.0001
Ca <sup>2+</sup> (cmol <sub>c</sub> kg <sup>-1</sup> )	-0.297	0.068	9.47	0.0082
pH	0.374	0.046	10.84	0.0058
oxalate Fe (mmol kg <sup>-1</sup> )	0.103	0.030	14.22	0.0027

Table 2.10 Stepwise regression results on the effect of soil properties on PAM effectiveness (Superfloc A100) for soil samples with > 20% smectite or vermiculite clay mineralogy. All other soil properties were not significant at p = 0.05.

<b>Summary of individual regression analysis</b>			
<b>Variable</b>	<b>Adjusted R<sup>2</sup></b>	<b>t-value</b>	<b>P-value</b>
sand (g kg <sup>-1</sup> )	0.584	4.85	0.0002
silt (g kg <sup>-1</sup> )	0.227	-2.39	0.0306
clay (g kg <sup>-1</sup> )	0.612	-5.12	<.0001
Ca <sup>2+</sup> (cmol <sub>c</sub> kg <sup>-1</sup> )	0.000	0.42	0.6790
Mg <sup>2+</sup> (cmol <sub>c</sub> kg <sup>-1</sup> )	0.119	-1.78	0.0956
sodium adsorption ratio	0.046	-1.33	0.2023
pH	0.251	2.52	0.0236
organic carbon (g kg <sup>-1</sup> )	0.002	-1.01	0.3275
CBD Fe (mmol kg <sup>-1</sup> )	0.820	-8.58	<.0001
oxalate Fe (mmol kg <sup>-1</sup> )	0.026	-1.19	0.2517

Table 2.11 Summary of individual regression analysis on the effect of soil properties on PAM effectiveness (Superfloc A100) for soil samples with > 20% smectite or vermiculite clay mineralogy.



<b>Summary of stepwise regression</b>				
<b>Variable included</b>	<b>Parameter Estimate</b>	<b>Partial R<sup>2</sup></b>	<b>F-value</b>	<b>P-value</b>
sand (g kg <sup>-1</sup> )	0.004	0.617	45.1	<0.0001
mica (1-2 μm)	-17.934	0.187	25.8	<0.0001
mica (< 1 μm)	27.018	0.125	45.9	<0.0001
smectite (< 1 μm)	1.055	0.042	37.2	<0.0001
sodium adsorption ratio	-0.217	0.005	5.13	0.0328

Table 2.12 Stepwise regression results on the effect of soil properties on PAM effectiveness (Superfloc A100) for all 13 NC DOT soil samples. All other soil properties were not significant at p = 0.05.

	<b>variable</b>	sand	silt	clay	Ca <sup>2+</sup>	Mg <sup>2+</sup>	SAR	pH	organic carbon	smectite (< 1 μm)
r-value	sand	1.000	-0.776	-0.821	0.505	-0.309	0.121	0.488	-0.118	0.659
p-value		0.000	0.002	0.001	0.079	0.305	0.695	0.091	0.702	0.038
	<b>variable</b>	smectite (1-2 μm)	vermiculite (< 1 μm)	vermiculite (1-2 μm)	mica (< 1 μm)	mica (1-2 μm)	kaolinite (< 1 μm)	kaolinite (1-2 μm)	oxalate Fe	CBD Fe
r-value	sand	0.586	0.200	0.232	0.548	0.377	-0.902	-0.872	-0.484	-0.823
p-value		0.075	0.580	0.519	0.101	0.283	0.000	0.001	0.111	0.001

Table 2.13 Pearson correlation coefficients for sand correlation to all other soil properties.

<b>Summary of individual regression analysis</b>			
<b>Variable</b>	<b>Adjusted R<sup>2</sup></b>	<b>t-value</b>	<b>P-value</b>
sand (g kg <sup>-1</sup> )	0.567	7.13	<0.0001
silt (g kg <sup>-1</sup> )	0.503	-6.28	<0.0001
clay (g kg <sup>-1</sup> )	0.245	-3.65	0.0008
Ca <sup>2+</sup> (cmol <sub>c</sub> kg <sup>-1</sup> )	0.073	2.00	0.0534
Mg <sup>2+</sup> (cmol <sub>c</sub> kg <sup>-1</sup> )	0.152	-2.80	0.0081
sodium adsorption ratio	0.000	0.93	0.3564
pH	0.111	2.40	0.0216
organic carbon (g kg <sup>-1</sup> )	0.000	0.94	0.353
CBD Fe (mmol kg <sup>-1</sup> )	0.334	-4.48	<0.0001
oxalate Fe (mmol kg <sup>-1</sup> )	0.132	-2.51	0.0169
vermiculite (<1 μm)	0.219	3.02	0.0053
mica (< 1 μm)	0.054	1.63	0.1148
kaolinite (< 1 μm)	0.537	-5.88	<0.0001
smectite (< 1 μm)	0.130	2.31	0.0284
vermiculite (1-2 μm)	0.248	3.25	0.003
mica (1-2 μm)	0.000	-0.56	0.5824
kaolinite (1-2 μm)	0.436	-4.84	<0.0001
smectite (1-2 μm)	0.051	1.60	0.1199

Table 2.14 Summary of individual regression analysis on the effect of soil properties on PAM effectiveness (Superfloc A100) for all 13 NC DOT soil samples.

# Combined Gypsum and PAM Treatment

## Introduction

Previous laboratory testing using PAM resulted in considerable turbidity reduction in soil suspensions (Chapter 2). However, reductions in turbidity with PAM were not similar for all soils, and some soils did not respond at all to PAM treatments. Six of the thirteen soils tested reached the 50 NTU standard with 30 seconds of settling time. The majority of Coastal Plain soils did not flocculate well with PAM treatments (3 of 4). In addition, three of five soils from the Piedmont and one of four soils from the Mountain Region did not reach 50 NTU with the addition of PAM. These recalcitrant soils had more 2:1 clays (vermiculite and smectite) than soil samples that had turbidity reductions achieving 50 NTU (Table 3.1).

Gypsum has shown to be effective in reducing the turbidity of construction site runoff in sediment basins (Przepiora et al., 1998). Gypsum can be an effective flocculant when used alone, although application rates are high ( $\geq 22$  lb/1000 ft<sup>3</sup> ( $\geq 350$  mg L<sup>-1</sup>)) and settling times are long ( $\geq 3$  hours) in order to reach the 50 NTU water quality standard (Przepiora et al., 1997). Sulfate levels in discharge water cannot exceed 250 mg L<sup>-1</sup> (NC DENR, 2002), a level that was exceeded in all eleven reported field experiments using gypsum (Przepiora et al., 1998).

Combined treatment of PAM and electrolytes (e.g. gypsum, alum) has been used in water treatment and it is a possible solution to construction site runoff turbidity (Barvenik, 1994). In agricultural field studies, combined treatment led to improvements in soil properties greater than either treatment alone. Infiltration increased 7-8 fold; soil sealing, percent runoff, and turbidity of runoff water were all decreased more than control

treatments or PAM treatment alone with the addition of PAM plus gypsum. (Shainberg et al., 1990; Shainberg and Levy, 1994; Levin et al., 1991, Shainberg et al., 1992, Smith et al., 1990). Shainberg and Levy, (1994) concluded that when anionic polymers (PAM) are used in erosion control, their efficacy is enhanced with the addition of electrolytes. Ben-Hur et al., (1992) stated that anionic polymers are repelled by the similarly charged clay surfaces and little adsorption occurs in suspension unless an electrolyte source is present. In contrast, Peng and Di (1994) showed that multivalent cations in solution decreased PAM efficacy in flocculation of kaolinitic soils. They said that the mechanism causing decreased PAM efficacy was the adsorption of  $\text{Ca}^{2+}$  and  $\text{Ca}(\text{OH})^+$  on anionic PAM, which blocked the interactions between PAM and kaolinite (Ligand exchange). The neutralization of PAM by  $\text{Ca}^{2+}$  was also believed to cause the polymer to coil in suspension making it less effective as a flocculant (Peng and Di, 1994).

In 2:1 clays, cation bridging may be a major factor in polymer adsorption by soil (Laird, 1997; Theng 1982; Aly and Letey 1988). Negatively charged PAM would be expected to be repulsed from negatively charged clay surfaces, but through a phenomenon known as cation-bridging PAM is attracted to clay surfaces (Green et al., 2000; Lentz, 1996). Cation-bridging occurs when the negative clay surface charge is screened by high electrolyte concentrations or when multivalent cations are present on the clay surfaces. The multivalent cations act as bridges between the anionic groups of the polymer and the negative clay surfaces. In the presence of electrolytes, the negative charge and the thickness of the diffuse double layer at the clay and polymer surfaces are suppressed, resulting in decreased repulsion forces and greater adsorption (Shainberg and

Levy, 1994). We conducted experiments to determine if adding an electrolyte would enhance flocculation with PAM, using gypsum as the electrolyte source.

## Materials and Methods

A soil sample from NC DOT Division 8 (Piedmont) was selected to perform replicated tests of PAM/gypsum interactions in order to conduct statistical analyses. An evaluation of the efficacy of combined PAM and gypsum application was performed on six additional North Carolina soils without replication to see if the trends observed in the replicated tests were similar for other soils. Soil samples used in additional evaluations were from Highway Divisions: 1, 2, 3, 4, 11, and 13 represent a wide range of soil properties from around the state (Fig. 3.1).

In all tests the gypsum used was construction grade material (88% pure) from a local building supply retailer. The concentrations of gypsum used for sample 8 were 0, 10, 20, 50 and 100 mg L<sup>-1</sup> (0.1, 0.2, 0.5 and 1 kg m<sup>-3</sup>).

In the evaluation of the six additional North Carolina soils, the gypsum levels were 5, 50, and 200 mg L<sup>-1</sup>. PAM used in the evaluation of soil sample 8 was both in granular and solid block form (Applied Polymer Systems). The PAM products used were: Superfloc A110 (Cytec Industries, West Paterson, NJ, USA), Chemtall 923 VHM (Chemtall Inc., Riceboro, GA, USA), Soilfix Polybead (Ciba Specialty Chemicals, Suffolk, VA, USA), and APS 705 (granular) and APS 706b (solid block) (Applied Polymer Systems Inc., Woodstock, GA, USA). Properties for the polymers used in this experiment are listed in table 3.2. The PAM product used in the evaluation of the six additional North Carolina soils was Cytec Superfloc A100 (Table 3.2) and was applied at 0, 0.5 and 1 mg L<sup>-1</sup>.

Each polymer was first weighed and then added to turbulent (magnetically-stirred) distilled water. PAM solutions (0.1%) were allowed to mix for at least 24 hours

at room temperature. PAM solutions were added by a pipette to the soil suspension immediately after pouring 100 ml of distilled water over 5 g air-dried soil, for final concentrations of 0, 0.05, 0.125, 1 and 2 mg L<sup>-1</sup> in the mixture. Each soil suspension with PAM and gypsum was shaken for 10 seconds by hand. A nephelometer (Analite 152, McVan Instruments, Mulgrave, Australia) probe was inserted into the solution 20 seconds after shaking and nephelometric turbidity unit (NTU) reading was taken 10 seconds later.



## Results and Discussion

In tests of the single component PAMs, gypsum usually increased turbidity significantly ( $p=0.05$ ) with no or low PAM concentrations ( $<1 \text{ mg L}^{-1}$ ) (Fig. 3.2-3.6). However, the turbidity of a soil suspension should decrease with the addition of a divalent cation such as gypsum (Sposito, 1984). It is possible that the addition of gypsum (no PAM) caused an increase in soil particle size (increasing light scattering and turbidity) but particles were not large enough to settle in the specified time (30 sec). However, as the PAM concentration approached  $1 \text{ mg L}^{-1}$ , differences in turbidity reduction due to gypsum concentration were no longer present. At higher PAM concentrations, soil particles were bridged by PAM which led to rapid flocculation. At the highest concentration of PAM ( $5 \text{ mg L}^{-1}$ ), increasing the gypsum concentration significantly (Tukey,  $p = 0.05$ ) reduced turbidity (Fig. 3.2-3.4). However, increasing gypsum concentrations above  $50 \text{ mg L}^{-1}$  does not appear to have any significant effect.

Chemtall 923 VHM (30% c.d.,  $14\text{-}17.5 \text{ Mg Mole}^{-1}$ ) had the most significant diminished PAM effect of all PAMs tested (Fig. 3.7-3.10) at the highest PAM concentration ( $5 \text{ mg L}^{-1}$ ). The optimal PAM for turbidity reduction was APS 705 (mixed polymer) at a concentration of  $5 \text{ mg L}^{-1}$  with a gypsum rate of 25 or  $50 \text{ mg L}^{-1}$ . The turbidity of this combination resulted in turbidity reduction from 1780-1900 NTU down to 28-45 NTU. This combination was significantly better than any other polymer or combined treatment ( $p = 0.05$ ).

Gypsum diminished the flocculation effectiveness of PAM at low PAM concentrations. The negative effect below PAM concentrations of  $1 \text{ mg L}^{-1}$  is similar to the effect seen by Peng and Di (1994) where multivalent cations in solution decreased

PAM efficacy in flocculation of kaolinitic soils. The mechanism is believed to be  $\text{Ca}^{2+}$  adsorption on the carboxylic ( $\text{R-COO}^-$ ) functional group of PAM to form  $(\text{R-COO})_2\text{Ca}$ , which diminishes repulsive forces between functional groups and decreases polymer extension in solution. Orts et al. (1999) also stated that neutron scattering pattern of Cytec Superfloc A110 (18% c.d.,  $15 \text{ Mg mole}^{-1}$ ) suggests that the radius of gyration of the polymer chain in water decreases almost linearly with increasing concentration of calcium in solution. In addition, complexation of  $\text{Ca}^{2+}$  to carboxyl groups inhibits ligand exchange.

Gypsum improved the performance of PAM at high concentrations ( $>1 \text{ mg L}^{-1}$ ). With no gypsum application, an increase in PAM (Superfloc A110) concentration from 1 to  $5 \text{ mg L}^{-1}$  resulted in a turbidity increase from 123 to 640 NTU. At a gypsum concentration of  $100 \text{ mg L}^{-1}$ , the same increase in concentration from 1 to  $5 \text{ mg L}^{-1}$  only caused an increase in turbidity from 93 to 168 NTU.

The lack of diminished PAM effect at high PAM concentrations due to the addition of gypsum for several reasons. Gypsum causes  $\text{Ca}^{2+}$  complexation of polymer carboxyl groups (Peng and Di, 1994; Laird, 1997). The decrease in negative intramolecular charge causes a decrease in polymer extension, and possibly a decrease in solution viscosity. The addition of gypsum may destabilize soil colloids, causing them to complex with PAM more readily. Gregory (1989) reported that in some cases adding salts (especially sulfates) will cause flocculation of stabilized colloid systems. This flocculation effect is seen in Figures 3.2-3.4 at the highest PAM concentration ( $5 \text{ mg L}^{-1}$ ). In these experiments gypsum ( $\text{CaSO}_4 \cdot 2\text{H}_2\text{O}$ ) was added to the soil suspension, and with increasing salt concentration there was increased flocculation.

PAM products sold by Applied Polymer Systems are combinations of multiple polymers and in some cases coagulants. Application with APS 705 was the optimal PAM treatment with no diminished flocculation with concentrations up to  $5 \text{ mg L}^{-1}$ . APS 705 at the highest concentration ( $5 \text{ mg L}^{-1}$ ) was significantly more effective than any single PAM product at all gypsum application rates (Fig. 3.7-3.11). The APS 706b solid block material was much less effective than granular PAM (Fig. 3.6). In all cases, the PAM was weighed and dissolved in water prior to the testing, so it is possible that the block form had a greatly reduced PAM content. Granular PAM consists of approximately 90% active ingredients (PAM), the remainder being water, processing aids, and buffers (Barvenik, 1994). APS 706b contains a lower percentage PAM than granular form (between 5 and 85% PAM, Steve Iwinski, APS, pers. Comm.) and as a result would require a higher application rates in order to reach optimal levels of flocculation. No diminished effect or plateau in turbidity reduction was reached, even at the highest concentration ( $5 \text{ mg L}^{-1}$ ) of log material. Optimal turbidity reductions with APS 706b may be reached above 5 mg of log per liter. APS 706b reportedly contains a coagulant (salt) along with two types of polymer (Steve Iwinski, APS, pers. comm.). It is also possible that these PAMs are not as effective as the others included in the tests. The addition of gypsum at any concentration had no beneficial effect on APS 706b performance, possibly because of the presence of an electrolyte source in the solid blocks. APS 706b was significantly less effective as a flocculant than single PAMs at concentrations less than or equal to  $1 \text{ mg L}^{-1}$  at any gypsum concentration (Fig. 3.7-3.10).

In the evaluation of other soil samples, the soils from the mountain region responded in a manner similar to the Piedmont soil (soil 8). In both cases, the addition of

gypsum negatively affected the performance of PAM in reducing turbidity (Fig. 3.12-3.13).

In soils from the Coastal Plain there was a positive combined PAM and gypsum effect. In most soil samples from the Coastal Plain Region, PAM plus gypsum in initial testing resulted in turbidity reductions of 50 to 1000 NTU greater than PAM alone (Fig 3.14-3.16), with increasing gypsum concentrations improving PAM performance measurably. Soil samples taken from the Coastal Plain Region contain large amounts of smectite and vermiculite in the clay fraction. The primary binding mechanism to these clays has been reported to be cation bridging (Laird, 1997; Ben-Hur et al., 1992; Aly and Letey, 1988; Nadler and Letey, 1989; Green et al., 2000; Orts et al., 1999; Sojka and Lentz, 1997). Gypsum provided the divalent cations required for cation bridging. In contrast, soils from the Piedmont and Mountain Regions, which had limited benefit from gypsum application, are dominated by kaolinite and illite. Soil 3 (Coastal Plain) was an exception, with little or no improved turbidity reduction with the addition of gypsum to PAM (Fig. 3.17). Soil 3 is similar to other Coastal Plain soils in most properties (Table 3.3), but the turbidity produced in our tests was much lower for this soil compared to the others. Although there was no positive combined gypsum plus PAM effect, there were no negative effects as was evident for soils 8, 11, and 13 (Fig. 3.2, 3.12, 3.13). Therefore, the use of gypsum on Coastal Plain soils to improve PAM performance would still be recommended. Overall, the combined treatment of PAM plus gypsum did not reduce the turbidity of Coastal Plain soils to the 50 NTU standard within 30 seconds settling time. The addition of gypsum may improve PAM performance in reducing

turbidity if longer settling times are imposed, but additional testing is needed to validate this hypothesis.

## Conclusions

In our laboratory tests, PAM substantially reduced the turbidity of soil suspensions, particularly for our Piedmont and Mountain region soils. However, in many cases there is an optimal dose of PAM, usually around  $1 \text{ mg L}^{-1}$ , above which turbidity polymer effectiveness diminishes. We found that adding gypsum to these suspensions decreases PAM performance below  $1 \text{ mg L}^{-1}$ , but appears to improve performance at higher PAM concentrations. For several Coastal Plain soils, which did not respond as well to PAM, the addition of gypsum improved PAM effectiveness in reducing turbidity. When PAM concentrations used in field application may exceed optimal levels ( $1 \text{ mg L}^{-1}$ ), and the addition of gypsum may be a more effective treatment than PAM alone. There was no significant improvement with gypsum concentrations greater than  $50 \text{ mg L}^{-1}$  with any PAM product. Keeping the gypsum application at or below  $50 \text{ mg L}^{-1}$  would yield a  $\text{SO}_4^{2-}$  concentration that is  $\geq 5$ -fold less than the  $250 \text{ mg L}^{-1}$  water quality requirements in North Carolina.

A mixed polymer available commercially (Applied Polymer Systems 705) had a similar effect in reducing turbidity in Coastal Plain soils as a combined treatment of gypsum and single component PAM. Additional testing with polymer/electrolyte mixtures should be performed to see if combinations exist that can reduce the turbidity of all soil suspensions in North Carolina to the 50 NTU water quality standard.

## References

- Alley, S.M. and J. Letey. 1988. Polymer and water quality effects on flocculation of montmorillonite. *Soil Sci. Soc. Am. J.* 52:1453-1458.
- Barvenik, F.W. 1994. Polyacrylamide characteristics related to soil applications. *Soil Sci.* 158:235-243.
- Ben-Hur, M., M. Malik, J. Letey, and U. Mingelgrin. 1992. Adsorption of polymers on clays as affected by clay charge and structure, polymer properties, and water quality. *Soil Sci.* 153:349-356.
- Green, S.V., D.E. Stott, L.D. Norton, and J.G. Graveel. 2000. Polyacrylamide molecular weight and charge effects on infiltration under simulated rainfall. *Soil Sci. Soc. Am. J.* 64:1786-1791.
- Gregory, J. 1989. Fundamentals of flocculation. *Crit. Rev. Environ. Control.* 19:185-230.
- Iwinski, S. Personal Communication. *Applied Polymer Systems.* (June 4, 2003 12:06pm)
- Laird, D.A. 1997. Bonding between polyacrylamide and clay mineral surfaces. *Soil Sci.* 162:826-832.
- Lentz, R.D., R.E. Sojka, and J.A. Foerster. 1996. Estimating polyacrylamide concentration in irrigation water. *J. Environ. Qual.* 25:1015-1024.
- Levin, J., M. Ben-Hur, M. Gal, and G.J. Levy. 1991. Rain energy and soil amendments effects on infiltration and erosion of three different soil types. *Aust. J. Soil Res.* 29:455-465.
- Nadler, A and J. Letey. 1989. Adsorption isotherms of polyanions on soils using tritium labeled compounds. *Soil Sci. Soc. Am. J.* 53:1375-1378.
- North Carolina Department of Environment and Natural Resources. 2002. Administrative code section 15ANCAC 02B .0211. Fresh surface water quality standards for class c waters. NC DENR, Div. Of Environmental Management, Raleigh, NC.
- Orts, W.J., R.E. Sojka, G.M. Glenn, and R.A. Gross. 1999. Preventing soil erosion with polymer additives. *Polymer News.* 24:406-413.
- Peng, F.F., and P. Di. 1994. Effect of multivalent salts—calcium and aluminum on the flocculation of kaolin suspension with anionic polyacrylamide. *J. Colloid Interface Sci.* 164:229-237.

- Przepiora, A., D. Hesterberg, J.E. Parsons, J.W. Gilliam, D.K. Cassel, and W. Faircloth. 1997. Calcium sulfate as a flocculant to reduce sedimentation basin water turbidity. *J. Environ. Qual.* 26:1605-1611.
- Przepiora, A., D. Hesterberg, J.E. Parsons, J.W. Gilliam, D.K. Cassel, and W. Faircloth. 1998. Field evaluation of calcium sulfate as a Chemical Flocculant for Sedimentation Basins. *J. Environ. Qual.* 27:669-678.
- Shainberg, I. and G.J. Levy. 1994. Organic polymers and soil sealing in cultivated soils. *Soil Sci.* 158:267-273.
- Shainberg, I., G.J. Levy, P. Rengasamy, and H. Frenkel. 1992. Aggregate stability and seal formation as affected by drops' impact energy and soil amendments. *Soil Sci.* 154:113-119.
- Shainberg, I., D.N. Warrington, and P. Rengasamy. 1990. Water quality and PAM interactions in reducing surface sealing. *Soil Sci.* 149:301-307.
- Smith, H.J.C., G.J. Levy, and I. Shainberg. 1990. Water-Droplet energy and soil amendments: effect on infiltration and erosion. *Soil Sci. Soc. Am. J.* 54:1084-1087.
- Sojka, R.E., and R.D. Lentz. 1997. Reducing Furrow Irrigation Erosion with Polyacrylamide (PAM). *J. Prod. Agric.* 10:47-51.
- Sposito, G. 1984. *The surface chemistry of soils.* Oxford Univ. Press. NY.
- Theng, B.K.G. 1982. Clay-Polymer interactions: summary and perspectives. *Clays Clay Min.* 30:1-10.



## NCDOT Divisions

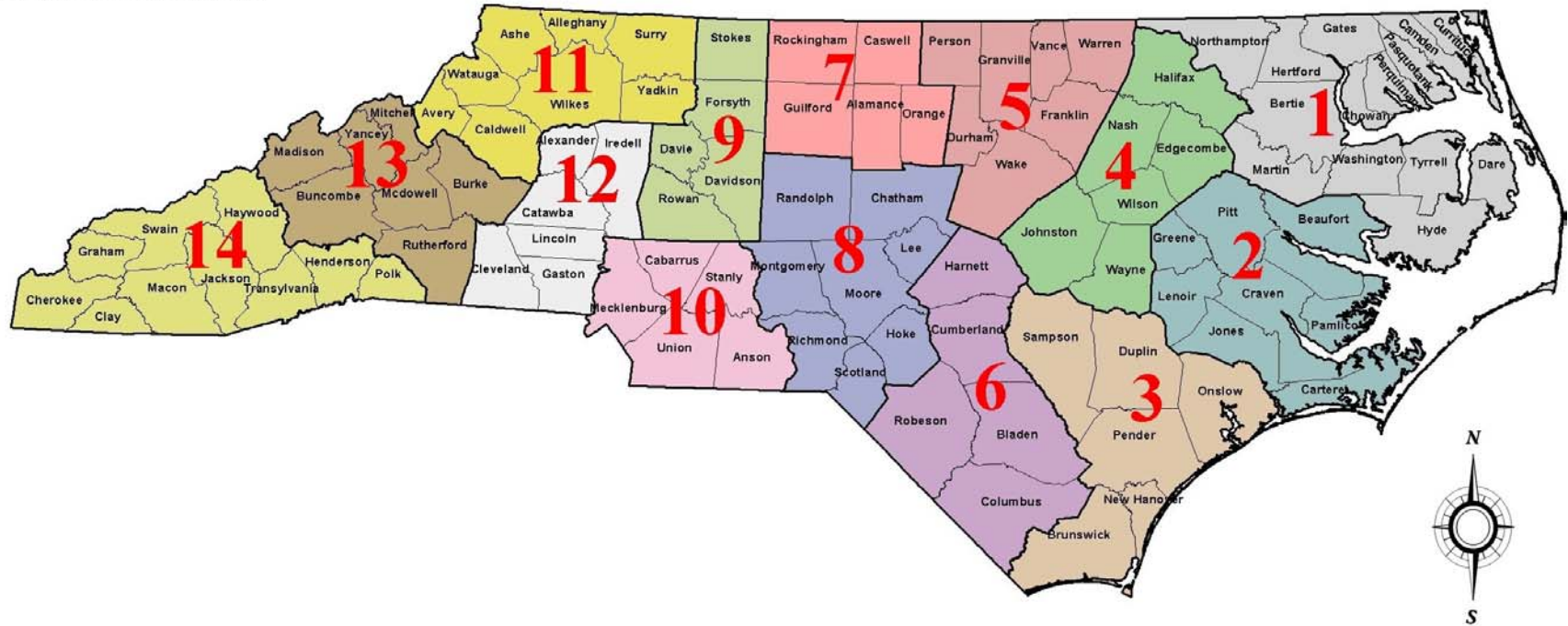


Figure 3.1 Soil sample numbers coincide with the highway division they originated from. Soil samples used in gypsum evaluation came from 1, 2, 3, 4, 8, 11 and 13 (NCDOT Divisions).

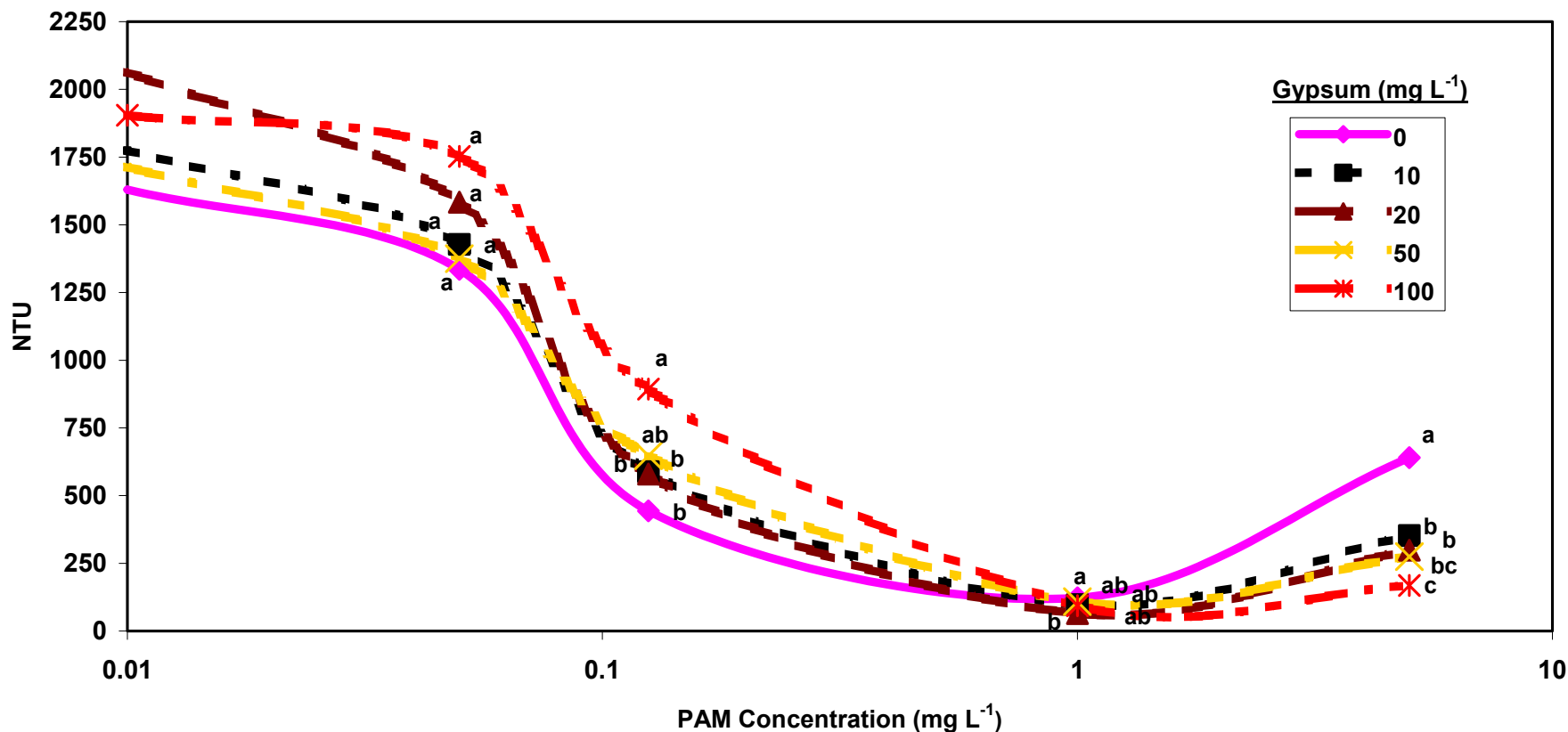


Figure 3.2 Turbidity reduction as a function of input PAM concentration. Flocculation by Superfloc A110 (18% charge density, 15 Mg mol<sup>-1</sup> molecular weight) alone and with gypsum at four different concentrations on soil 8. For each PAM concentration, data points with different letters are significantly different ( $p = 0.05$ ). The “0” data point for PAM is graphed at 0.01 due to limitations in using a linear-log scale.

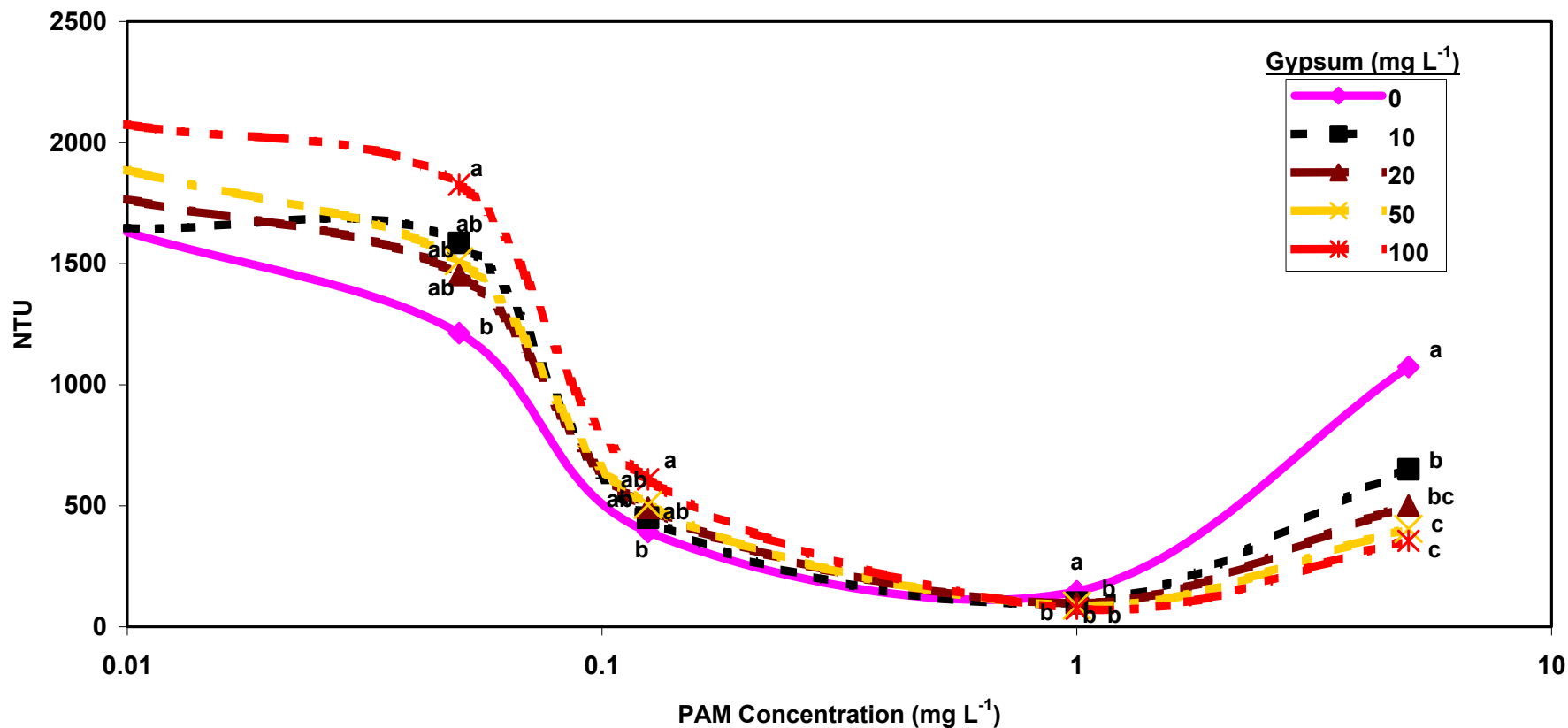


Figure 3.3 Turbidity reduction as a function of input PAM concentration. Flocculation by Chemtall 923VHM (30% charge density, 14-17.5 Mg mol<sup>-1</sup> molecular weight) alone and with gypsum at four different concentrations on soil 8. For each PAM concentration, data points with different letters are significantly different ( $p = 0.05$ ). The “0” data point for PAM is graphed at 0.01 due to limitations in using a linear-log scale.

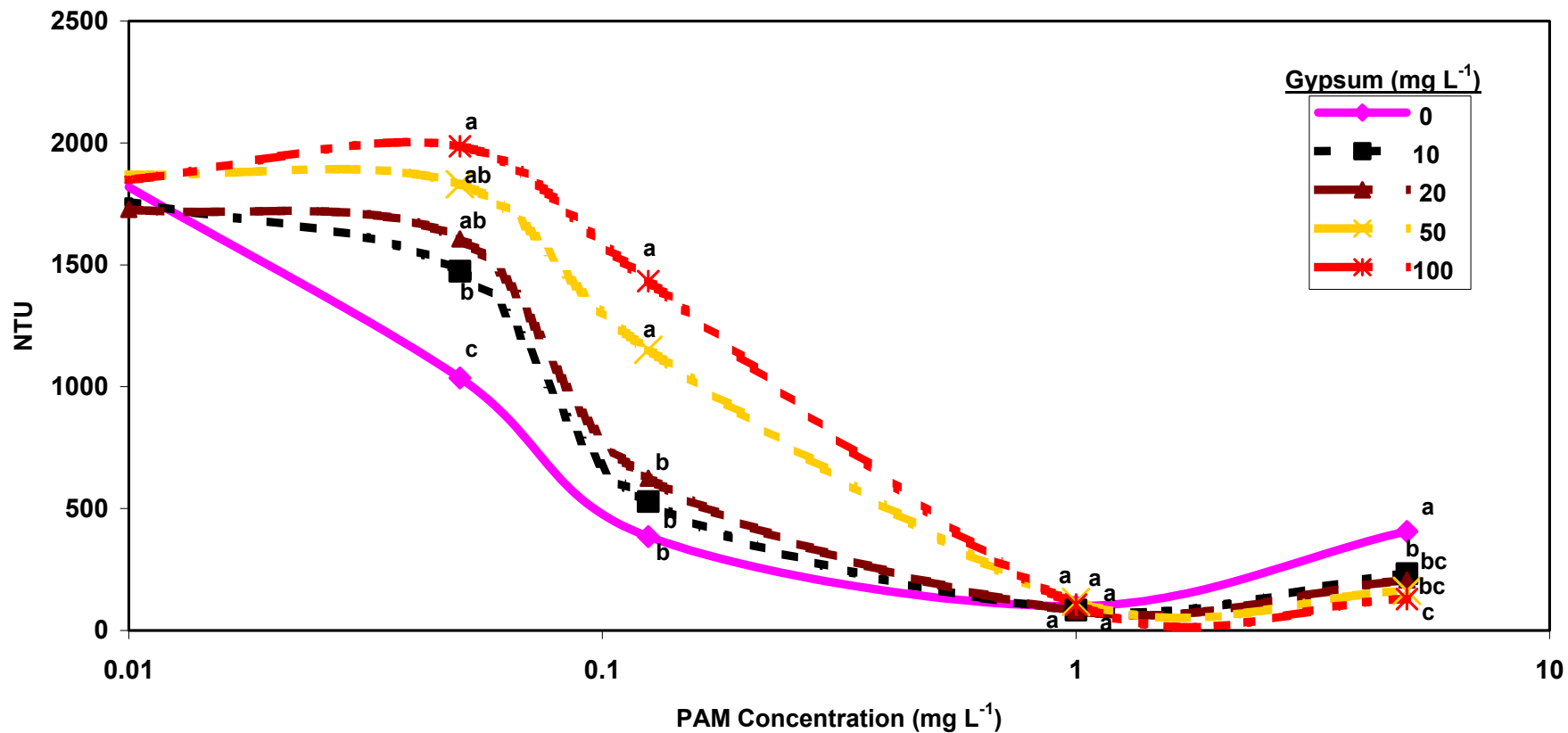


Figure 3.4 Turbidity reduction as a function of input PAM concentration. Flocculation by Ciba Soilfix (30% charge density, 15 Mg mol<sup>-1</sup> molecular weight) alone and with gypsum at four different concentrations on soil 8. For each PAM concentration, data points with different letters are significantly different (p = 0.05). The “0” data point for PAM is graphed at 0.01 due to limitations in using a linear-log scale.

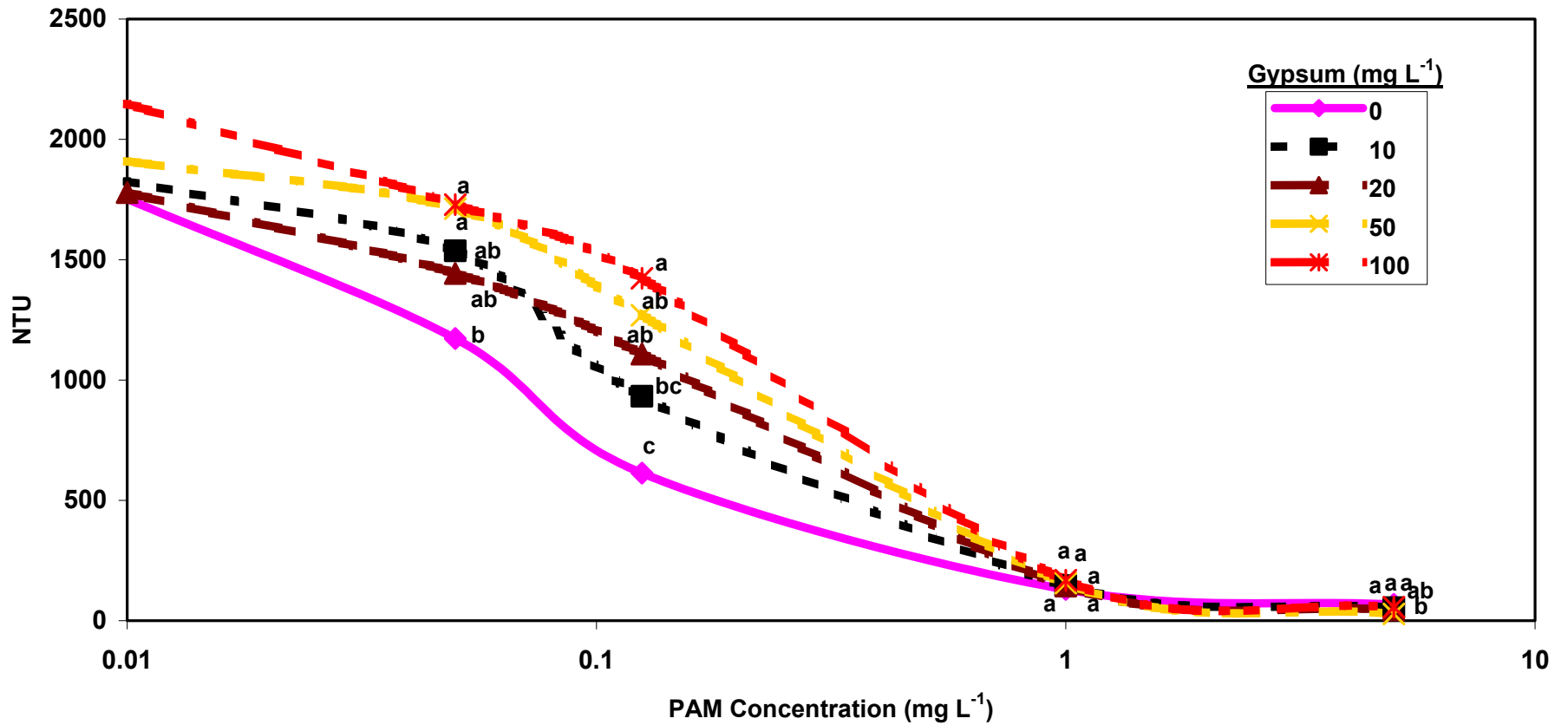


Figure 3.5 Turbidity reduction as a function of input PAM concentration. Flocculation by APS 705 (mixed charge density, mixed molecular weight) alone and with gypsum at four different concentrations on soil 8. For each PAM concentration, data points with different letters are significantly different ( $p = 0.05$ ). The “0” data point for PAM is graphed at 0.01 due to limitations in using a linear-log scale.

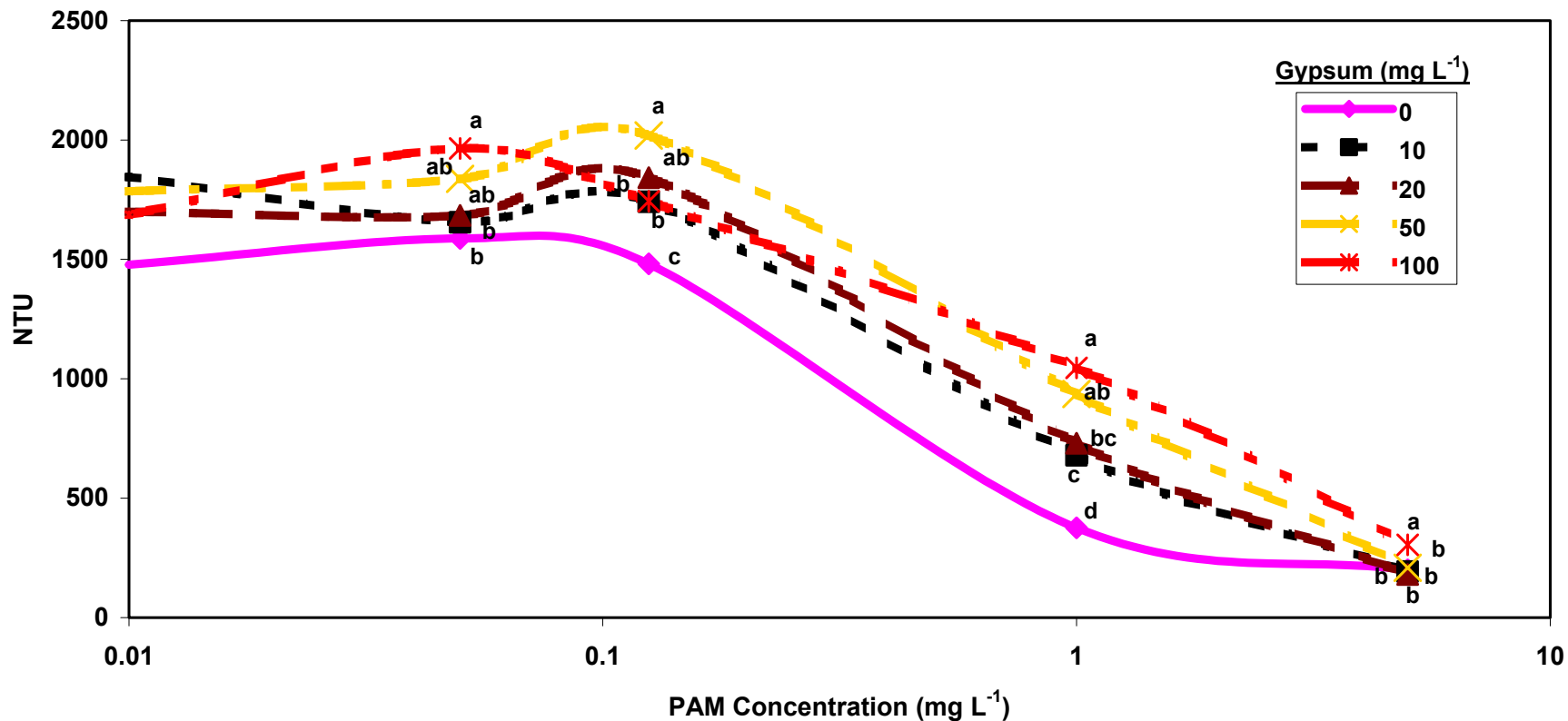


Figure 3.6 Turbidity reduction as a function of input PAM concentration. Flocculation by APS 706b (block) (mixed charge density, mixed molecular weight) alone and with gypsum at four different concentrations on soil 8. For each PAM concentration, data points with different letters are significantly different ( $p = 0.05$ ). The “0” data point for PAM is graphed at 0.01 due to limitations in using a linear-log scale.

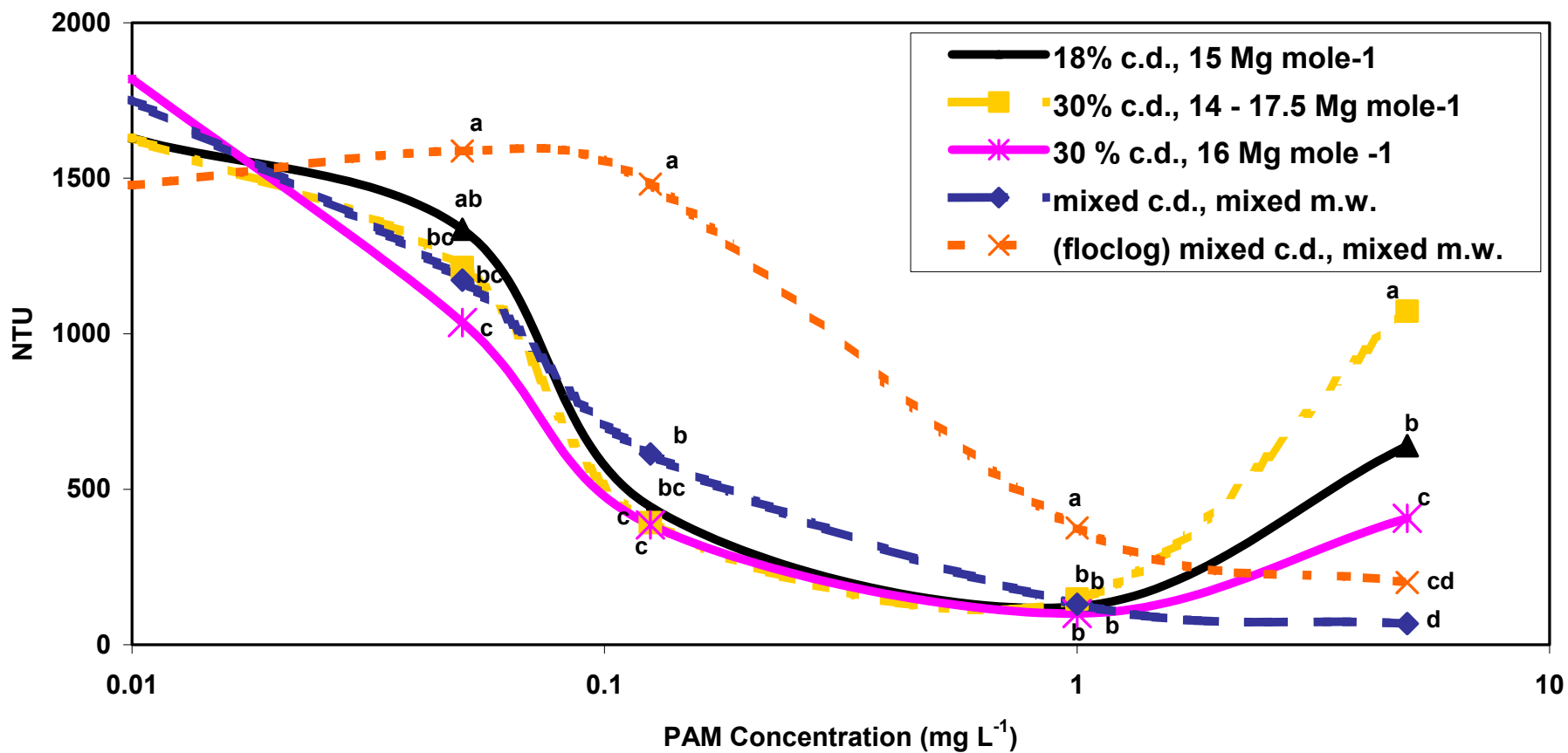


Figure 3.7 Turbidity reduction as a function of input PAM concentration with no gypsum and 5 different PAM products on soil 8. For each PAM concentration, data points with different letters are significantly different ( $p = 0.05$ ). The “0” data point for PAM is graphed at 0.01 due to limitations in using a linear-log scale.

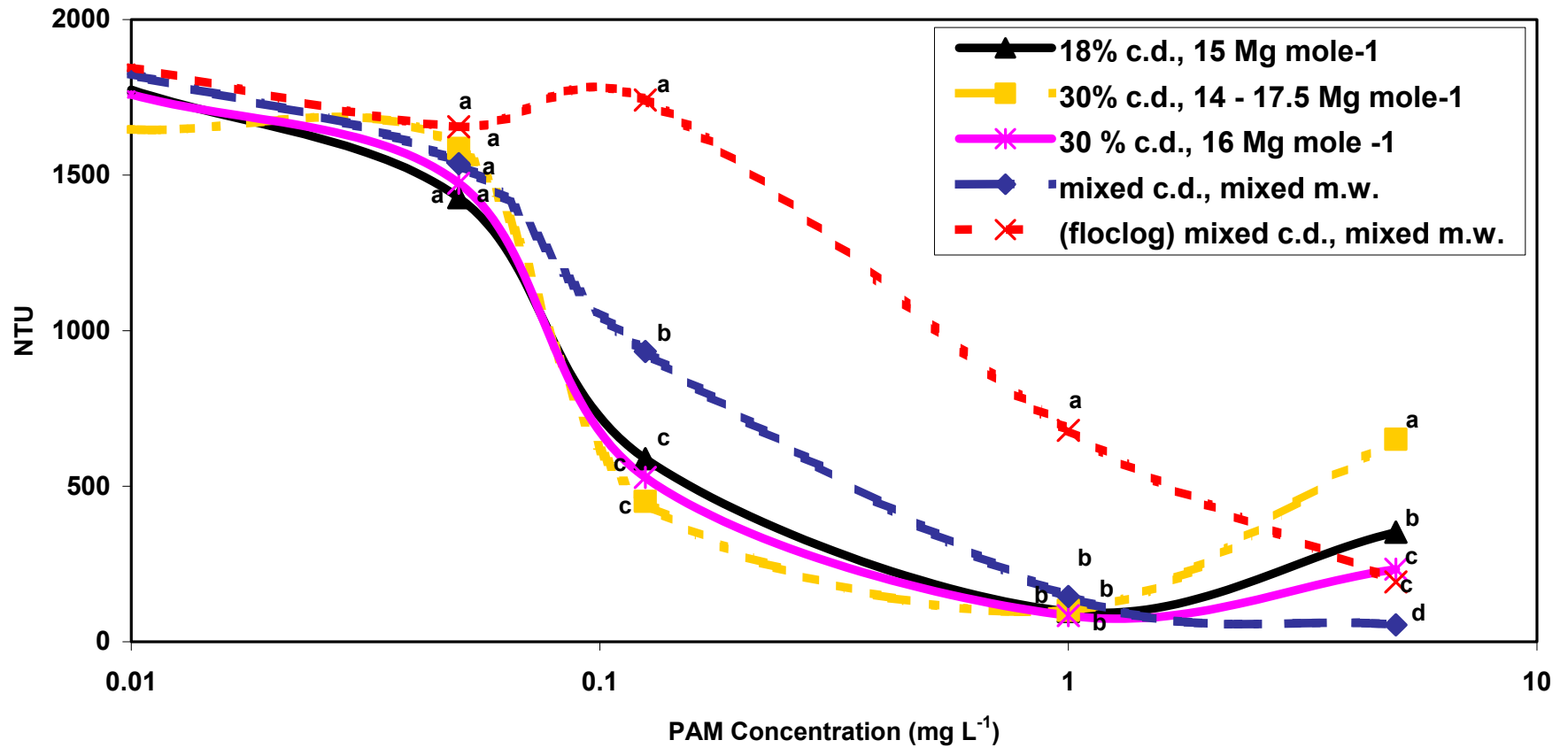


Figure 3.8 Turbidity reduction as a function of input PAM concentration with 10 mg L<sup>-1</sup> gypsum and 5 different PAM products on soil 8. For each PAM concentration, data points with different letters are significantly different ( $p = 0.05$ ). The “0” data point for PAM is graphed at 0.01 due to limitations in using a linear-log scale.



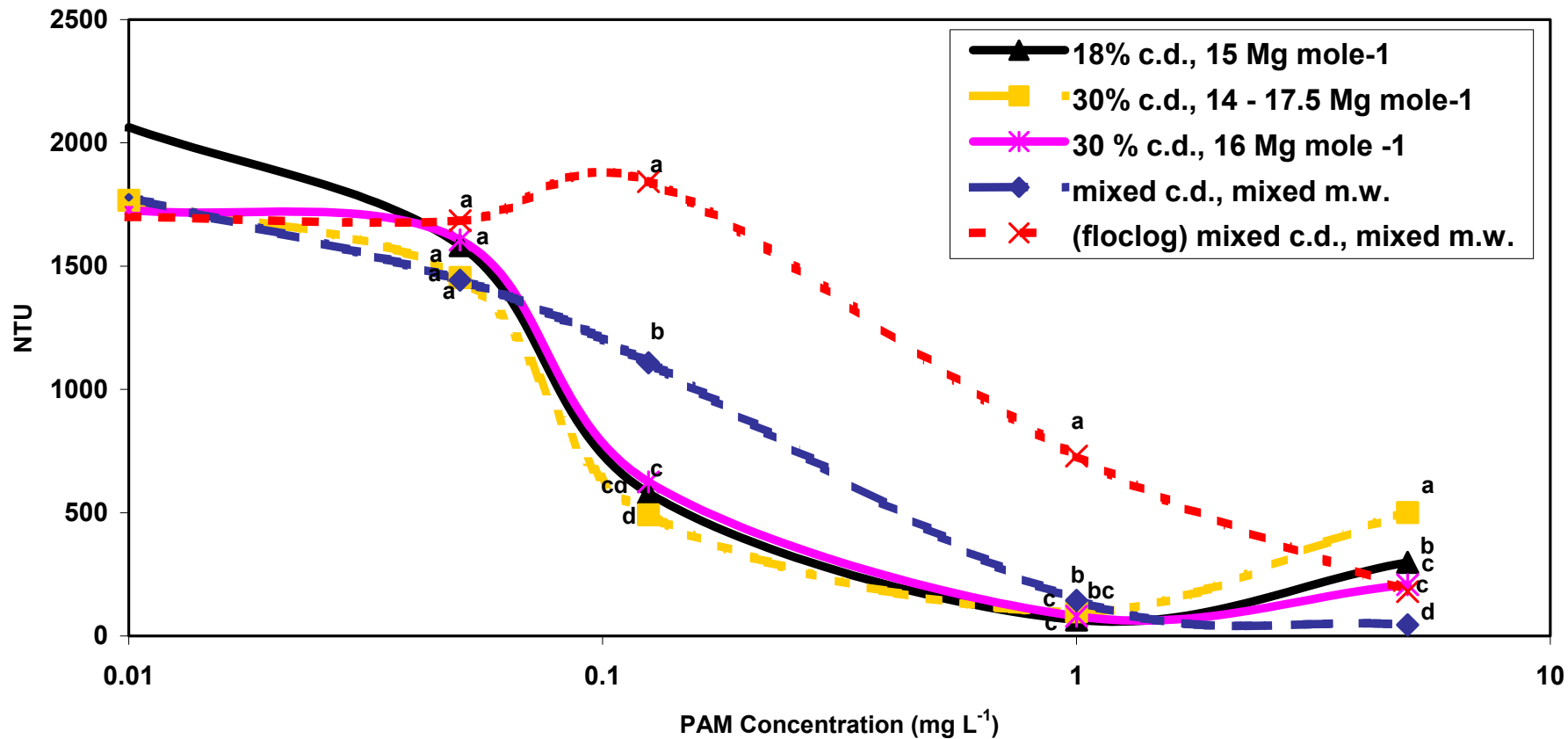


Figure 3.9 Turbidity reduction as a function of input PAM concentration with 20 mg L<sup>-1</sup> gypsum and 5 different PAM products on soil 8. For each PAM concentration, data points with different letters are significantly different ( $p = 0.05$ ). The “0” data point for PAM is graphed at 0.01 due to limitations in using a linear-log scale.

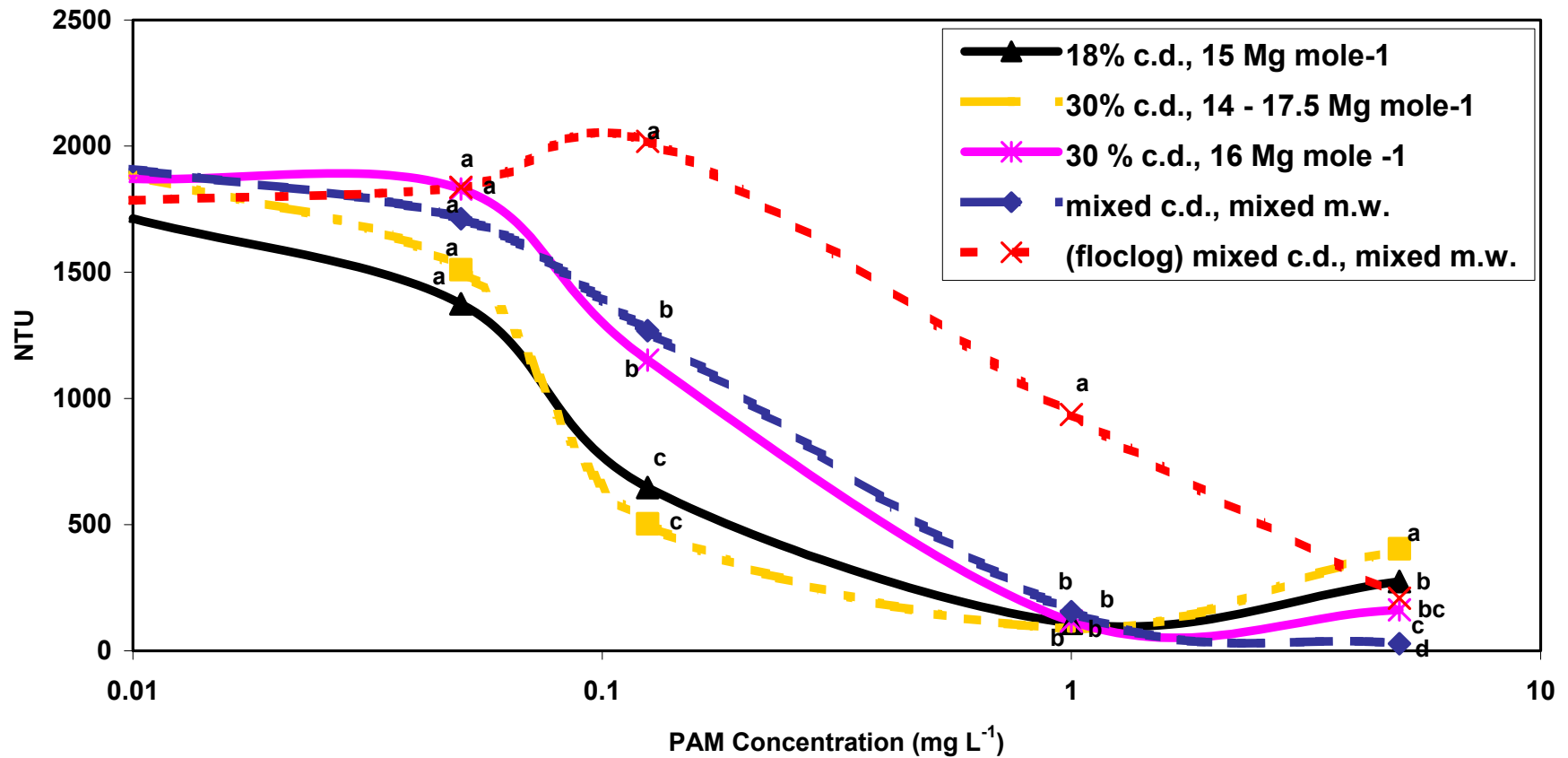


Figure 3.10 Turbidity reduction as a function of input PAM concentration with 50 mg L<sup>-1</sup> gypsum and 5 different PAM products on soil 8. For each PAM concentration, data points with different letters are significantly different ( $p = 0.05$ ). The “0” data point for PAM is graphed at 0.01 due to limitations in using a linear-log scale.

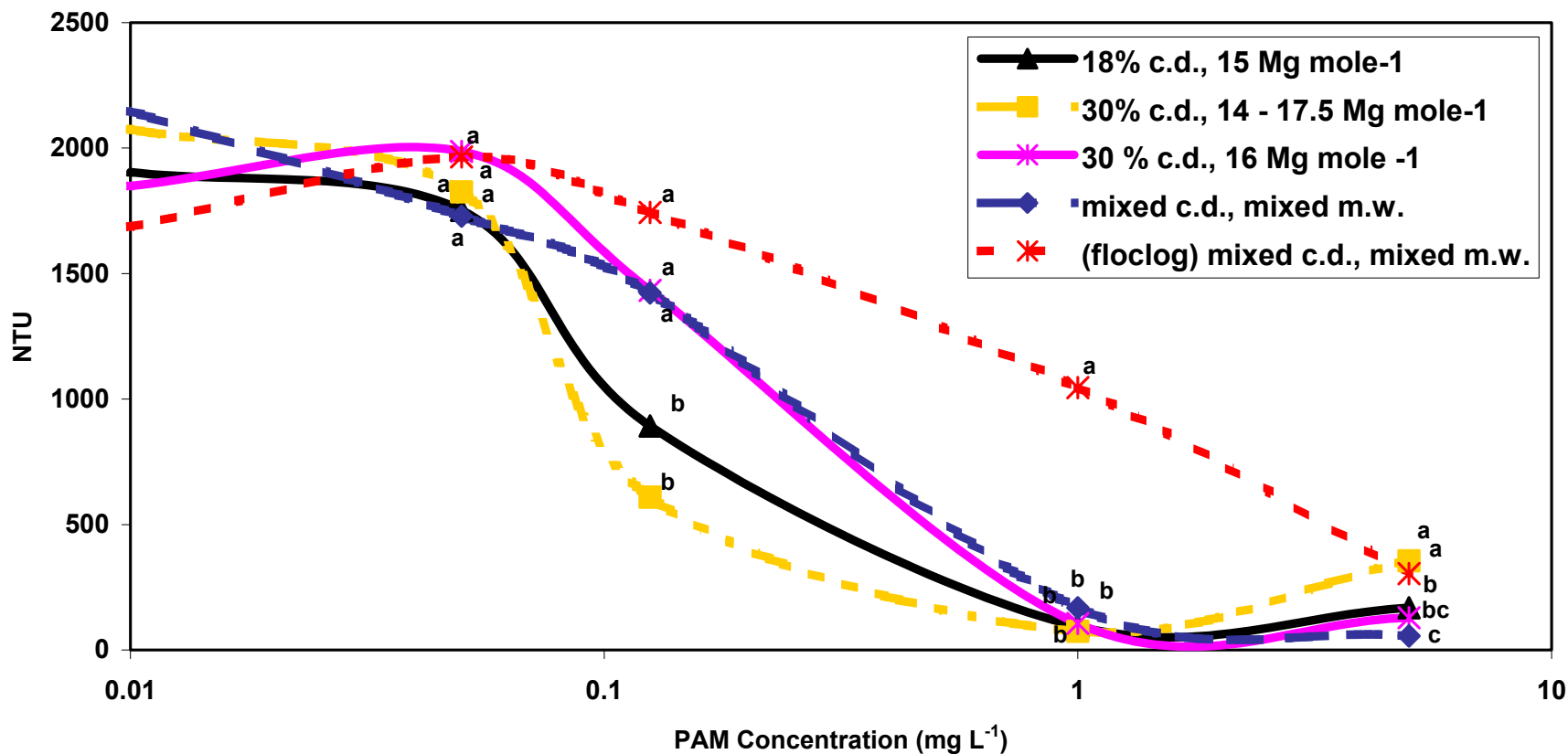


Figure 3.11 Turbidity reduction as a function of input PAM concentration with 100mg L<sup>-1</sup> gypsum and 5 different PAM products on soil 8. For each PAM concentration, data points with different letters are significantly different ( $p = 0.05$ ). The “0” data point for PAM is graphed at 0.01 due to limitations in using a linear-log scale.

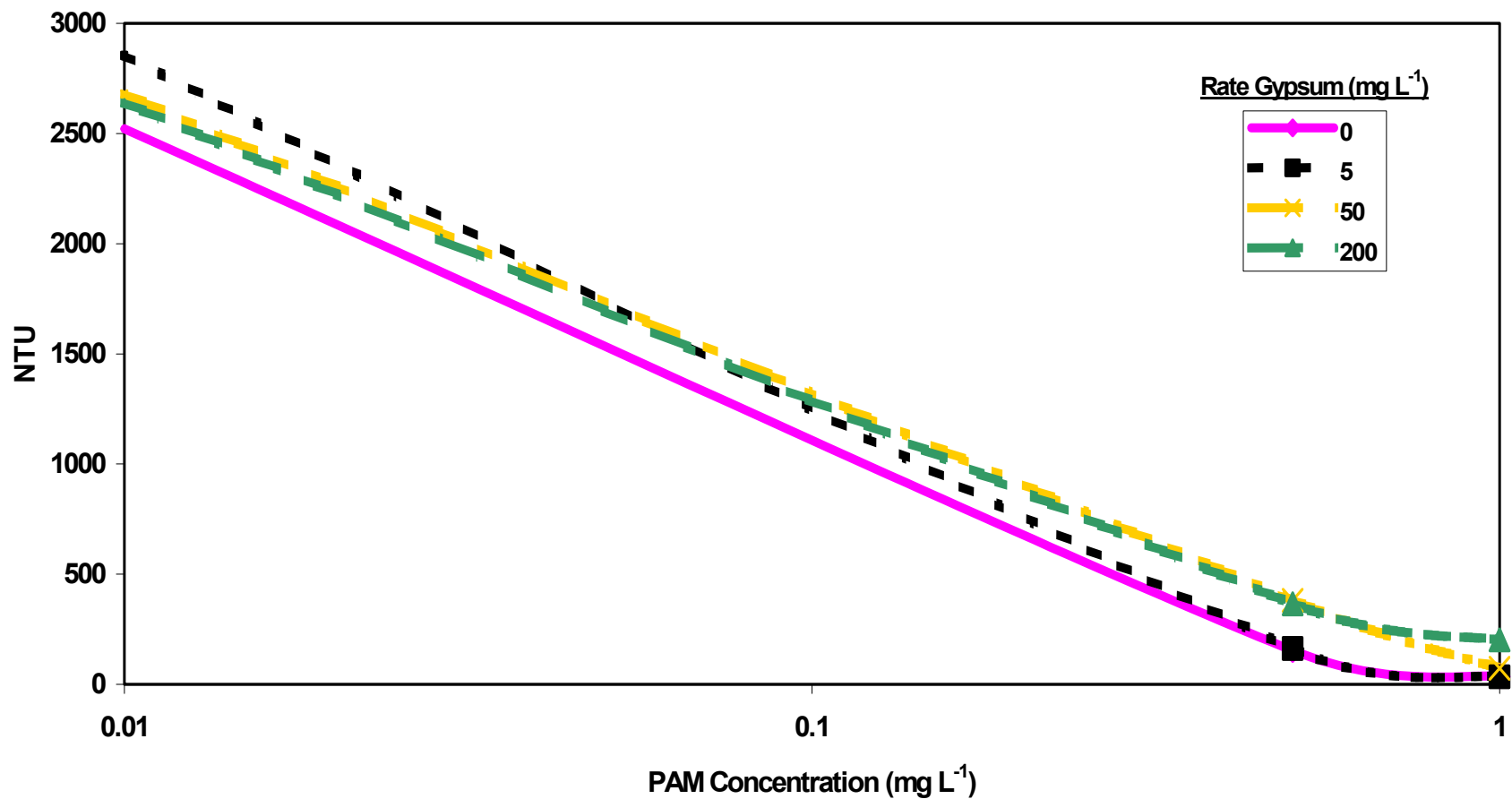


Figure 3.12 Turbidity reduction by Superfloc A100 (7% charge density, 16 Mg mol<sup>-1</sup> molecular weight) alone and with gypsum at three different concentrations for soil sample 11. The “0” data point for PAM is graphed at 0.01 due to limitations in using a linear-log scale.

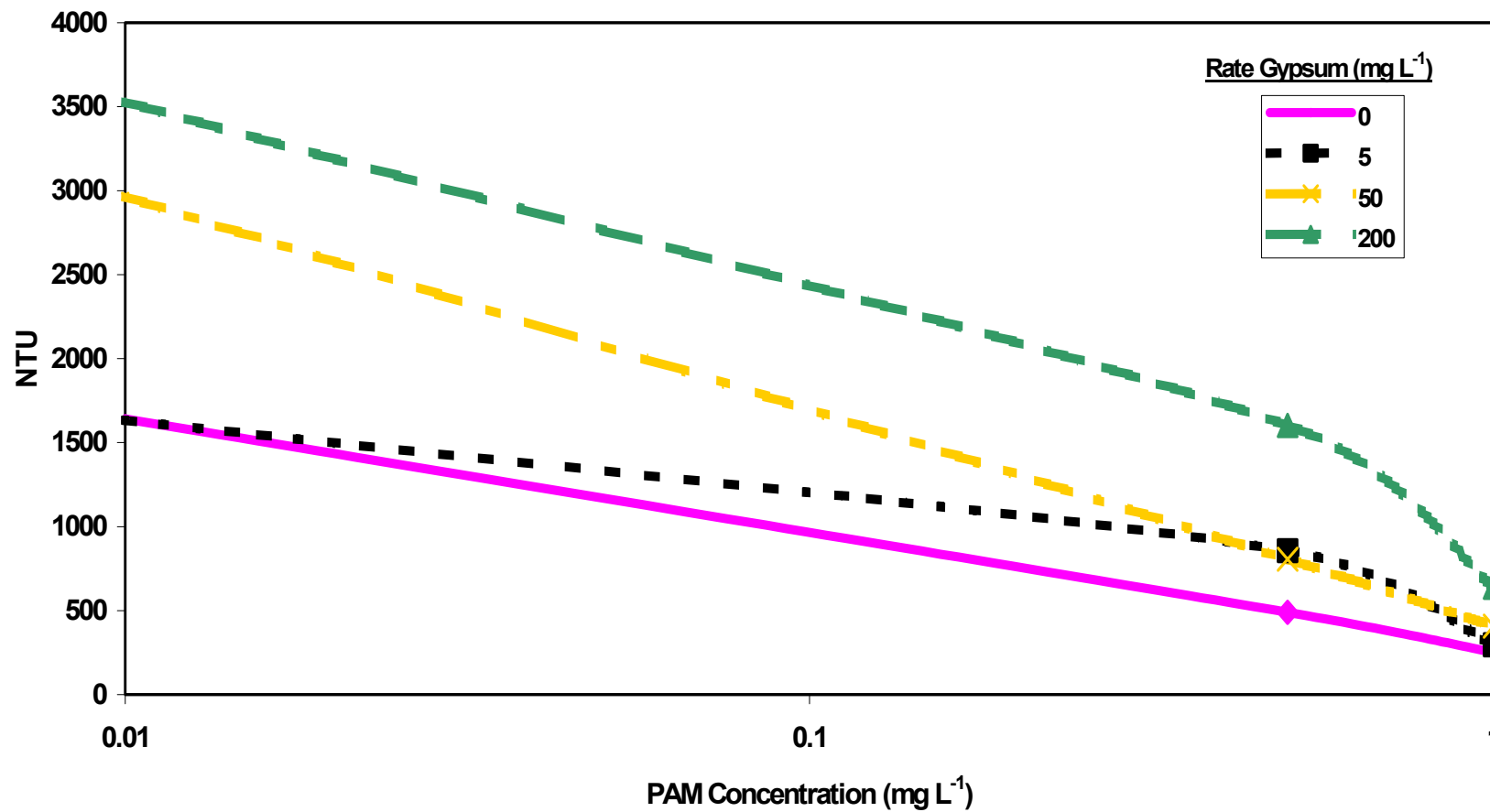


Figure 3.13 Turbidity reduction by Superfloc A100 (7% charge density, 16 Mg mol<sup>-1</sup> molecular weight) alone and with gypsum at three different concentrations for soil sample 13. The “0” data point for PAM is graphed at 0.01 due to limitations in using a linear-log scale.

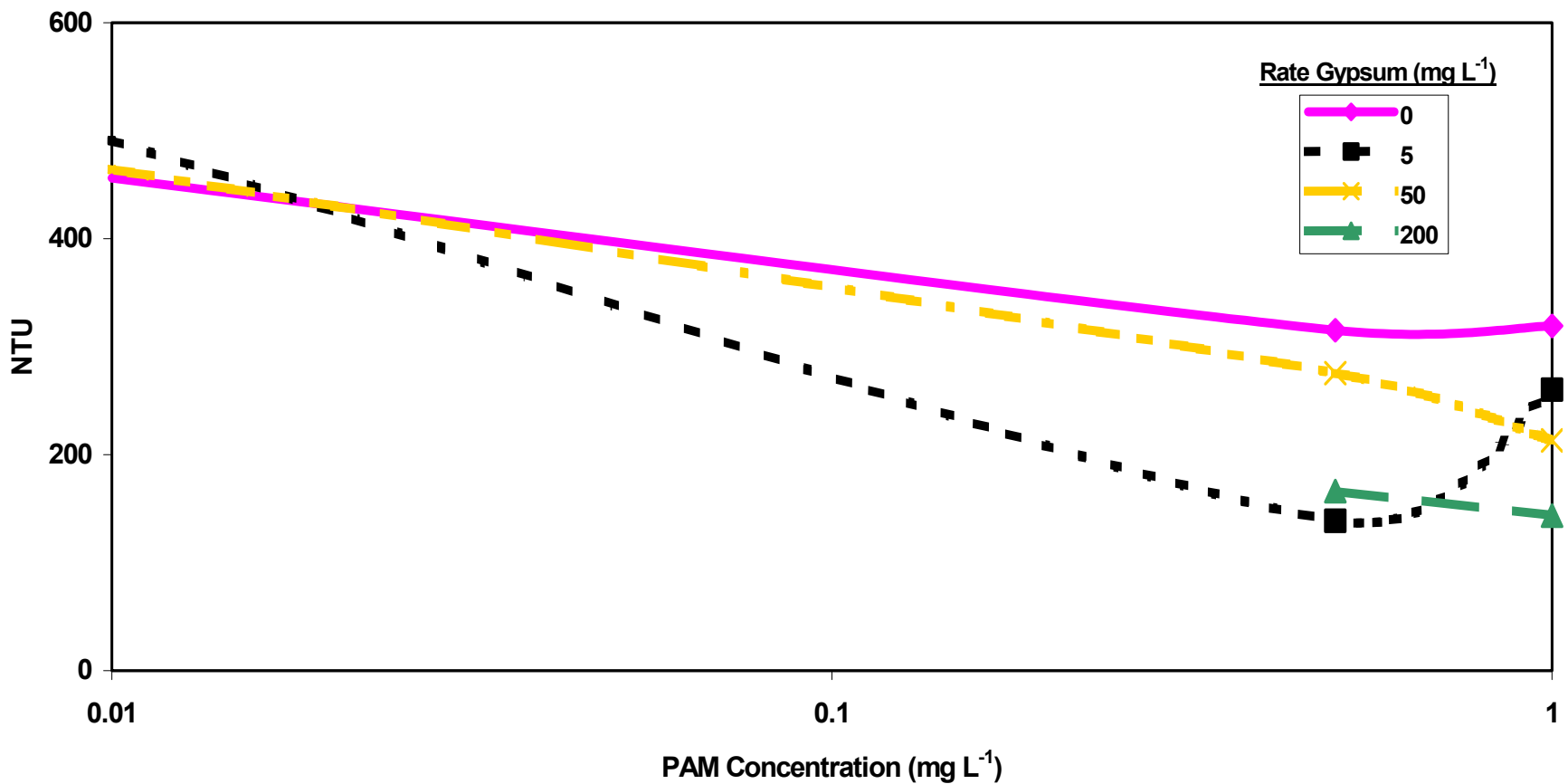


Figure 3.14 Turbidity reduction by Superfloc A100 (7% charge density, 16 Mg mol<sup>-1</sup> molecular weight) alone and with gypsum at four different concentrations for soil sample 1. The “0” data point for PAM is graphed at 0.01 due to limitations in using a linear-log scale.

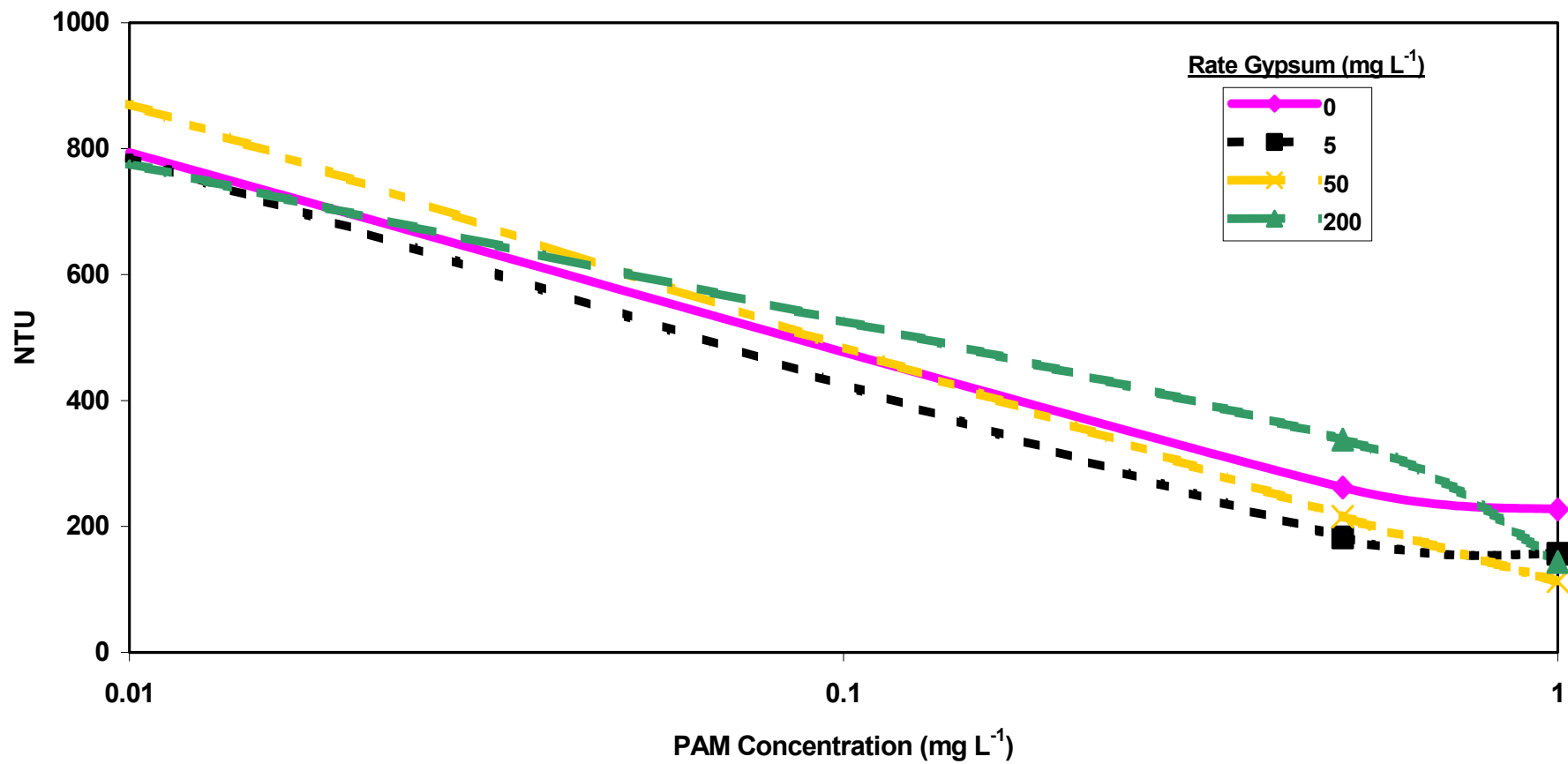


Figure 3.15 Turbidity reduction by Superfloc A100 (7% charge density, 16 Mg mol<sup>-1</sup> molecular weight) alone and with gypsum at three different concentrations for soil sample 2. The “0” data point for PAM is graphed at 0.01 due to limitations in using a linear-log scale.

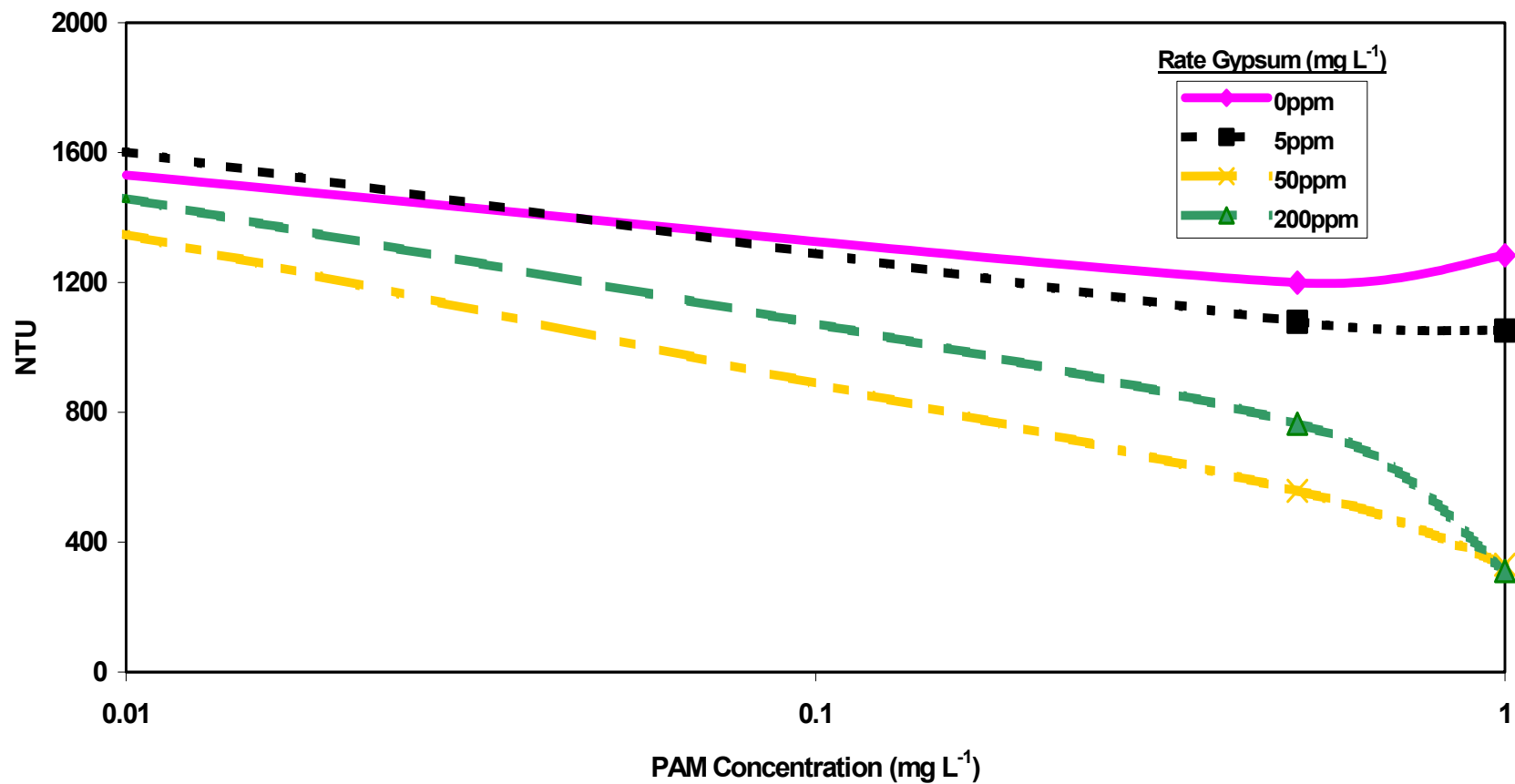


Figure 3.16 Turbidity reduction by Superfloc A100 (7% charge density, 16 Mg mol<sup>-1</sup> molecular weight) alone and with gypsum at three different concentrations for soil sample 4. The “0” data point for PAM is graphed at 0.01 due to limitations in using a linear-log scale.



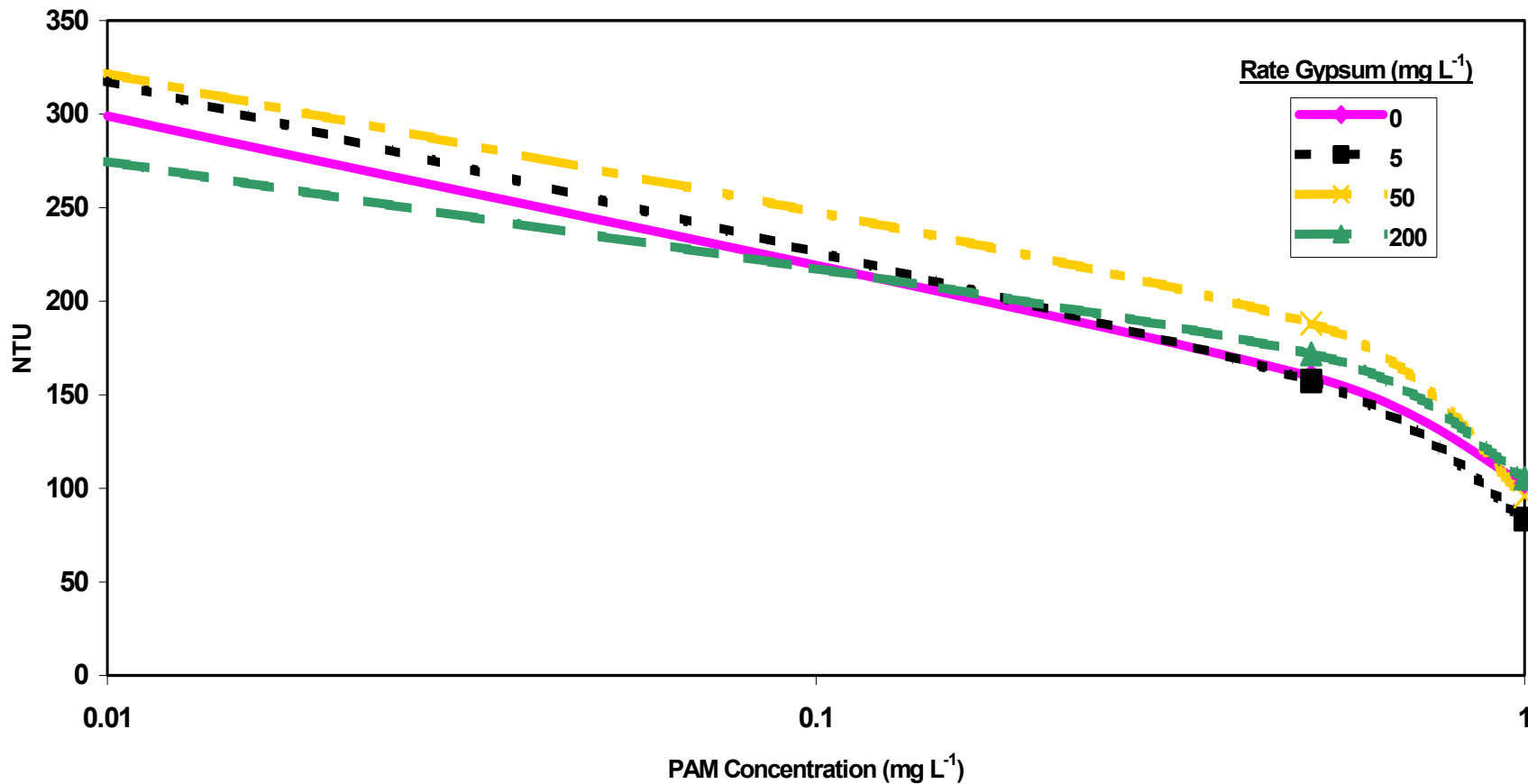


Figure 3.17 Turbidity reduction by Superfloc A100 (7% charge density, 16 Mg mol<sup>-1</sup> molecular weight) alone and with gypsum at three different concentrations for soil sample 3. The “0” data point for PAM is graphed at 0.01 due to limitations in using a linear-log scale.

Soil	Smectite (<1 μm)	Smectite (1-2 μm)	Vermiculite (<1 μm)	Vermiculite (1-2 μm)	Mica (<1 μm)	Mica (1-2 μm)	Kaolinite (<1 μm)	Kaolinite (1-2 μm)
1	64%	13%	7%	11%	18%	26%	11%	42%
2	0%	0%	42%	59%	7%	4%	52%	37%
4	0%	0%	52%	50%	10%	7%	38%	43%
6	21%	13%	0%	4%	0%	5%	79%	78%
7	0%	1%	19%	49%	0%	0%	81%	50%

Soil	Smectite (<1 μm)	Smectite (1-2 μm)	Vermiculite (<1 μm)	Vermiculite (1-2 μm)	Mica (<1 μm)	Mica (1-2 μm)	Kaolinite (<1 μm)	Kaolinite (1-2 μm)
5	8%	0%	12%	10%	0%	1%	80%	88%
9	6%	0%	9%	3%	10%	30%	75%	68%
11	0%	0%	10%	2%	19%	34%	71%	64%
13	0%	0%	9%	2%	1%	2%	90%	96%

Table 3.1 Comparison of the amount of smectite and vermiculite in the clay fraction of recalcitrant soils (1, 2, 4, 6, 7) with soils that had turbidity reductions (with PAM) that met the 50 NTU standard (5, 9, 11, 13).

<b>Flocculant</b>	<b>Molecular Weight</b>	<b>Charge Density</b>
SF A100	16 Mg mol <sup>-1</sup>	7%
SF A110	15 Mg mol <sup>-1</sup>	18%
Soilfix Polybead	16 Mg mol <sup>-1</sup>	30%
APS706b (block)	mixed	mixed
APS705	mixed	mixed
Chemtall 923VHM	14-17.5 Mg mol <sup>-1</sup>	20%

Table 3.2 Properties of PAM products used in gypsum evaluation. All polymers except for SF A100 were used in replicate testing (soil 8).

Soil	Texture	Sand (g kg <sup>-1</sup> )	Silt (g kg <sup>-1</sup> )	Clay (g kg <sup>-1</sup> )	Ca <sup>2+</sup> (cmol <sub>c</sub> Kg <sup>-1</sup> )	Mg <sup>2+</sup> (cmol <sub>c</sub> Kg <sup>-1</sup> )	SAR	pH (1:1, H <sub>2</sub> O)	Organic Carbon (g kg <sup>-1</sup> )
1	sand	900	54	46	4.3	0.2	0.5	8.0	1.5
2	sandy loam	720	178	102	0.5	0.3	1.6	4.8	3.3
3	sand	932	30	38	9.0	0.20	0.2	7.4	2.0
4	loamy sand	840	110	50	0.2	0.1	0.7	5.0	4.6

Soil	Smectite (<1 μm)	Smectite (1-2 μm)	Vermiculite (<1 μm)	Vermiculite (1-2 μm)	Mica (<1 μm)	Mica (1-2 μm)	Kaolinite (<1 μm)	Kaolinite (1-2 μm)	Oxalate Fe (mmol kg <sup>-1</sup> )	CBD Fe (mmol kg <sup>-1</sup> )
1	64%	13%	7%	11%	18%	26%	11%	42%	5.2	8.2
2	0%	0%	42%	59%	7%	4%	52%	37%	2.6	16.4
3	90%	60%	0%	2%	10%	27%	0%	11%	9.6	10.2
4	0%	0%	52%	50%	10%	7%	38%	43%	6.8	18.2

Table 3.3 Table comparing the soil properties of the four Coastal Plain soils.

# Appendix

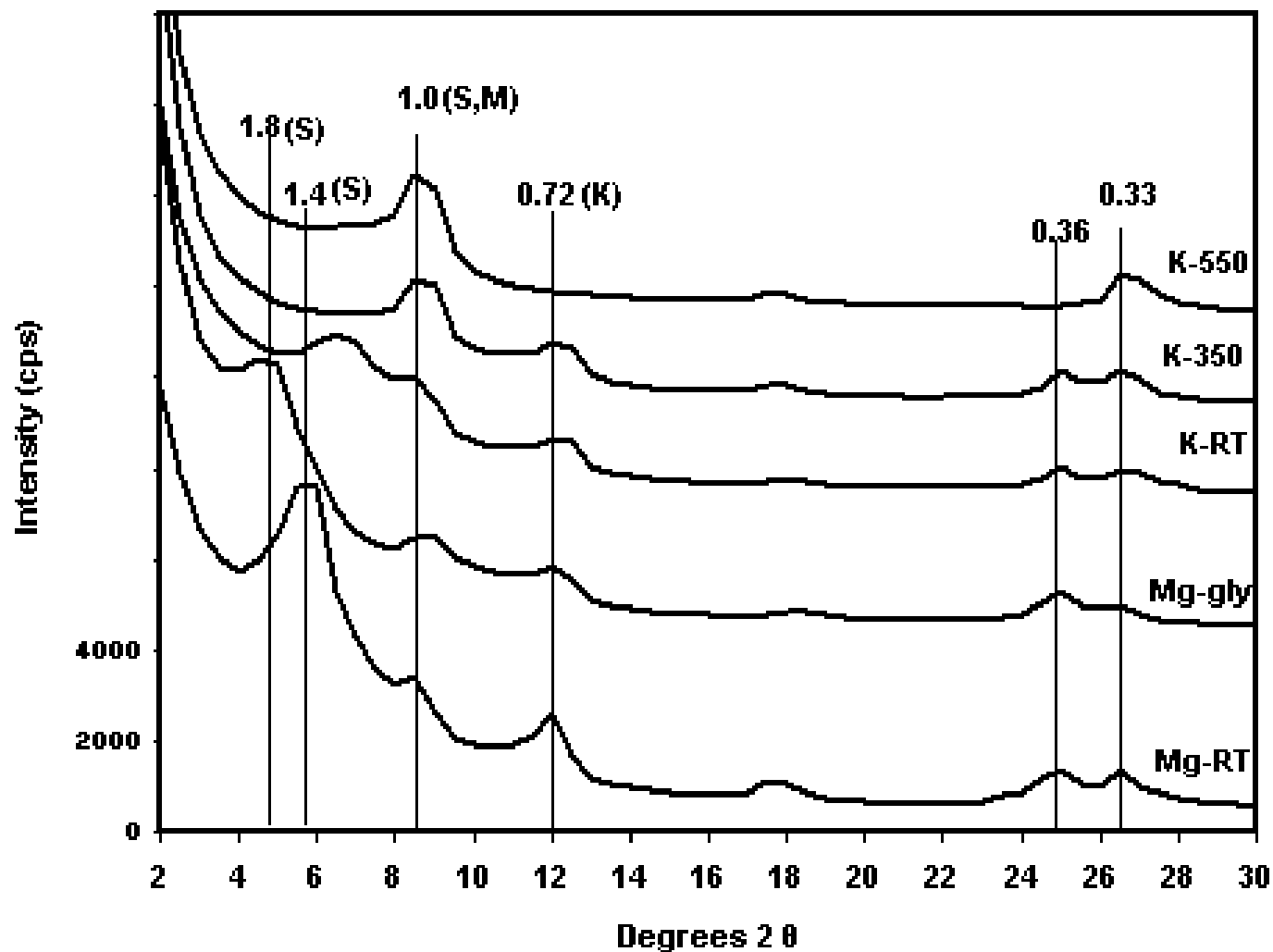


Figure A.1 X-ray diffraction (xrd) patterns for phyllosilicate mineralogy of the fine clay fraction of soil sample 1. Numbers above peaks are d-spacings in nanometers. Letters above peaks designate clay mineralogy (s = smectite, v = vermiculite, m = mica, and k = kaolinite). Treatments include:  $Mg^{2+}$  saturation at room temperature (Mg-RT) and with glycerol (Mg-gly),  $K^+$  saturation at room temperature (K-RT), 350 °C (K-350), and 550 °C (K-550). Area under each peak of the Mg-gly xrd pattern was compared to specify the percent of each clay mineral.

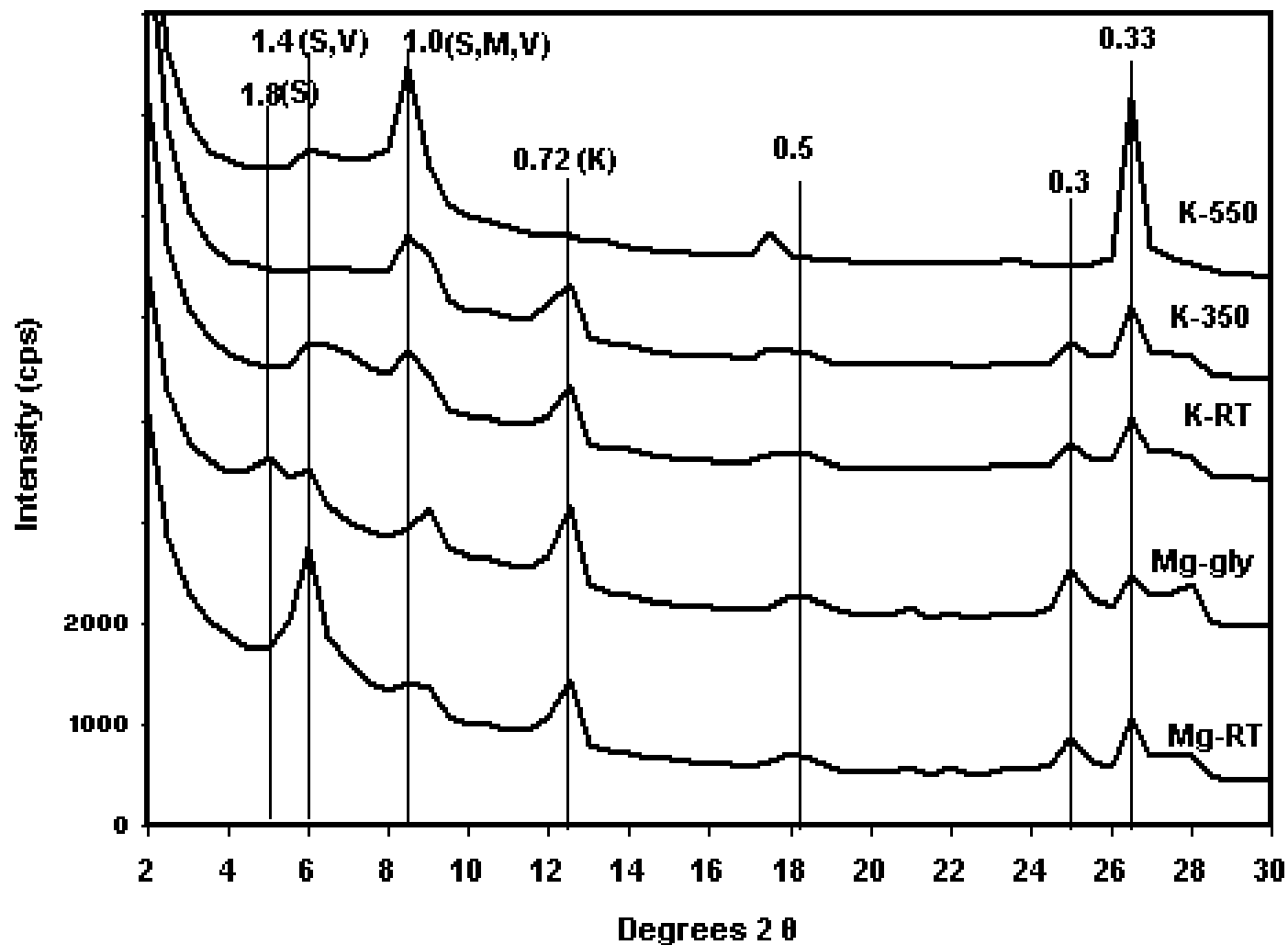


Figure A.2 X-ray diffraction (xrd) patterns for phyllosilicate mineralogy of the coarse clay fraction of soil sample 1. Numbers above peaks are d-spacings in nanometers. Letters above peaks designate clay mineralogy (s = smectite, v = vermiculite, m = mica, and k = kaolinite). Treatments include:  $Mg^{2+}$  saturation at room temperature (Mg-RT) and with glycerol (Mg-gly),  $K^+$  saturation at room temperature (K-RT), 350 °C (K-350), and 550 °C (K-550). Area under each peak of the Mg-gly xrd pattern was compared to specify the percent of each clay mineral.

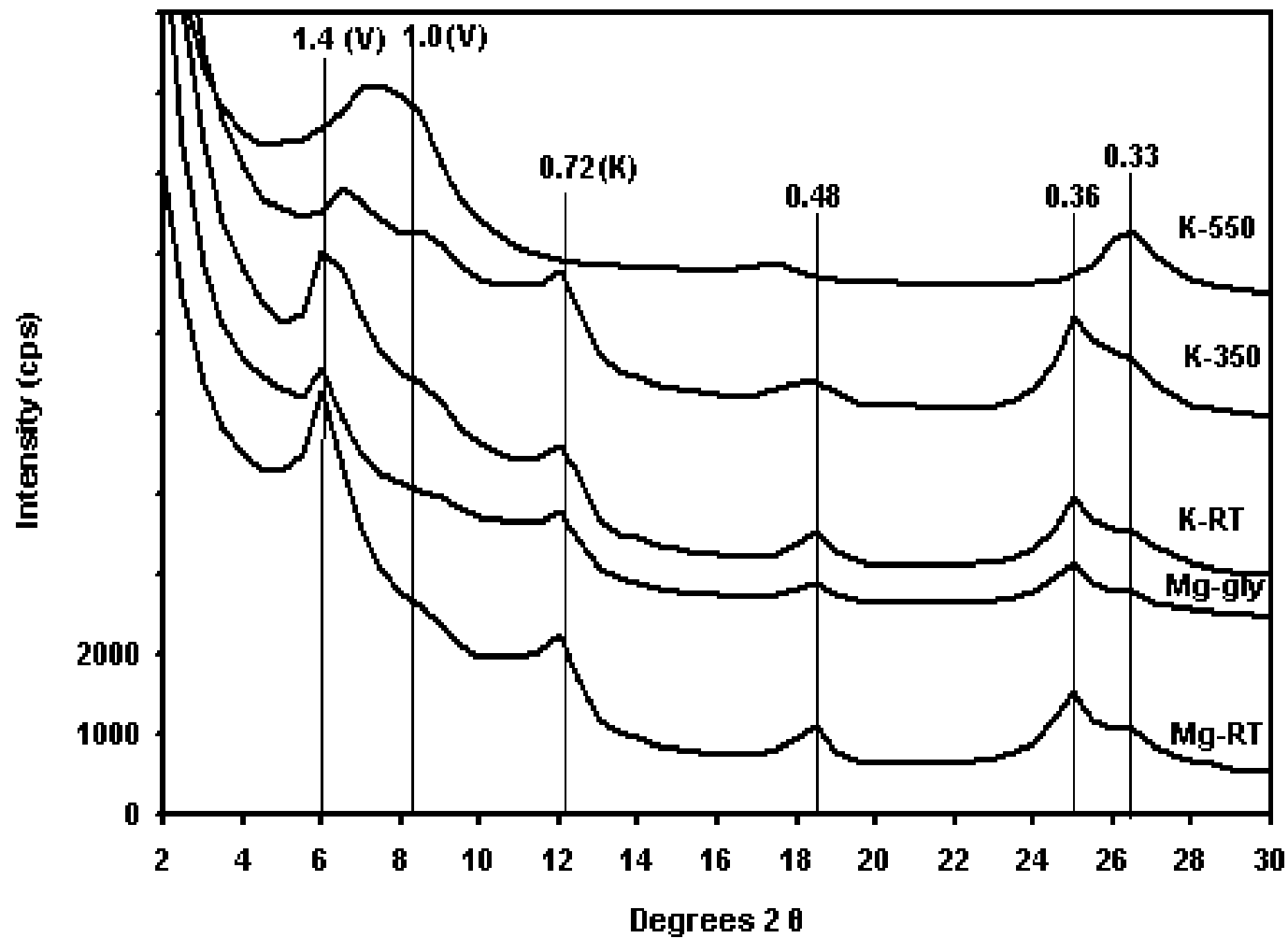


Figure A.3 X-ray diffraction (xrd) patterns for phyllosilicate mineralogy of the fine clay fraction of soil sample 2. Numbers above peaks are d-spacings in nanometers. Letters above peaks designate clay mineralogy (s = smectite, v = vermiculite, m = mica, and k = kaolinite). Treatments include: Mg<sup>2+</sup> saturation at room temperature (Mg-RT) and with glycerol (Mg-gly), K<sup>+</sup> saturation at room temperature (K-RT), 350 °C (K-350), and 550 °C (K-550). Area under each peak of the Mg-gly xrd pattern was compared to specify the percent of each clay mineral.



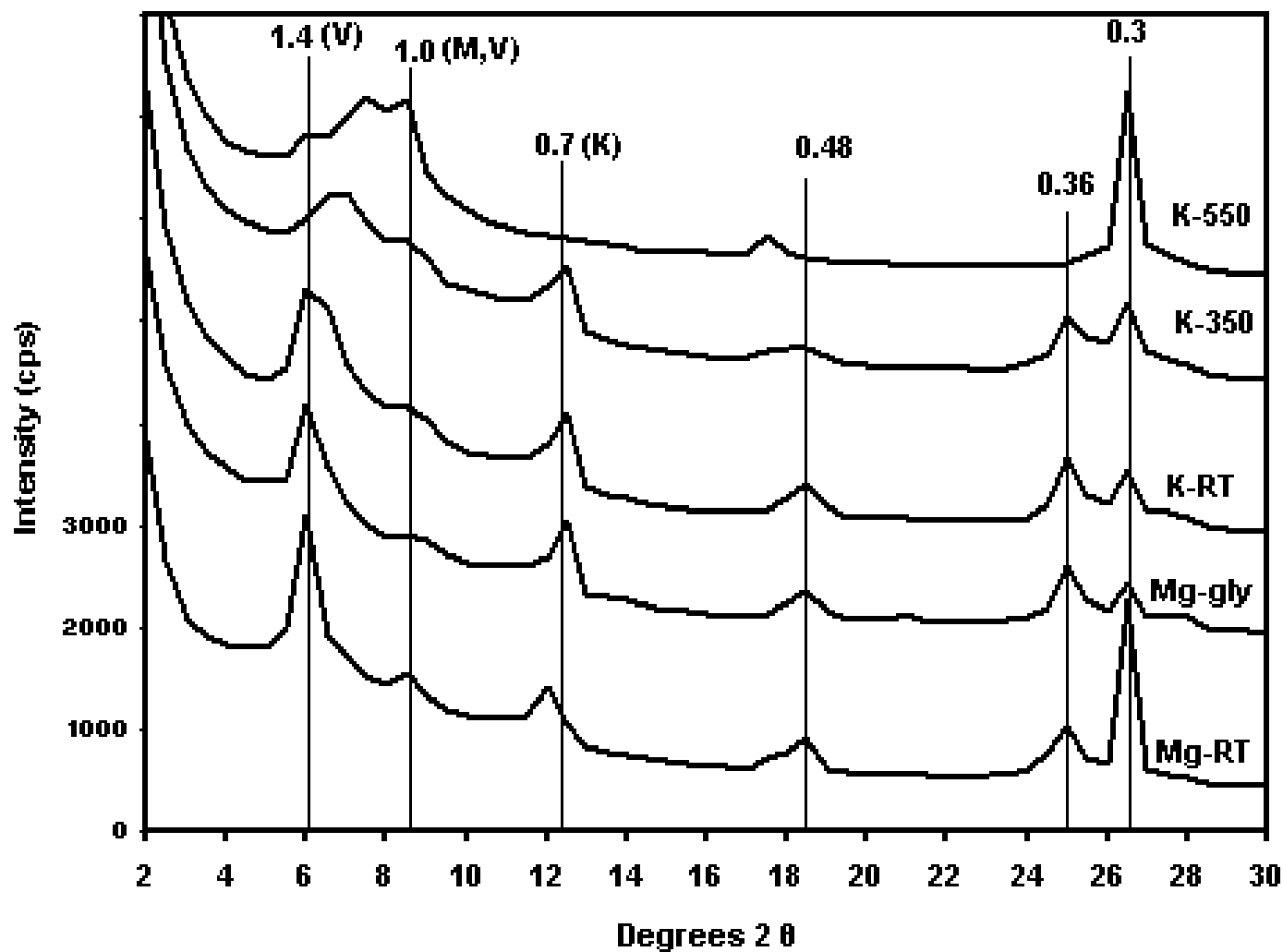


Figure A.4 X-ray diffraction (xrd) patterns for phyllosilicate mineralogy of the coarse clay fraction of soil sample 2. Numbers above peaks are d-spacings in nanometers. Letters above peaks designate clay mineralogy (s = smectite, v = vermiculite, m = mica, and k = kaolinite). Treatments include:  $Mg^{2+}$  saturation at room temperature (Mg-RT) and with glycerol (Mg-gly),  $K^{+}$  saturation at room temperature (K-RT), 350 °C (K-350), and 550 °C (K-550). Area under each peak of the Mg-gly xrd pattern was compared to specify the percent of each clay mineral.

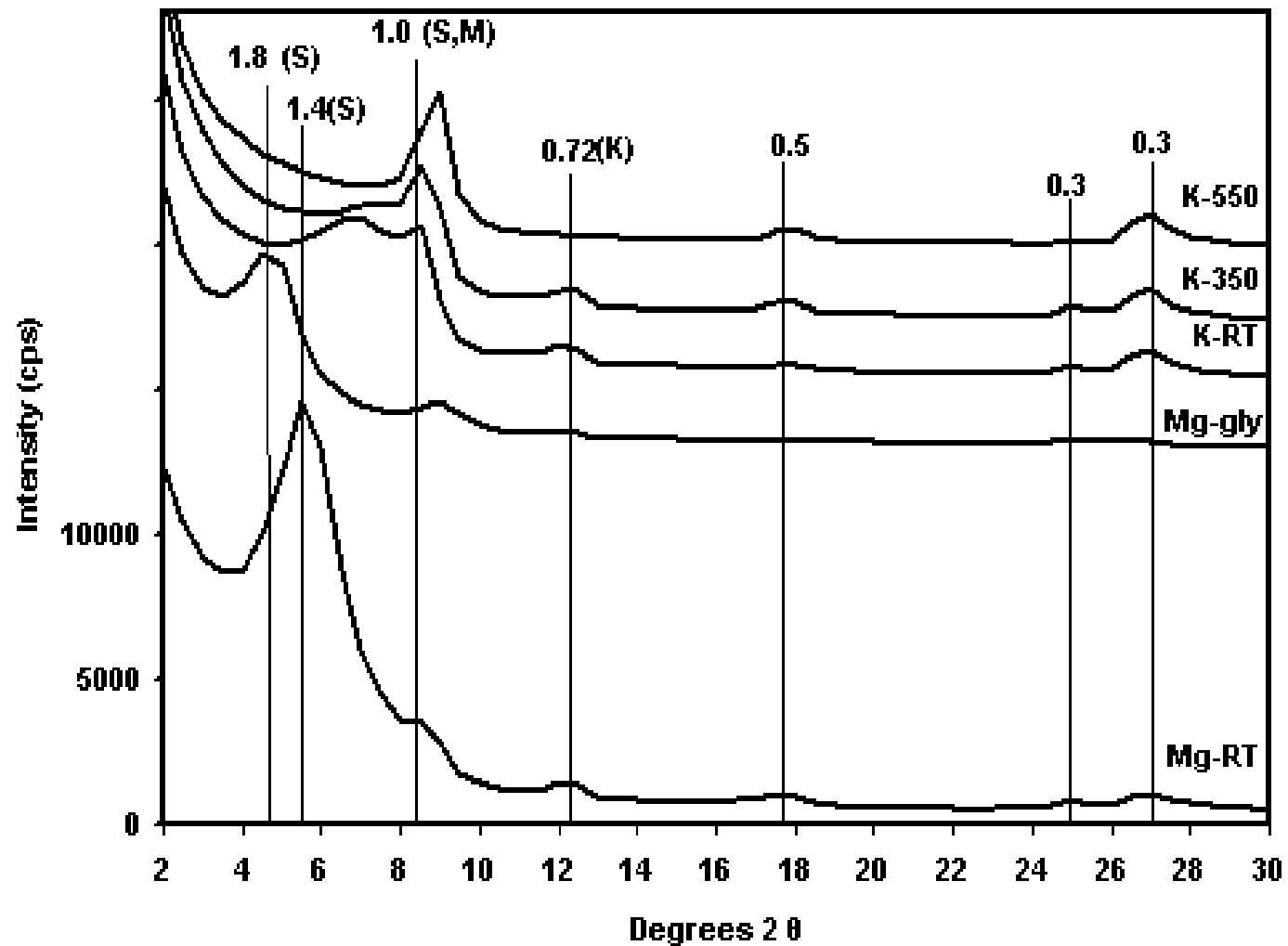


Figure A.5 X-ray diffraction patterns for phyllosilicate mineralogy of the fine clay fraction of soil sample 3. Numbers above peaks are d-spacings in nanometers. Letters above peaks designate clay mineralogy (s = smectite, v = vermiculite, m = mica, and k = kaolinite). Treatments include:  $Mg^{2+}$  saturation at room temperature (Mg-RT) and with glycerol (Mg-gly),  $K^+$  saturation at room temperature (K-RT), 350 °C (K-350), and 550 °C (K-550). Area under each peak of the Mg-gly xrd pattern was compared to specify the percent of each clay mineral.

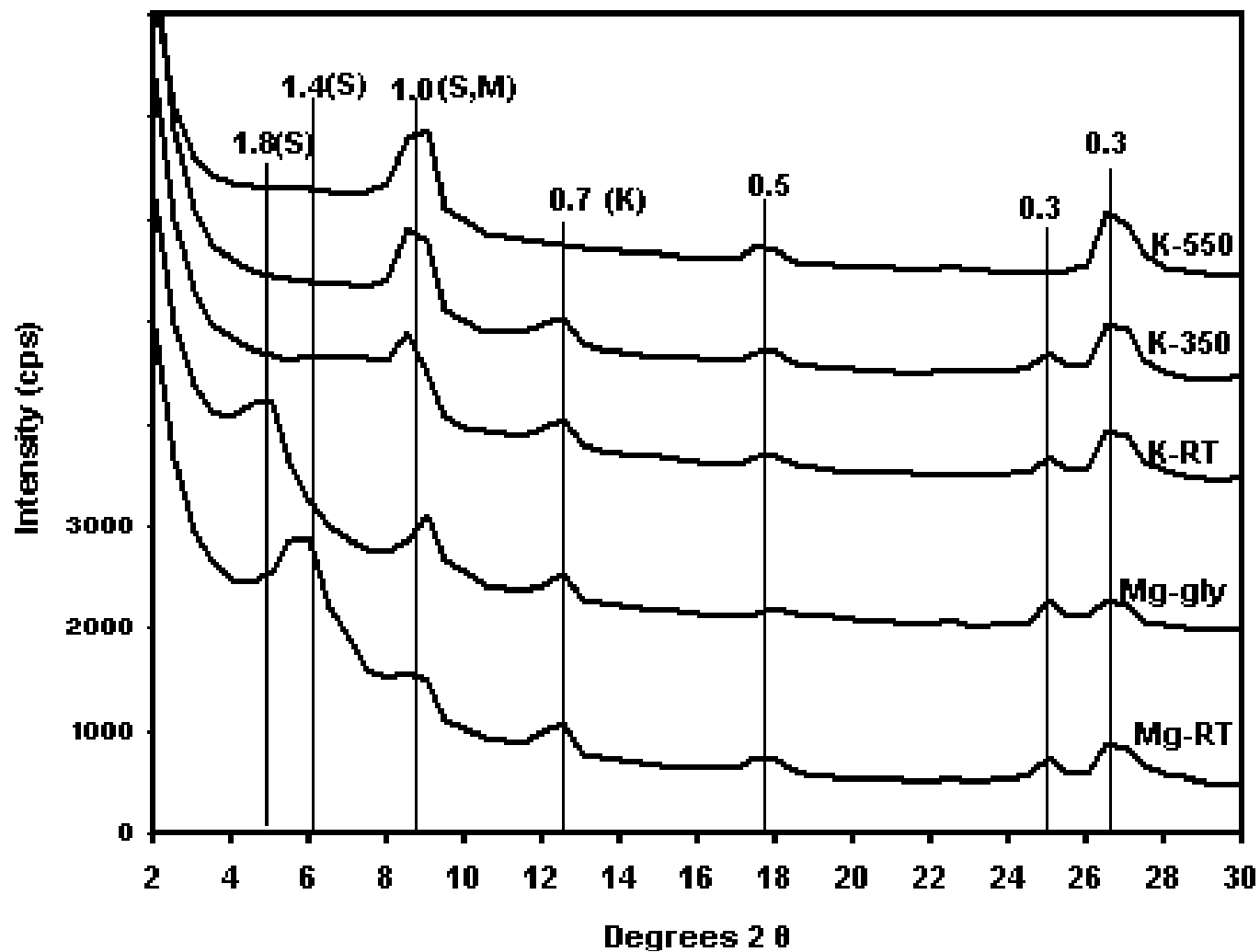


Figure A.6 X-ray diffraction patterns for phyllosilicate mineralogy of the coarse clay fraction of soil sample 3. Numbers above peaks are d-spacings in nanometers. Letters above peaks designate clay mineralogy (s = smectite, v = vermiculite, m = mica, and k = kaolinite). Treatments include:  $Mg^{2+}$  saturation at room temperature (Mg-RT) and with glycerol (Mg-gly),  $K^+$  saturation at room temperature (K-RT), 350 °C (K-350), and 550 °C (K-550). Area under each peak of the Mg-gly xrd pattern was compared to specify the percent of each clay mineral.

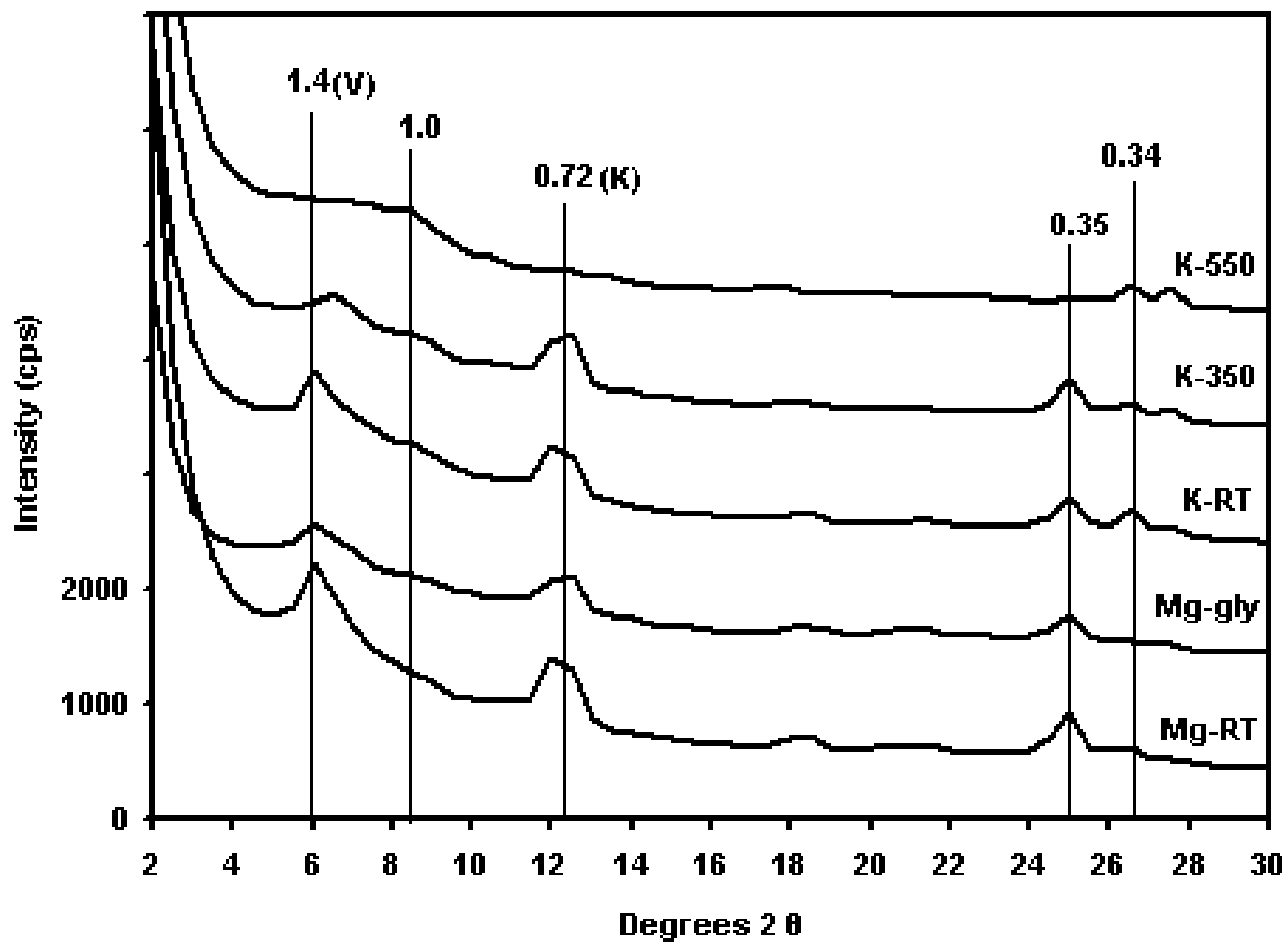


Figure A.7 X-ray diffraction (xrd) patterns for phyllosilicate mineralogy of the fine clay fraction of soil sample 4. Numbers above peaks are d-spacings in nanometers. Letters above peaks designate clay mineralogy (s = smectite, v = vermiculite, m = mica, and k = kaolinite). Treatments include:  $Mg^{2+}$  saturation at room temperature (Mg-RT) and with glycerol (Mg-gly),  $K^+$  saturation at room temperature (K-RT), 350 °C (K-350), and 550 °C (K-550). Area under each peak of the Mg-gly xrd pattern was compared to specify the percent of each clay mineral.

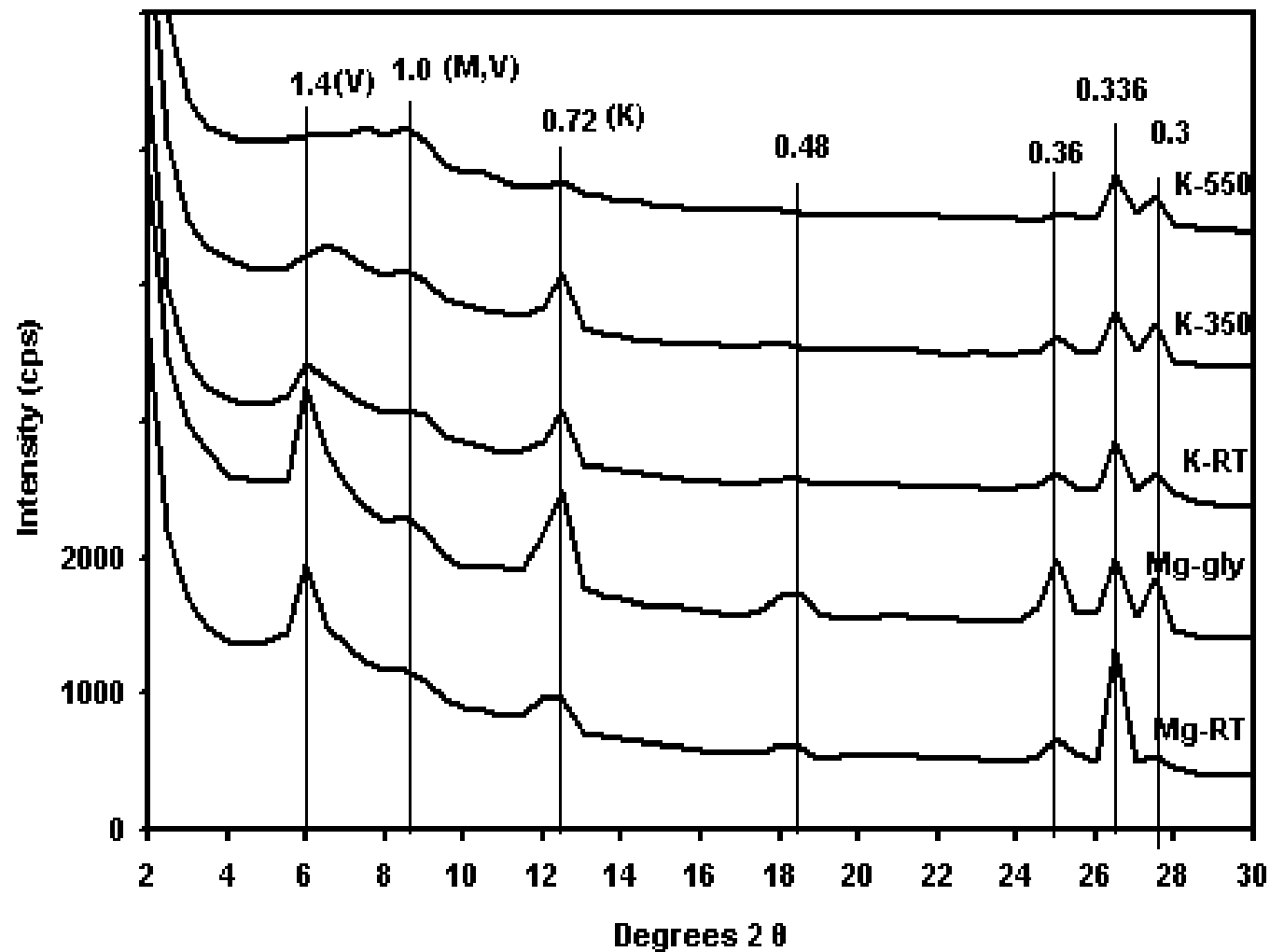


Figure A.8 X-ray diffraction (xrd) patterns for phyllosilicate mineralogy of the coarse clay fraction of soil sample 4. Numbers above peaks are d-spacings in nanometers. Letters above peaks designate clay mineralogy (s = smectite, v = vermiculite, m = mica, and k = kaolinite). Treatments include:  $Mg^{2+}$  saturation at room temperature (Mg-RT) and with glycerol (Mg-gly),  $K^+$  saturation at room temperature (K-RT), 350 °C (K-350), and 550 °C (K-550). Area under each peak of the Mg-gly xrd pattern was compared to specify the percent of each clay mineral.

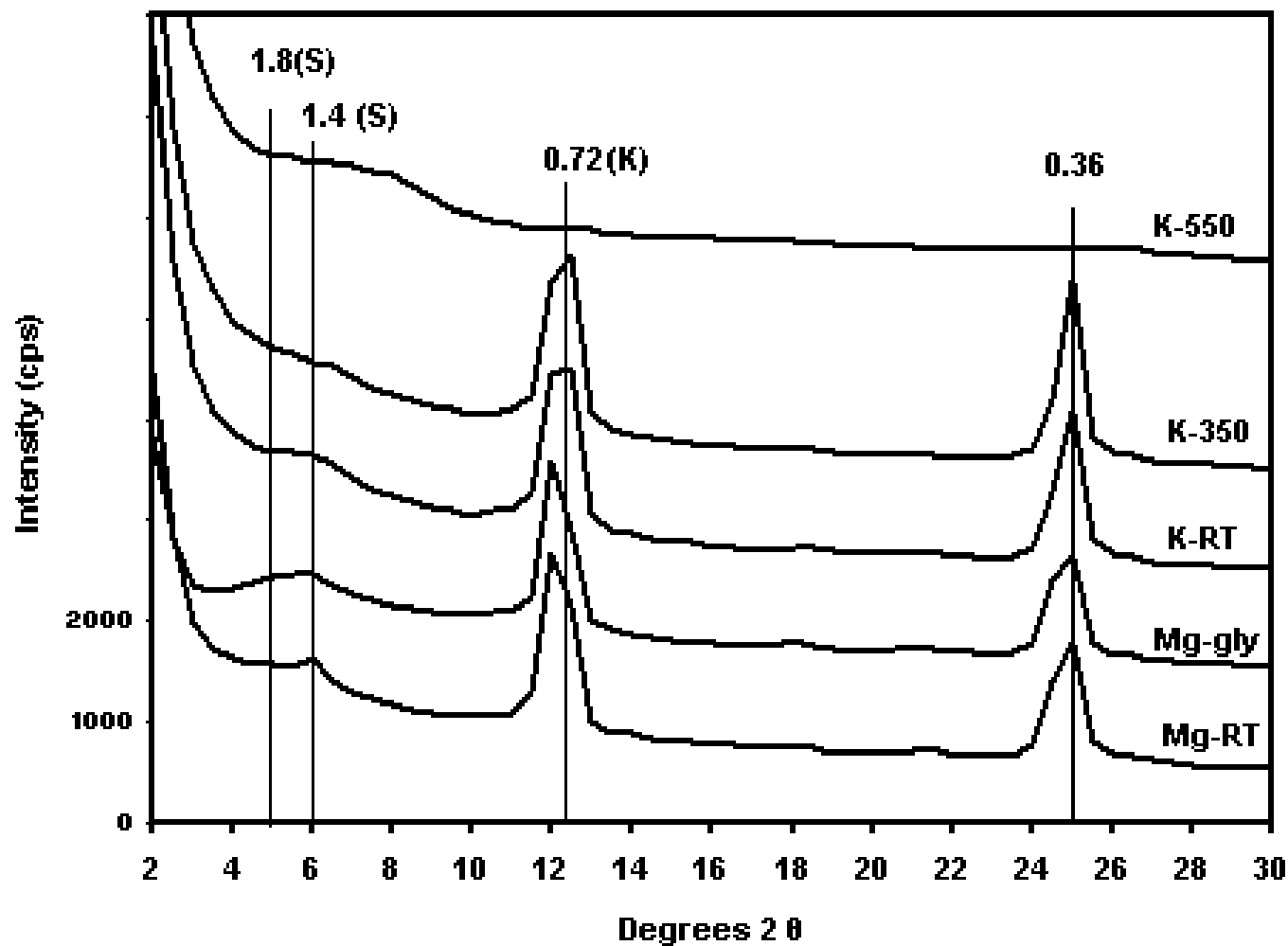


Figure A.9 X-ray diffraction patterns for phyllosilicate mineralogy of the fine clay fraction of soil sample 5. Numbers above peaks are d-spacings in nanometers. Letters above peaks designate clay mineralogy (s = smectite, v = vermiculite, m = mica, and k = kaolinite). Treatments include:  $Mg^{2+}$  saturation at room temperature (Mg-RT) and with glycerol (Mg-gly),  $K^+$  saturation at room temperature (K-RT), 350 °C (K-350), and 550 °C (K-550). Area under each peak of the Mg-gly xrd pattern was compared to specify the percent of each clay mineral.

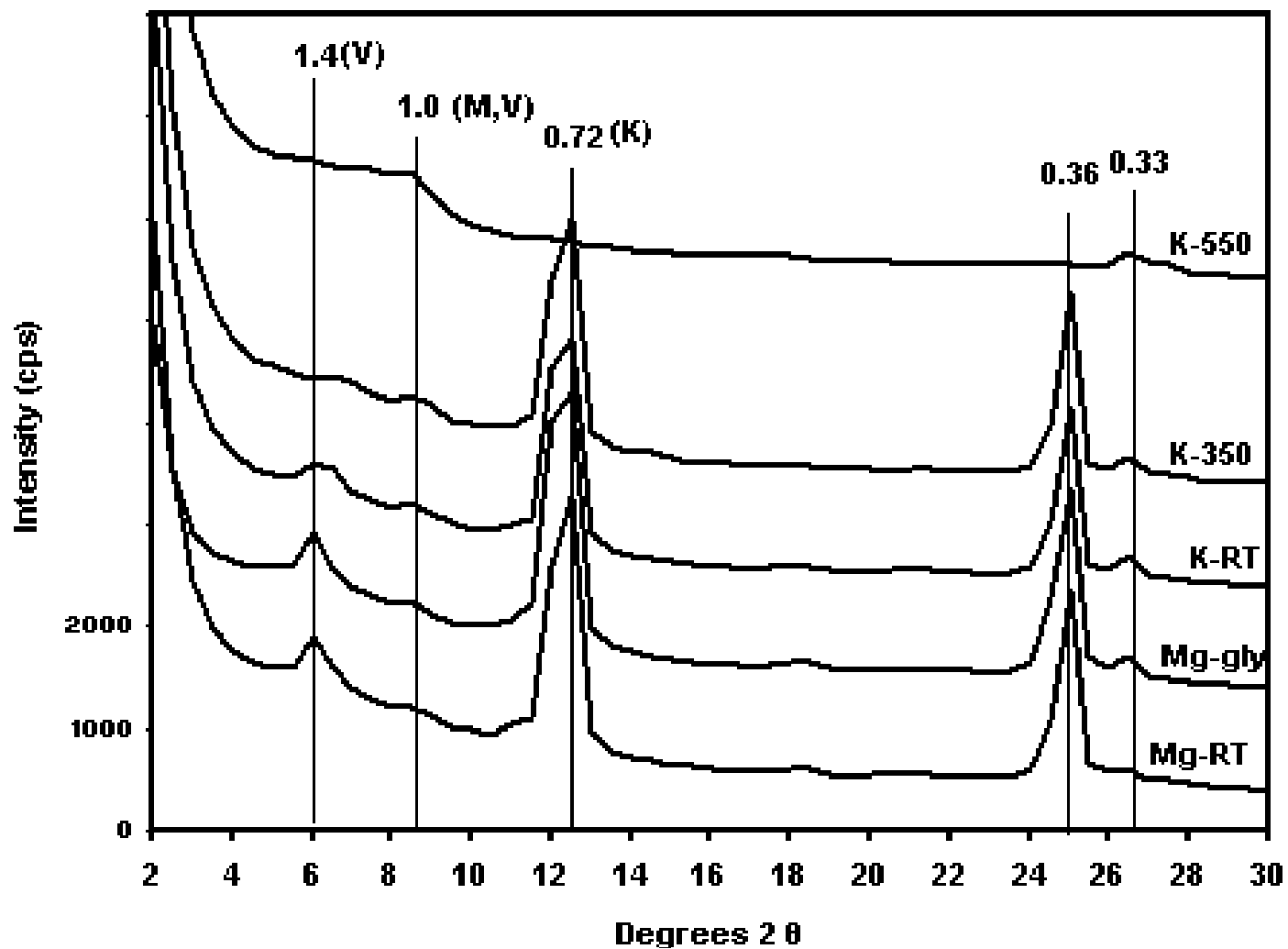


Figure A.10 X-ray diffraction patterns for phyllosilicate mineralogy of the coarse clay fraction of soil sample 5. Numbers above peaks are d-spacings in nanometers. Letters above peaks designate clay mineralogy (s = smectite, v = vermiculite, m = mica, and k = kaolinite). Treatments include:  $Mg^{2+}$  saturation at room temperature (Mg-RT) and with glycerol (Mg-gly),  $K^+$  saturation at room temperature (K-RT), 350 °C (K-350), and 550 °C (K-550). Area under each peak of the Mg-gly xrd pattern was compared to specify the percent of each clay mineral.

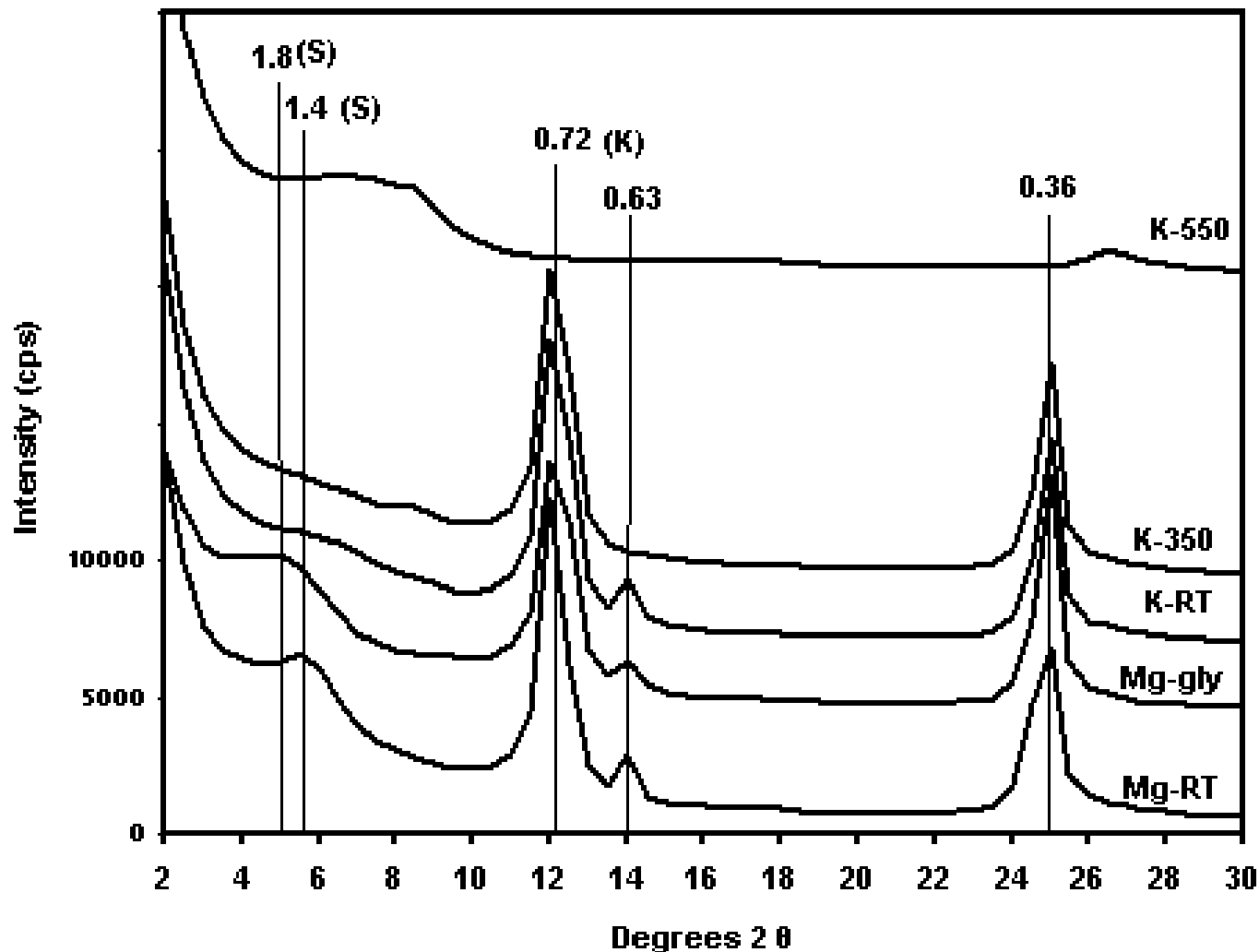


Figure A.11 X-ray diffraction (xrd) patterns for phyllosilicate mineralogy of the fine clay fraction of soil sample 6. Numbers above peaks are d-spacings in nanometers. Letters above peaks designate clay mineralogy (s = smectite, v = vermiculite, m = mica, and k = kaolinite). Treatments include:  $Mg^{2+}$  saturation at room temperature (Mg-RT) and with glycerol (Mg-gly),  $K^+$  saturation at room temperature (K-RT), 350 °C (K-350), and 550 °C (K-550). Area under each peak of the Mg-gly xrd pattern was compared to specify the percent of each clay mineral.



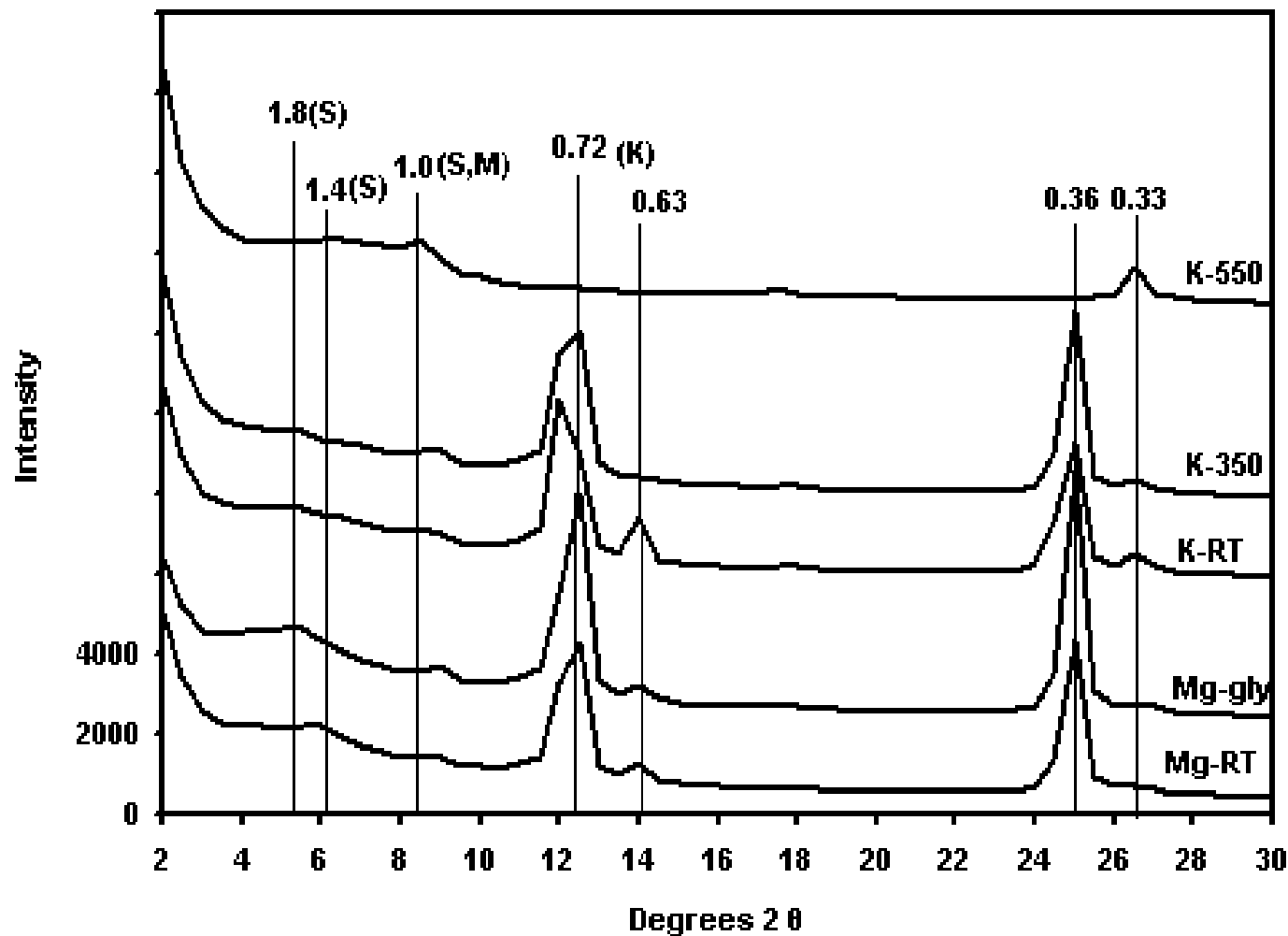


Figure A.12 X-ray diffraction (xrd) patterns for phyllosilicate mineralogy of the coarse clay fraction of soil sample 6. Numbers above peaks are d-spacings in nanometers. Letters above peaks designate clay mineralogy (s = smectite, v = vermiculite, m = mica, and k = kaolinite). Treatments include:  $Mg^{2+}$  saturation at room temperature (Mg-RT) and with glycerol (Mg-gly),  $K^+$  saturation at room temperature (K-RT), 350 °C (K-350), and 550 °C (K-550). Area under each peak of the Mg-gly xrd pattern was compared to specify the percent of each clay mineral.

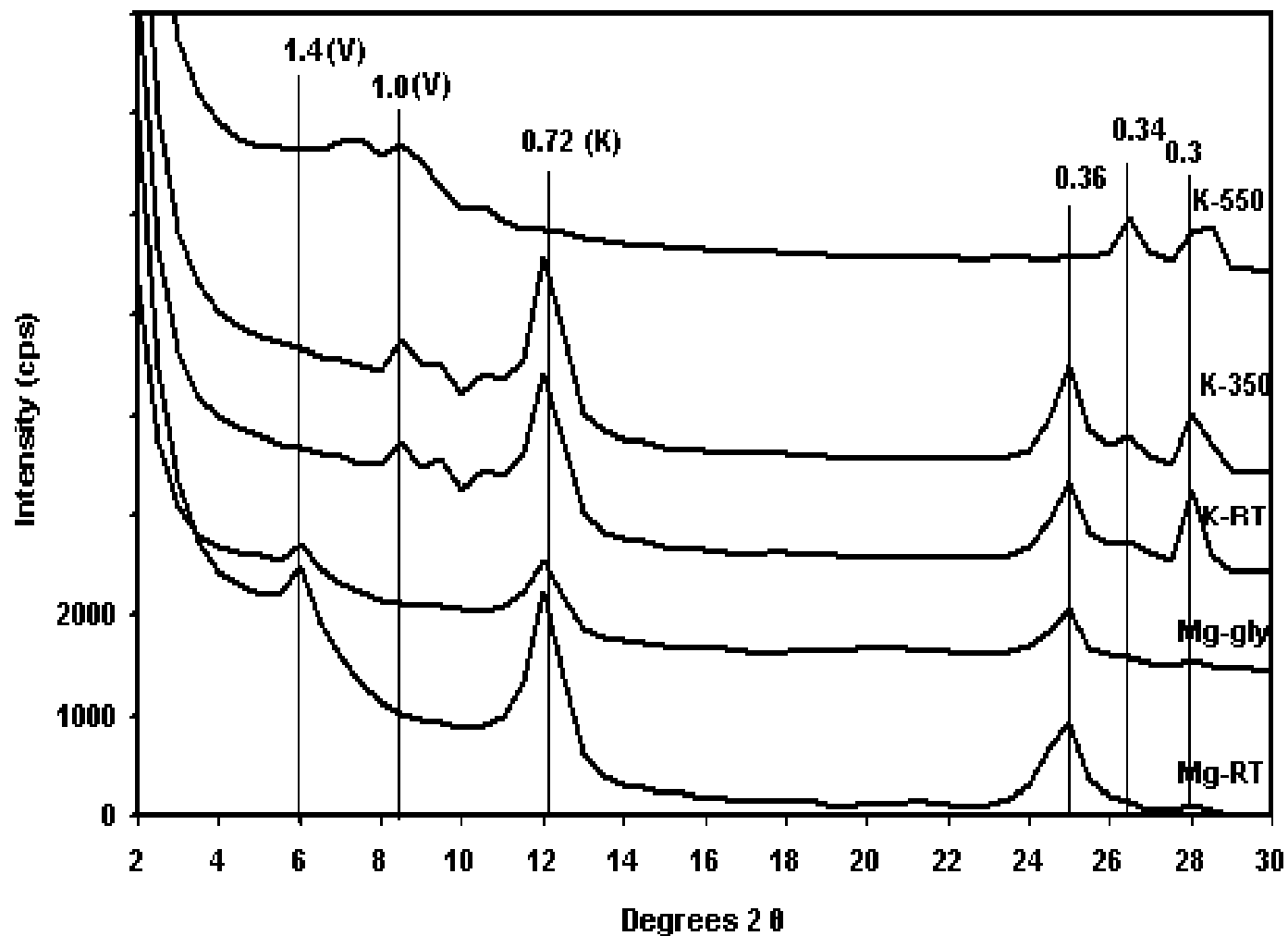


Figure A.13 X-ray diffraction (xrd) patterns for phyllosilicate mineralogy of the fine clay fraction of soil sample 7. Numbers above peaks are d-spacings in nanometers. Letters above peaks designate clay mineralogy (s = smectite, v = vermiculite, m = mica, and k = kaolinite). Treatments include:  $Mg^{2+}$  saturation at room temperature (Mg-RT) and with glycerol (Mg-gly),  $K^+$  saturation at room temperature (K-RT), 350 °C (K-350), and 550 °C (K-550). Area under each peak of the Mg-gly xrd pattern was compared to specify the percent of each clay mineral.

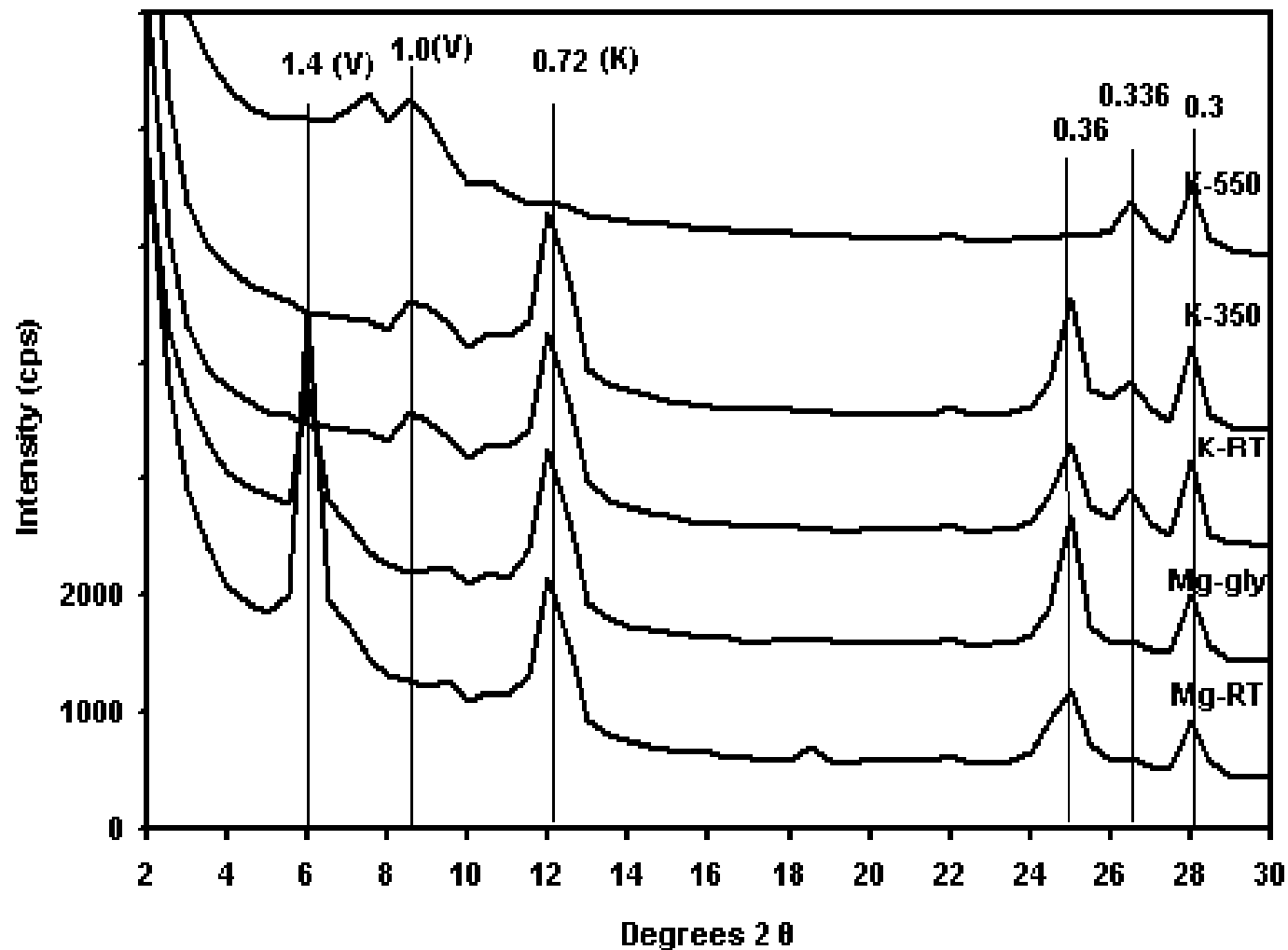


Figure A.14 X-ray diffraction (xrd) patterns for phyllosilicate mineralogy of the coarse clay fraction of soil sample 7. Numbers above peaks are d-spacings in nanometers. Letters above peaks designate clay mineralogy (s = smectite, v = vermiculite, m = mica, and k = kaolinite). Treatments include:  $Mg^{2+}$  saturation at room temperature (Mg-RT) and with glycerol (Mg-gly),  $K^+$  saturation at room temperature (K-RT), 350 °C (K-350), and 550 °C (K-550). Area under each peak of the Mg-gly xrd pattern was compared to specify the percent of each clay mineral.

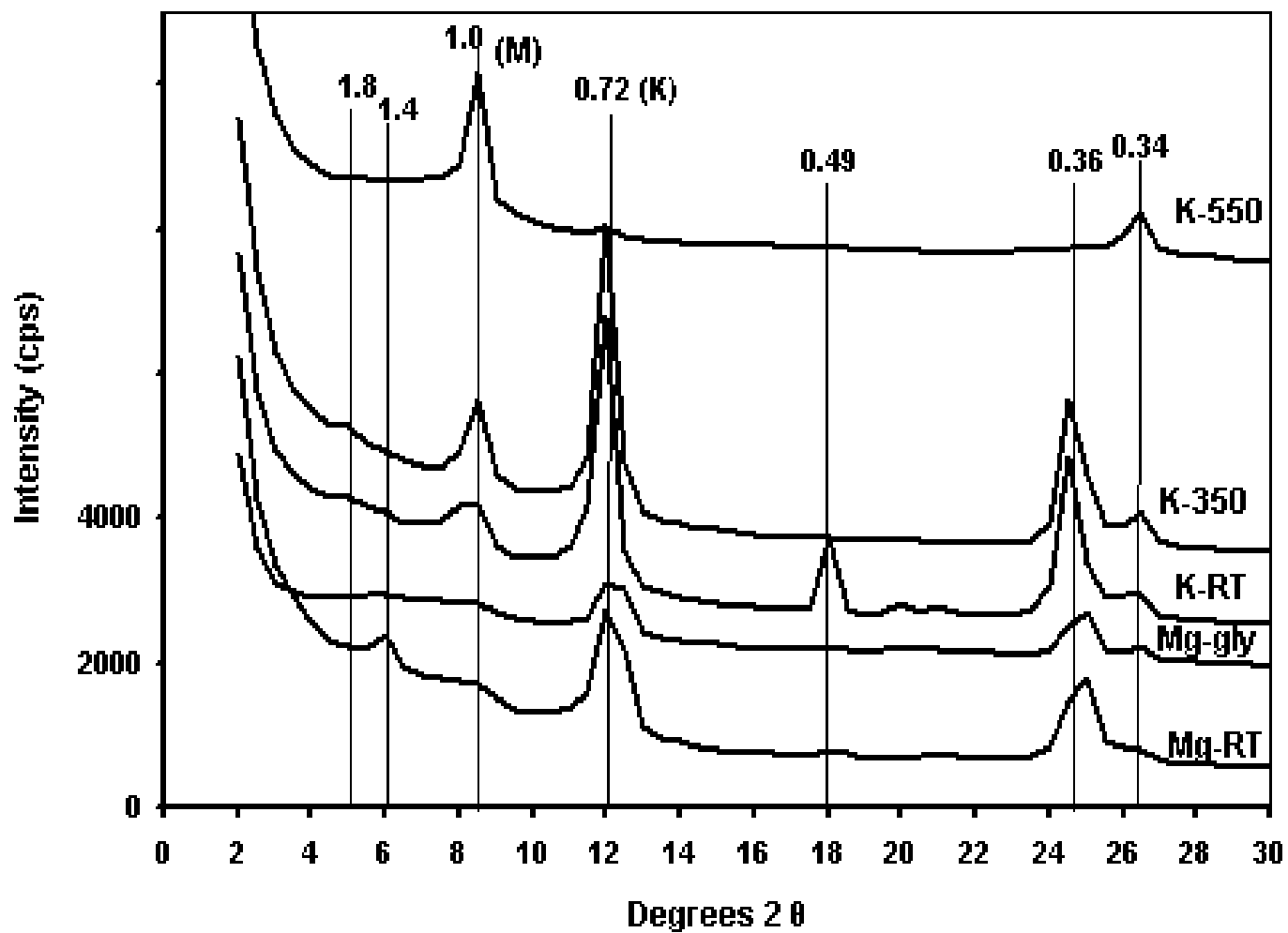


Figure A.15 X-ray diffraction (xrd) patterns for phyllosilicate mineralogy of the fine clay fraction of soil sample 9. Numbers above peaks are d-spacings in nanometers. Letters above peaks designate clay mineralogy (s = smectite, v = vermiculite, m = mica, and k = kaolinite). Treatments include:  $Mg^{2+}$  saturation at room temperature (Mg-RT) and with glycerol (Mg-gly),  $K^+$  saturation at room temperature (K-RT), 350 °C (K-350), and 550 °C (K-550). Area under each peak of the Mg-gly xrd pattern was compared to specify the percent of each clay mineral.

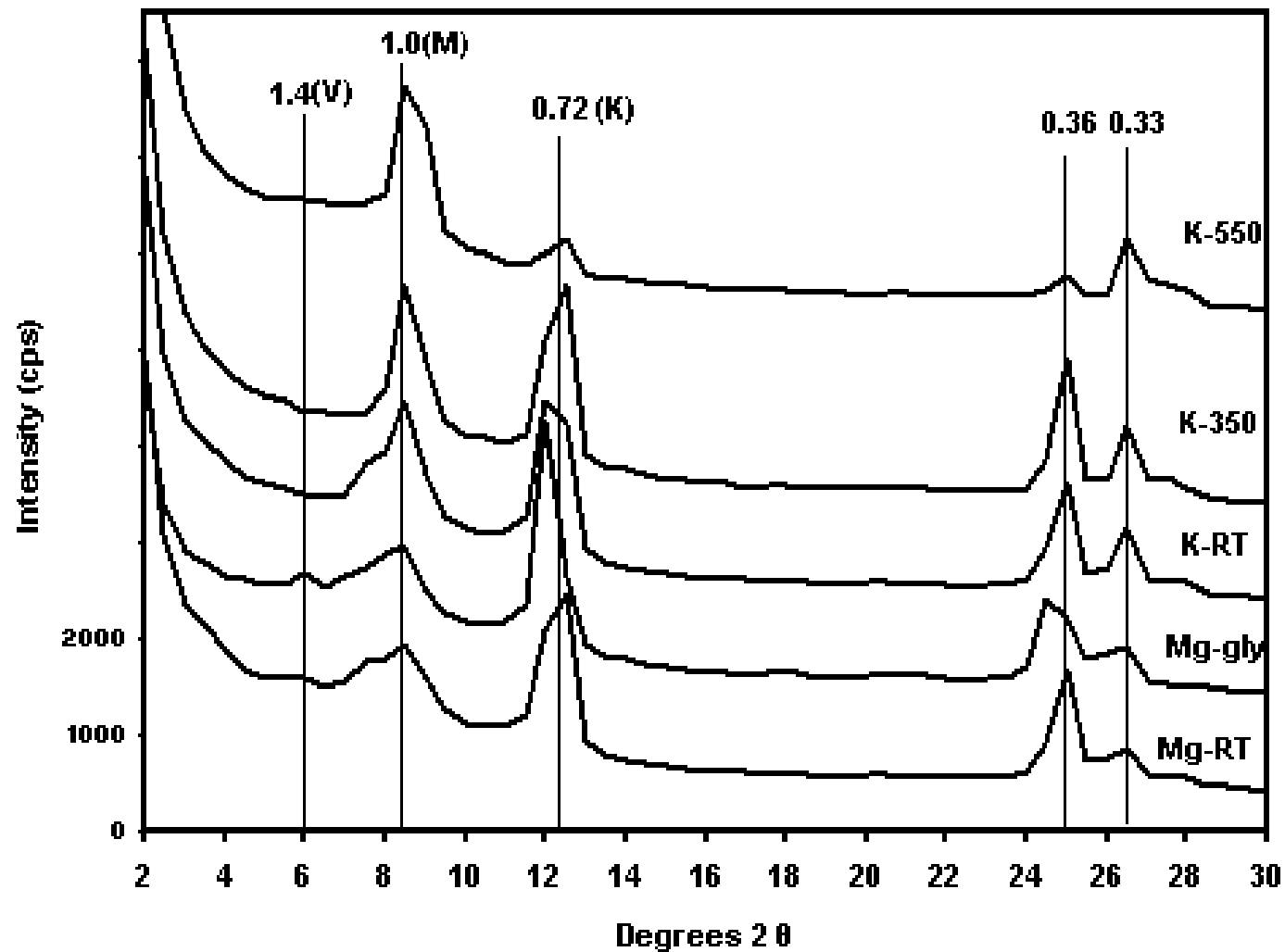


Figure A.16 X-ray diffraction (xrd) patterns for phyllosilicate mineralogy of the coarse clay fraction of soil sample 9. Numbers above peaks are d-spacings in nanometers. Letters above peaks designate clay mineralogy (s = smectite, v = vermiculite, m = mica, and k = kaolinite). Treatments include: Mg<sup>2+</sup> saturation at room temperature (Mg-RT) and with glycerol (Mg-gly), K<sup>+</sup> saturation at room temperature (K-RT), 350 °C (K-350), and 550 °C (K-550). Area under each peak of the Mg-gly xrd pattern was compared to specify the percent of each clay

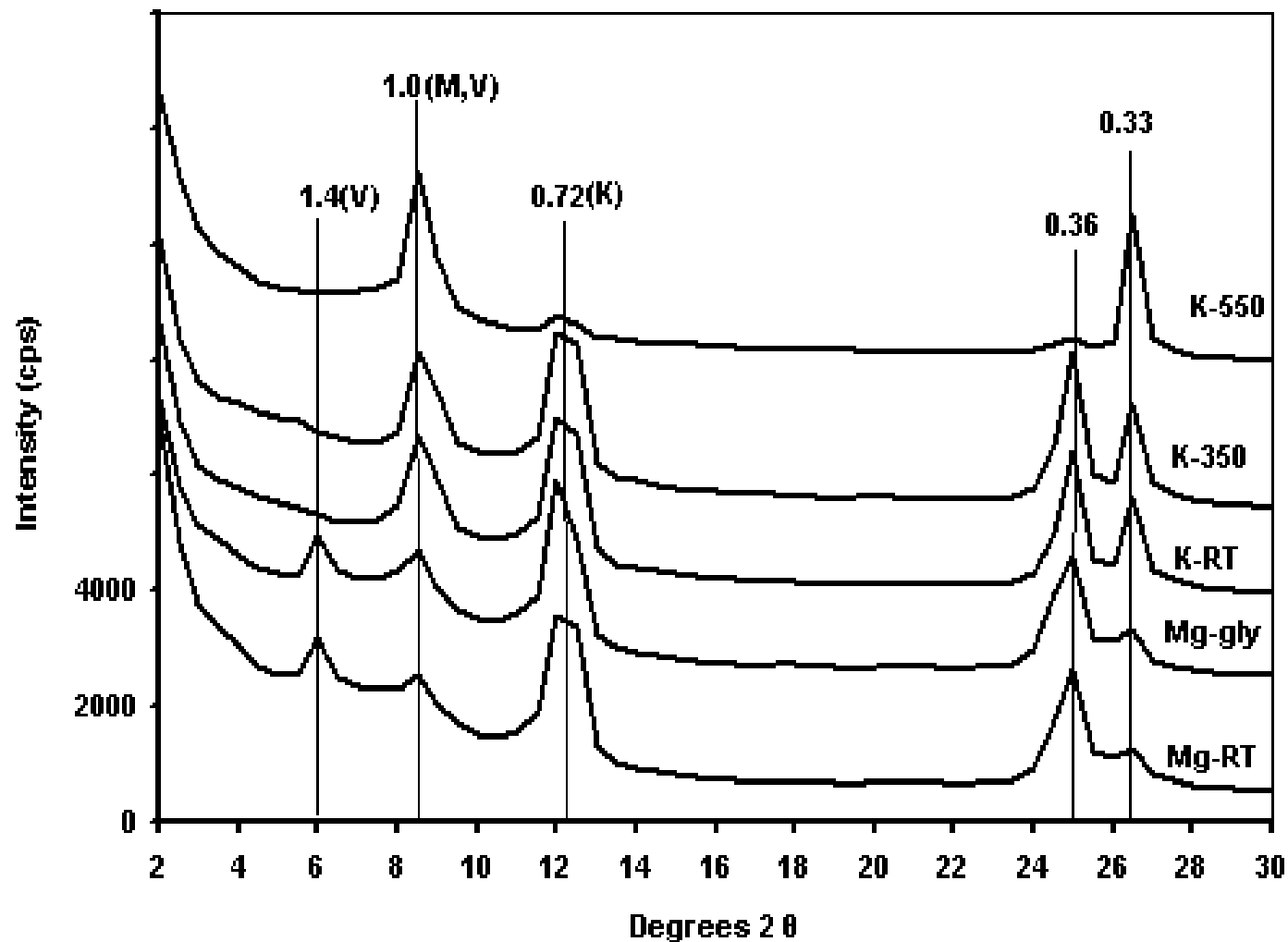


Figure A.17 X-ray diffraction (xrd) patterns for phyllosilicate mineralogy of the fine clay fraction of soil sample 11. Numbers above peaks are d-spacings in nanometers. Letters above peaks designate clay mineralogy (s = smectite, v = vermiculite, m = mica, and k = kaolinite). Treatments include:  $Mg^{2+}$  saturation at room temperature (Mg-RT) and with glycerol (Mg-gly),  $K^+$  saturation at room temperature (K-RT), 350 °C (K-350), and 550 °C (K-550). Area under each peak of the Mg-gly xrd pattern was compared to specify the percent of each clay mineral.

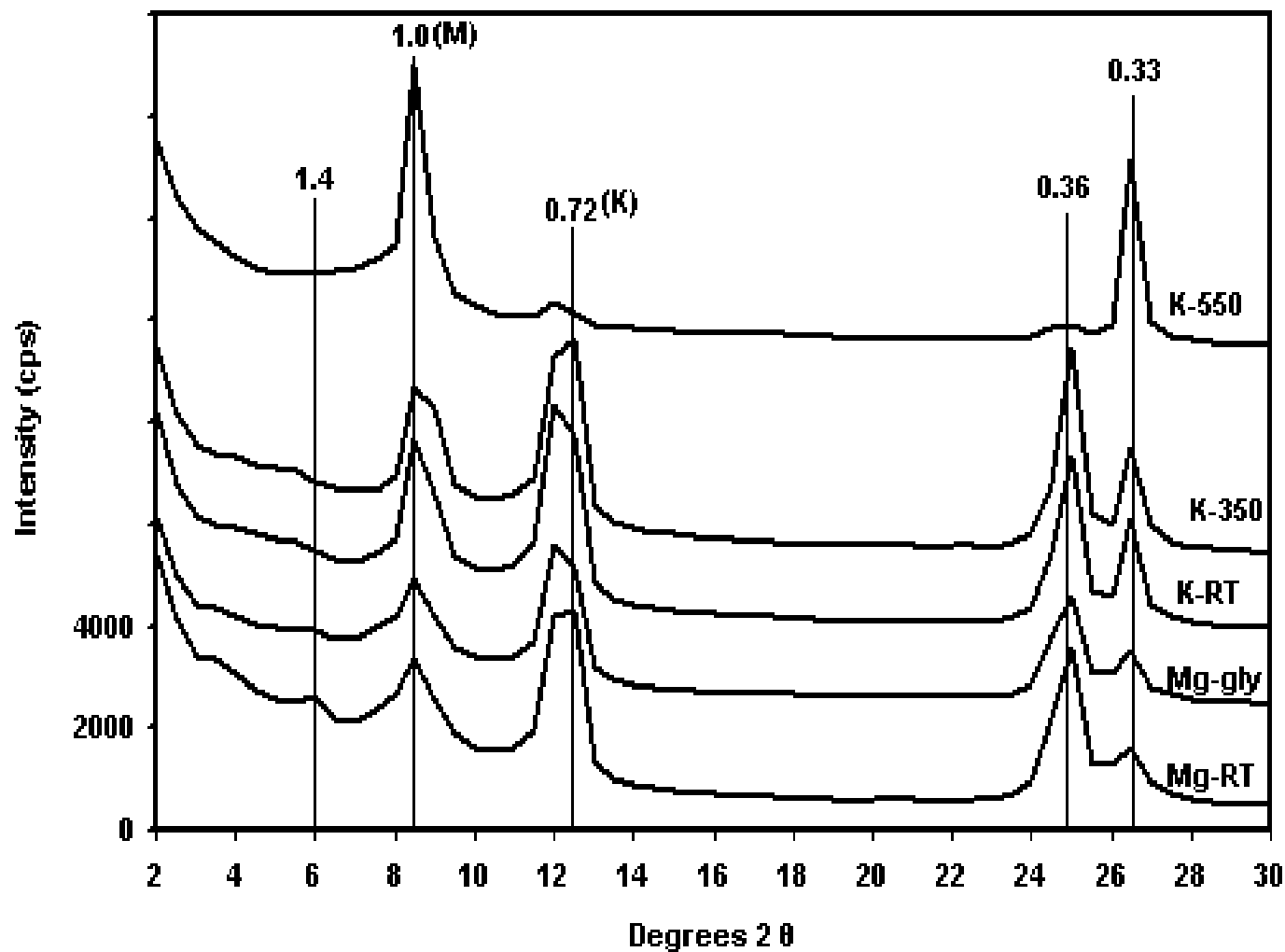


Figure A.18 X-ray diffraction (xrd) patterns for phyllosilicate mineralogy of the coarse clay fraction of soil sample 11. Numbers above peaks are d-spacings in nanometers. Letters above peaks designate clay mineralogy (s = smectite, v = vermiculite, m = mica, and k = kaolinite). Treatments include:  $Mg^{2+}$  saturation at room temperature (Mg-RT) and with glycerol (Mg-gly),  $K^+$  saturation at room temperature (K-RT), 350 °C (K-350), and 550 °C (K-550). Area under each peak of the Mg-gly xrd pattern was compared to specify the percent of each clay mineral.

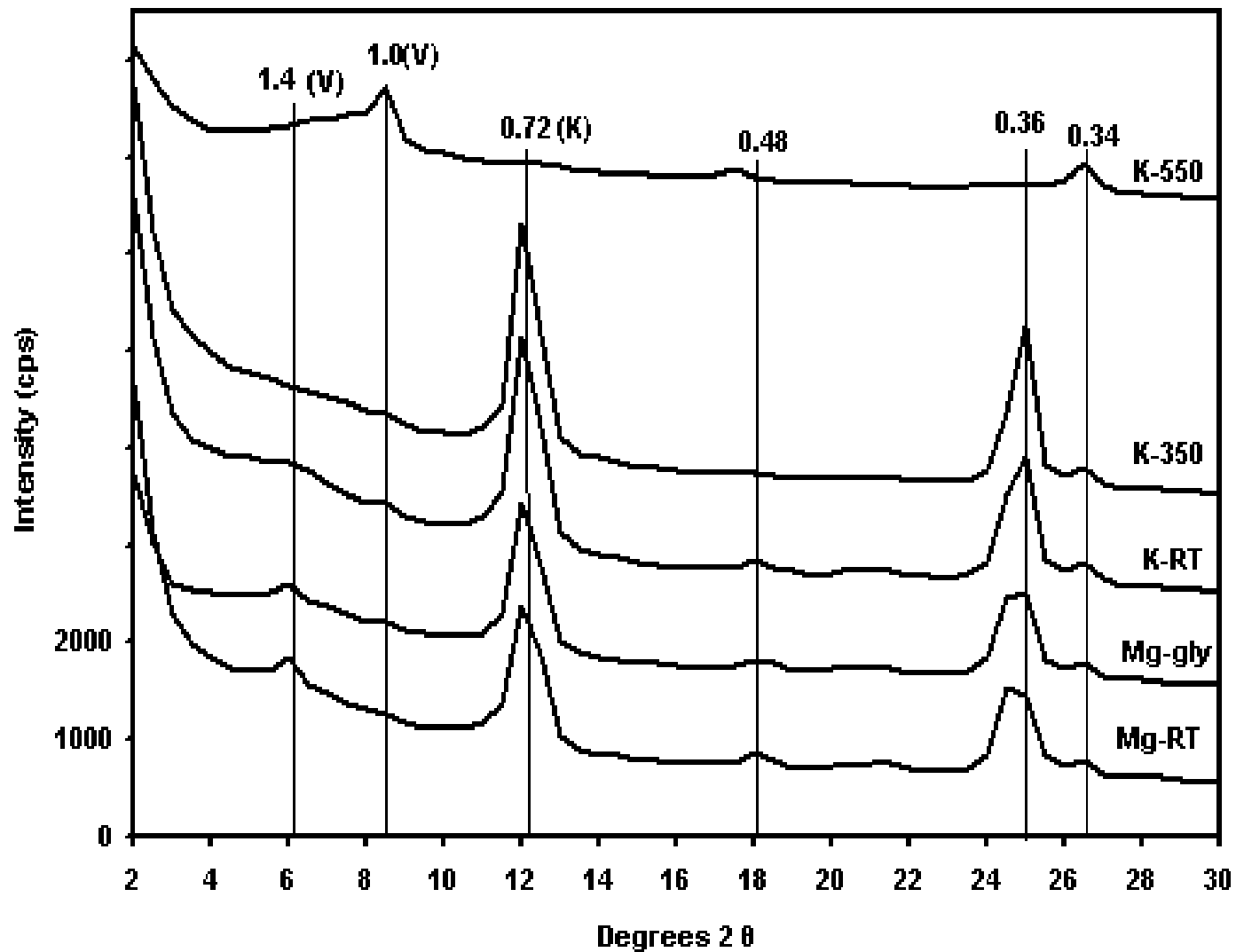


Figure A.19 X-ray diffraction (xrd) patterns for phyllosilicate mineralogy of the fine clay fraction of soil sample 13. Numbers above peaks are d-spacings in nanometers. Letters above peaks designate clay mineralogy (s = smectite, v = vermiculite, m = mica, and k = kaolinite). Treatments include:  $Mg^{2+}$  saturation at room temperature (Mg-RT) and with glycerol (Mg-gly),  $K^+$  saturation at room temperature (K-RT), 350 °C (K-350), and 550 °C (K-550). Area under each peak of the Mg-gly xrd pattern was compared to specify the percent of each clay mineral.



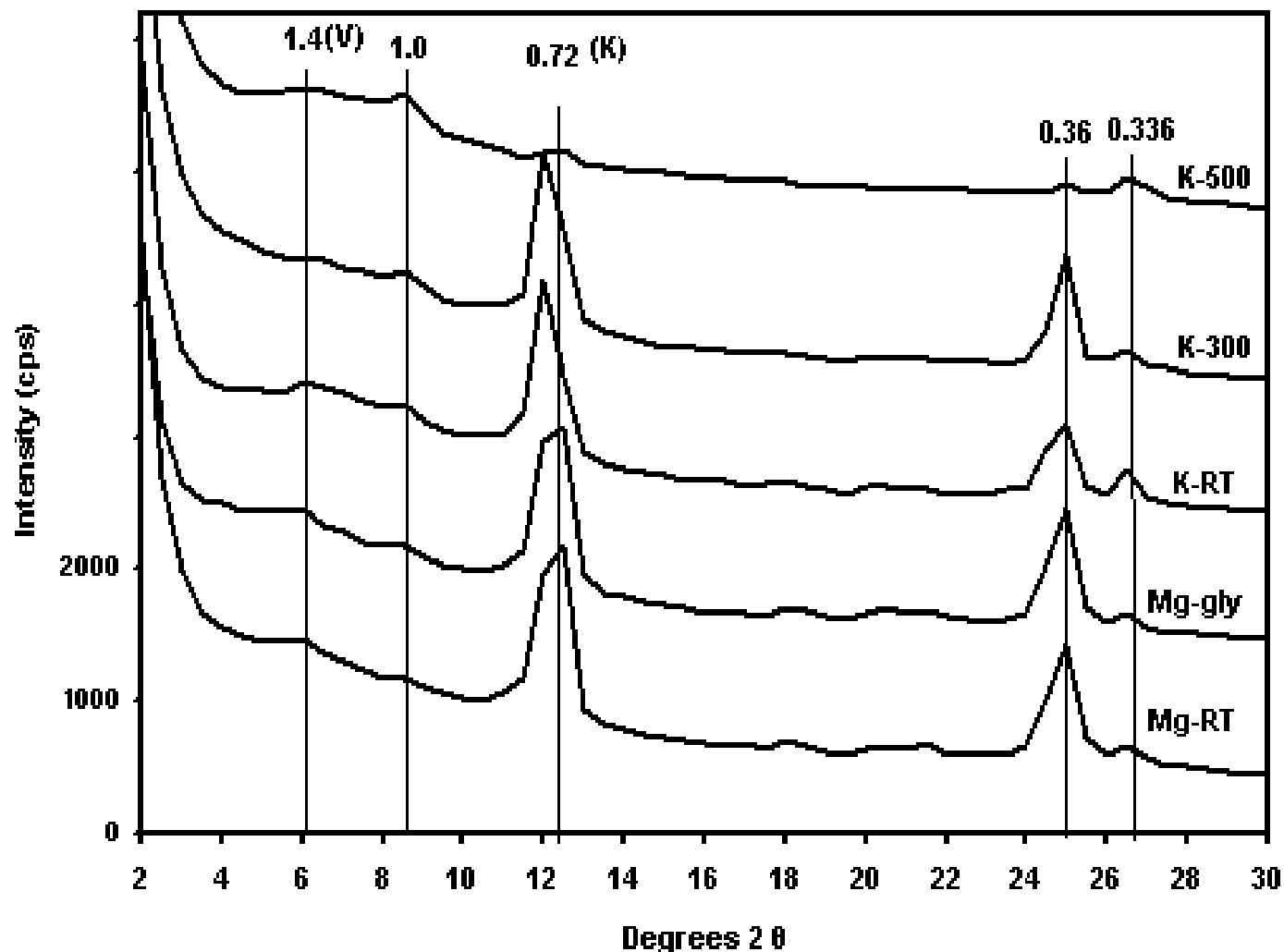


Figure A.20 X-ray diffraction (xrd) patterns for phyllosilicate mineralogy of the coarse clay fraction of soil sample 13. Numbers above peaks are d-spacings in nanometers. Letters above peaks designate clay mineralogy (s = smectite, v = vermiculite, m = mica, and k = kaolinite). Treatments include:  $Mg^{2+}$  saturation at room temperature (Mg-RT) and with glycerol (Mg-gly),  $K^+$  saturation at room temperature (K-RT), 350 °C (K-350), and 550 °C (K-550). Area under each peak of the Mg-gly xrd pattern was compared to specify the percent of each clay mineral.

9										
	0	0.0125	0.025	0.05	0.075	0.125	0.25	0.5	1	2
<b>A100</b>	3057.0 a	2657.4 a	2080.2 a	1777.8 a	1369.8 a	968.8 a	601.7 a	317.5 a	66.4 a	13.9 a
<b>A110</b>	2488.2 a	2563.1 a	2066.4 a	1547.4 a	1185.0 a	1057.9 a	515.1 ab	254.5 ab	32.8 a	12.8 a
<b>A150</b>	3001.5 a	2507.6 a	1913.7 a	1414.2 a	1103.4 a	876.1 a	419.4 ab	121.3 c	25.3 a	14.8 a
<b>SoilFix</b>	3118.1 a	2113.5 a	2024.7 a	1278.2 a	1097.9 a	783.2 a	369.4 b	137.7 bc	28.6 a	9.5 a
5										
	0	0.0125	0.025	0.05	0.075	0.125	0.25	0.5	1	2
<b>A100</b>	2139.0 a	1510.4 a	1464.5 a	1159.3 a	969.3 a	794.8 b	530.6 ab	284.3 ab	190.3 a	47.0 a
<b>A110</b>	1943.6 a	1773.7 a	1629.3 a	1323.8 a	1138.3 a	997.0 a	670.8 a	357.3 a	146.4 ab	21.5 a
<b>SF1606</b>	2269.2 a	1595.3 a	1516.9 a	1160.7 a	1084.5 a	805.0 b	429.0 b	170.5 b	59.2 b	10.8 a
<b>SoilFix</b>	2345.7 a	1734.1 a	1487.7 a	1305.6 a	1102.9 a	830.2 ab	481.4 ab	318.5 a	49.5 b	26.6 a
12										
	0	0.025	0.05	0.075	0.125	0.25	0.5	1	2	2.5
<b>A100</b>	2139.8 a	1480.0 b	1183.2 b	1048.8 ab	835.1 a	656.8 ab	328.2 a	190.8 a	73.3 a	71.4 a
<b>A110</b>	2155.1 a	1606.8 b	1315.4 ab	1064.2 ab	947.3 a	679.4 a	323.4 a	127.5 ab	52.3 a	40.0 a
<b>A150</b>	2446.6 a	2050.2 a	1795.2 a	1317.1 a	748.5 a	591.3 ab	340.4 a	99.1 ab	59.7 a	59.1 a
<b>SF1606</b>	2051.6 a	1531.0 b	1210.0 b	950.0 b	734.1 a	408.5 b	238.9 a	63.2 b	42.4 a	71.9 a
13										
	0	0.0125	0.025	0.05	0.075	0.125	0.25	0.5	1	2
<b>923VHM</b>	1875.7 a	1776.5 a	1366.0 a	1015.5 a	1139.0 a	988.2 a	581.5 ab	415.4 a	98.1 b	64.6 a
<b>A100</b>	2043.2 a	1473.0 a	1293.1 a	1249.0 a	1062.6 a	884.5 a	615.9 ab	431.6 a	184.3 a	60.8 a
<b>A110</b>	1824.3 a	1670.3 a	1375.8 a	1410.4 a	1172.8 a	943.4 a	734.8 a	393.2 a	147.6 ab	43.8 a
<b>Soilfix</b>	1924.3 a	1794.6 a	1386.6 a	1209.0 a	1126.6 a	1043.4 a	606.1 ab	432.4 a	98.6 b	61.1 a
<b>APS705</b>	1754.2 a	1706.5 a	1274.8 a	1220.5 a	902.7 a	982.5 a	522.4 b	317.4 a	165.9 ab	94.2 a

Table A.1 Average NTU readings for soils with the most effective flocculation with PAM. For each PAM concentration, data points with different letters are significantly different ( $p = 0.05$ ).

2										
	0	0.025	0.075	0.125	0.25	0.5	1	2.5	5	
A100	802.6 a	502.0 cd	324.5 b	291.4 bc	246.0 a	238.1 a	241.0 b	256.9 b	312.3 b	
A110	580.0 a	437.3 d	369.4 b	279.7 c	246.6 a	257.7 a	285.8 ab	309.7 ab	512.9 a	
A150	817.4 a	868.4 a	830.4 a	349.7 ab	282.9 a	262.2 a	310.2 ab	399.6 a	513.2 a	
SF1606	720.0 a	828.0 ab	740.3 a	268.9 c	213.3 a	217.5 a	348.8 a	422.4 a	562.6 a	
APS705	781.6 a	656.8 bc	629.2 a	385.1 a	274.1 a	303.8 a	123.5 c	77.4 c	53.2 c	
7										
	0	0.0125	0.025	0.05	0.075	0.125	0.25	0.5	1	2
A100	2799.3 a	1882.0 b	1528.2 b	930.9 b	678.9 b	418.9 b	253.2 b	162.8 b	160.9 c	470.9 b
A110	2779.7 a	1812.4 b	1336.5 bc	756.4 bc	632.5 b	300.4 b	231.4 b	166.4 b	231.1 bc	855.3 a
A150	2924.8 a	1530.3 b	1024.9 c	589.8 c	449.3 b	318.7 b	254.8 b	188.1 b	464.3 a	826.3 a
N300	3324.6 a	3443.3 a	3014.2 a	3027.7 a	2442.0 a	1953.5 a	1357.0 a	693.4 a	330.4 ab	194.1 c
11										
	0	0.0125	0.025	0.05	0.075	0.125	0.25	0.5	1	2
923VHM	2647.0 a	2000.8 b	1339.2 bc	619.4 b	460.6 bc	271.8 b	168.9 bc	210.4 b	285.5 a	790.1 a
A100	2913.6 a	2076.2 b	1632.2 b	927.2 b	814.1 b	508.8 b	268.6 b	116.7 b	68.5 c	158.4 c
A110	2568.9 a	2060.0 b	1386.8 bc	894.1 b	621.3 bc	352.9 b	182.4 bc	115.9 b	178.9 b	435.5 b
SF1606	2905.5 a	1489.2 c	991.3 c	627.0 b	394.3 c	238.9 b	131.0 c	162.5 b	332.9 a	764.8 a
APS705	2885.1 a	2614.9 a	2360.7 a	2180.6 a	1762.1 a	1136.9 a	657.0 a	355.8 a	120.7 bc	31.9 c
14										
	0	0.025	0.05	0.1	0.25	0.5	1	2.5	5	
923VHM	2616.0 a	1939.2 a	1421.7 a	1033.5 a	516.3 a	384.3 a	145.7 ab	95.1 a	239.5 ab	
A100	2845.1 a	1907.5 a	1430.6 a	1223.4 a	484.4 a	250.3 a	117.0 b	122.5 a	192.3 b	
A110	2486.9 a	2031.3 a	1841.7 a	1049.0 a	548.4 a	242.6 a	104.1 b	164.1 a	325.8 a	
A150	2385.4 a	2045.4 a	1705.6 a	1057.1 a	590.3 a	412.3 a	187.0 a	126.9 a	189.3 b	

Table A.2 Average NTU readings for soils with diminished turbidity reduction at high PAM concentrations. For each PAM concentration, data points with different letters are significantly different ( $p = 0.05$ ).

3										
	0	0.025	0.05	0.075	0.125	0.25	0.5	1	2	4
<b>923VHM</b>	393.0 a	302.0 ab	265.4 ab	237.6 b	226.0 ab	176.8 ab	182.7 a	153.8 a	160.7 a	149.4 a
<b>A100</b>	330.0 ab	256.4 b	215.0 b	254.7 ab	210.6 b	181.4 ab	154.2 ab	99.9 b	72.1 bc	69.7 c
<b>A110</b>	392.6 a	339.0 a	290.7 a	215.8 b	192.1 b	128.3 b	115.5 b	105.7 b	89.6 b	109.5 b
<b>N300</b>	335.4 ab	324.5 a	236.5 ab	308.2 a	267.0 a	222.3 a	186.3 a	135.1 ab	86.0 b	64.5 c
<b>APS705</b>	309.1 b	321.9 a	288.3 a	270.9 ab	262.5 a	192.3 a	146.2 ab	96.1 b	54.7 c	43.5 c
6										
	0	0.025	0.05	0.1	0.25	0.5	0.75	1	1.5	2
<b>A100</b>	3342.6 a	3149.8 a	2951.6 a	2256.5 a	1058.9 b	641.0 c	367.6 b	285.3 a	184.0 ab	123.5 a
<b>A110</b>	2996.9 a	3181.3 a	2880.2 a	2044.7 a	809.9 b	564.6 c	368.0 b	268.7 a	131.2 b	99.4 a
<b>A150</b>	3455.3 a	3072.8 a	3203.0 a	2668.6 a	2630.6 a	2362.1 a	1841.2 a	324.6 a	276.6 a	163.2 a
<b>Soifix</b>	3141.7 a	3106.4 a	3071.1 a	2750.7 a	2530.8 a	1248.1 b	1313.6 a	291.6 a	175.6 ab	137.9 a
8										
	0	0.0125	0.025	0.05	0.075	0.125	0.25	0.5	1	2
<b>A100</b>	2005.8 a	1784.3 a	1705.8 a	1672.1 ab	1523.5 ab	1368.5 ab	817.0 b	475.3 b	194.4 a	193.0 a
<b>A110</b>	1677.7 ab	1515.1 a	1551.6 a	1325.1 b	1361.8 b	922.5 b	640.1 b	369.9 b	207.6 a	149.0 b
<b>A150</b>	1935.7 ab	1907.6 a	1515.1 a	1778.7 a	1711.4 a	1689.0 a	1532.0 a	888.0 a	200.5 a	151.8 b
<b>SF1606</b>	1638.5 b	1475.9 a	1652.5 a	1425.4 ab	1600.1 a	1492.7 a	1397.1 a	1000.7 a	183.2 a	173.1 ab

Table A.3 Average NTU readings for soils with little flocculation at low PAM concentrations. For each PAM concentration, data points with different letters are significantly different ( $p = 0.05$ ).

1										
Flocculant	0	0.0125	0.025	0.05	0.075	0.125	0.25	0.5	1	2
A100	567.7 a	572.8 a	535.7 a	503.8 ab	492.7 a	434.1 b	405.6 c	412.3 a	380.5 b	368.2 bc
A110	573.3 a	518.9 ab	523.4 a	492.1 ab	491.8 a	483.5 ab	471.2 b	476.5 a	425.4 ab	419.8 ab
N300	572.2 a	536.5 ab	537.6 a	544.3 a	510.0 a	559.1 a	556.3 a	522.3 a	457.5 ab	326.4 c
SF1606	563.3 a	592.6 a	522.3 a	505.8 ab	526.4 a	508.0 ab	484.0 b	505.8 a	502.4 a	488.2 a
APS705	433.1 b	392.9 b	425.5 b	412.7 b	392.7 a	297.8 c	281.4 d	182.7 b	120.4 c	54.2 d
4										
	0	0.05	0.1	0.25	0.5	1	2.5	5	10	
923VHM	1289.6 a	1254.3 ab	1301.6 a	1352.7 a	1304.1 a	1097.9 a	1317.9 a	1110.1 a	1215.3 a	
A100	1298.2 a	1121.0 b	1027.8 b	967.5 b	957.9 b	1149.4 a	1164.7 a	1096.9 a	1127.8 a	
A150	1185.8 a	1297.3 ab	1190.9 ab	1216.3 a	1173.3 a	949.8 a	905.9 a	1218.6 a	1229.9 a	
APS705	1476.1 a	1411.5 a	1073.8 b	613.0 c	429.2 c	230.6 b	216.3 b	196.7 b	272.7 b	

Table A.4 Average NTU readings for soils with minimal PAM effect (except APS705). For each PAM concentration, data points with different letters are significantly different ( $p = 0.05$ ).

0 mg L <sup>-1</sup> Gypsum					
	PAM Concentration (mg L <sup>-1</sup> )				
Flocculant	0	0.05	0.125	1	5
Soilfix	1819.1 a	1035.9 c	385.0 c	100.4 b	406.5 c
A110	1752.2 a	1335.8 ab	443.9 bc	122.8 b	640.0 b
APS 705	1629.8 a	1172.5 bc	613.1 b	130.1 b	67.8 d
923 VHM	1629.4 a	1213.2 bc	392.7 c	147.0 b	1073.0 a
APS 706b	1477.9 a	1587.8 a	1481.3 a	375.2 a	199.9 cd
10 mg L <sup>-1</sup> Gypsum					
	PAM Concentration (mg L <sup>-1</sup> )				
Flocculant	0	0.05	0.125	1	5
Soilfix	1759.0 a	1473.8 a	528.4 c	83.6 b	233.1 c
A110	1774.2 a	1427.2 a	588.1 c	97.5 b	352.5 b
APS 705	1825.0 a	1536.7 a	933.0 b	145.4 b	54.0 d
923 VHM	1646.7 a	1585.7 a	451.4 c	100.6 b	650.9 a
APS 706b	1845.0 a	1655.3 a	1741.1 a	679.1 a	192.3 c
20 mg L <sup>-1</sup> Gypsum					
	PAM Concentration (mg L <sup>-1</sup> )				
Flocculant	0	0.05	0.125	1	5
Soilfix	1727.8 b	1606.2 a	624.3 c	79.9 c	207.4 c
A110	2063.9 a	1583.3 a	579.9 cd	64.7 c	298.6 b
APS 705	1779.1 ab	1433.0 a	1108.2 b	144.5 b	44.8 d
923 VHM	1766.7 ab	1453.6 a	491.4 d	97.8 bc	500.8 a
APS 706b	1699.5 b	1683.9 a	1842.4 a	729.8 a	179.9 c
50 mg L <sup>-1</sup> Gypsum					
	PAM Concentration (mg L <sup>-1</sup> )				
Flocculant	0	0.05	0.125	1	5
Soilfix	1870.8 a	1830.2 a	1152.1 b	117.2 b	162.5 c
A110	1713.5 a	1375.0 a	647.2 c	108.6 b	274.5 b
APS 705	1909.1 a	1712.2 a	1269.1 b	155.5 b	28.4 d
923 VHM	1887.0 a	1510.5 a	503.6 c	88.7 b	404.4 a
APS 706b	1785.0 a	1837.2 a	2019.0 a	936.0 a	208.7 bc
100 mg L <sup>-1</sup> Gypsum					
	PAM Concentration (mg L <sup>-1</sup> )				
Flocculant	0	0.05	0.125	1	5
Soilfix	1848.8 a	1986.4 a	1433.2 a	105.8 b	128.6 bc
A110	1904.5 a	1752.1 a	893.1 b	93.8 b	168.4 b
APS 705	2147.7 a	1728.9 a	1422.8 a	168.2 b	56.3 c
923 VHM	2075.0 a	1825.6 a	609.3 b	74.7 b	355.7 a
APS 706b	1686.8 a	1964.5 a	1743.7 a	1045.9 a	304.3 a

Table A.5 Statistical significance of flocculant treatment by gypsum concentration for soil 8 (lsd  $\alpha = 0.05$ ).

<b>Soilfix</b>					
	<b>PAM Concentration (mg L<sup>-1</sup>)</b>				
<b>Gypsum conc</b>	<b>0</b>	<b>0.05</b>	<b>0.125</b>	<b>1</b>	<b>5</b>
<b>0 mg L<sup>-1</sup></b>	1819.1 a	1035.9 c	385.0 b	100.4 a	406.5 a
<b>10 mg L<sup>-1</sup></b>	1759.0 a	1473.8 b	528.4 b	83.6 a	233.1 b
<b>20 mg L<sup>-1</sup></b>	1727.8 a	1606.2 ab	624.3 b	79.9 a	207.4 bc
<b>50 mg L<sup>-1</sup></b>	1870.8 a	1830.2 ab	1152.1 a	117.2 a	162.5 bc
<b>100 mg L<sup>-1</sup></b>	1848.8 a	1986.4 a	1433.2 a	105.8 a	128.6 c
<b>923VHM</b>					
	<b>PAM Concentration (mg L<sup>-1</sup>)</b>				
<b>Gypsum conc</b>	<b>0</b>	<b>0.05</b>	<b>0.125</b>	<b>1</b>	<b>5</b>
<b>0 mg L<sup>-1</sup></b>	1629.8 b	1213.2 b	392.7 b	147.0 a	1073.0 a
<b>10 mg L<sup>-1</sup></b>	1646.7 b	1585.7 ab	451.4 ab	100.6 b	650.9 b
<b>20 mg L<sup>-1</sup></b>	1766.7 ab	1453.6 ab	491.4 ab	97.8 b	500.8 bc
<b>50 mg L<sup>-1</sup></b>	1887.0 ab	1510.5 ab	503.6 ab	88.7 b	404.4 c
<b>100 mg L<sup>-1</sup></b>	2075.0 a	1825.6 a	609.3 a	74.7 b	355.7 c
<b>APS 705</b>					
	<b>PAM Concentration (mg L<sup>-1</sup>)</b>				
<b>Gypsum conc</b>	<b>0</b>	<b>0.05</b>	<b>0.125</b>	<b>1</b>	<b>5</b>
<b>0 mg L<sup>-1</sup></b>	1752.2 b	1172.5 b	613.1 c	130.1 a	67.8 a
<b>10 mg L<sup>-1</sup></b>	1825.0 ab	1536.7 ab	933.0 bc	145.4 a	54.0 a
<b>20 mg L<sup>-1</sup></b>	1779.1 b	1443.0 ab	1108.2 ab	144.5 a	44.8 ab
<b>50 mg L<sup>-1</sup></b>	1909.1 ab	1712.2 a	1269.1 ab	155.5 a	28.4 b
<b>100 mg L<sup>-1</sup></b>	2147.7 a	1728.9 a	1422.8 a	168.2 a	56.3 a
<b>APS 706b</b>					
	<b>PAM Concentration (mg L<sup>-1</sup>)</b>				
<b>Gypsum conc</b>	<b>0</b>	<b>0.05</b>	<b>0.125</b>	<b>1</b>	<b>5</b>
<b>0 mg L<sup>-1</sup></b>	1477.9 a	1587.8 b	1481.3 c	375.2 d	199.9 b
<b>10 mg L<sup>-1</sup></b>	1845.0 a	1655.3 b	1741.1 b	679.1 c	192.3 b
<b>20 mg L<sup>-1</sup></b>	1699.5 a	1683.9 ab	1842.4 ab	729.8 bc	179.9 b
<b>50 mg L<sup>-1</sup></b>	1785.0 a	1837.2 ab	2019.0 a	936.0 ab	208.7 b
<b>100 mg L<sup>-1</sup></b>	1686.8 a	1964.5 a	1743.7 b	1045.9 a	304.3 a
<b>A110</b>					
	<b>PAM Concentration (mg L<sup>-1</sup>)</b>				
<b>Gypsum conc</b>	<b>0</b>	<b>0.05</b>	<b>0.125</b>	<b>1</b>	<b>5</b>
<b>0 mg L<sup>-1</sup></b>	1629.4 c	1335.8 a	443.9 b	122.8 a	640.0 a
<b>10 mg L<sup>-1</sup></b>	1774.2 bc	1427.2 a	588.1 b	97.5 ab	352.5 b
<b>20 mg L<sup>-1</sup></b>	2063.9 a	1583.3 a	579.9 b	64.7 b	298.6 b
<b>50 mg L<sup>-1</sup></b>	1713.5 bc	1375.0 a	647.2 ab	108.6 ab	274.5 bc
<b>100 mg L<sup>-1</sup></b>	1904.5 ab	1752.1 a	893.1 a	93.8 ab	168.4 c

Table A.6 Statistical significance of gypsum concentration by PAM concentration for soil 8 (lsd  $\alpha = 0.05$ ).